A STUDY OF THE ELECTRICAL DOUBLE LAYER

A THESIS

submitted to the University of Glasgow

for the degree of

DOCTOR OF PHILOSOPHY

BY

Colin A. Vincent, B.Sc.

Supervisor

Dr. G. H. Nancollas.

July, 1963.

ProQuest LLC.
789 East Eisenhower Parkway
P.O. Box 1346
Ann Arbor, MI 48106 – 1346

A Study of the Electrical Double Layer.

Summary.

Colin A. Vincent.

At the interface between a metal and an electrolytic solution, there is in general an array of oppositely charged particles and oriented dipoles, known as the "electrical double layer". In the present work, a study was made of the double layer for perfectly polarised systems - i.e. where charge transfer across the interface did not occur. The metallic phase was mercury, while the solution consisted of alkali metal chlorides in aqueous and non-aqueous solvents. The main purpose of the research was to devise an accurate method of measuring differential capacitance at a dropping mercury electrode and thence to investigate, for various systems, the variation of double layer capacitance with applied potential and electrode charge, so that the effect of the dielectric constant and other properties of the solvent might be assessed. The thesis is divided into four sections. After a theoretical introduction, Part 1. describes the construction of apparatus for the measurement of the double layer impedance at a dropping mercury electrode. Part 2. is an investigation of certain aspects of the double layer in aqueous solutions, while in Part 3. consideration is made of the effect of solvent variation.

Since the impedance of the dropping mercury electrode, which was measured using a transformer ratio-arm bridge, varied with time, it was necessary to know the time interval between the birth of a mercury drop and the instant at which the bridge was balanced. This was achieved as set out in Part 1. by means of an

electronic interval timer which measured the period between pulses emitted respectively by a "drop birth detector" and a "bridge balance detector".

In Part 2. the factors determining the area of a growing mercury drop at a given time were considered and an accurate method of calculating differential capacitance per unit area was derived. Other aspects of the double layer in aqueous systems which were investigated included the effect of bridge frequency variation and the resistive component of the electrode impedance. A new method of determining differential capacitance was studied which was independent of timing and flow rate measurements.

The final section of the thesis, Part 3, is mainly concerned with the results of capacitance measurements of alkali metal chloride solutions in formamide. This solvent has a very high dielectric constant, and it was therefore of interest to compare measurements in it with those for aqueous solutions and for solvents of low dielectric constant such as methanol. Three main points were noted for formamide solutions. First, while there was no capacitance maximum on the anodic side of the charge/capacitance curves, such an effect did occur on the cathodic branch. Second, as the electrode charge was increased cathodically, the differential capacitance decreased. Finally, at high cathodic polarisation, the size of the cation had no effect on the differential capacitance. Explanations for these three results are suggested in terms of double layer theory and the molecular structure of formamide.

PREFACE.

The work described in this thesis was carried out in the Chemistry Department of the University of Glasgow under the direction of Professor J. Monteath Robertson, C.B.E., F.R.S.

The material of Part 1 has been published in the "Journal of Scientific Instruments" and a reprint is appended at the end of the thesis.

I wish to express my sincere gratitude to Dr. G. H. Nancollas for his guidance and encouragement during the period of research. Thanks are also due to Dr. M. S. Dunsmore for her help with Deuce computer programmes.

I also thank the Carnegie Trust for the Universities of Scotland and the Salters' Institute of Industrial Chemistry for the award of maintenance grants which made this research possible.

CONTENTS

INTRODUCTION

Across any phase boundary there generally exists a difference in electrical potential caused by the redistribution of electrical charges of particles coming from the bulk of the phases to form the interfacial layer. The array of oppositely charged particles and oriented dipoles in juxtaposition at a boundary is customarily referred to as the "electrical double layer". Such an effect is caused by the tendency of any system to assume a position of minimum free energy and it has been shown (1) that there are four main mechanisms responsible for its formation:

(i) charge transfer across the interface.

(ii) unequal adsorption of oppositely charged ions.

(iii) adsorption and orientation of dipolar molecules.

(iv) deformation of polarisable ions, atoms or molecules in the electric field at the interface.

Familiar examples of double layers are those formed when a metal dips into a solution of its ions, at liquid junctions, or when a metal is heated in a vacuum. An exact study of the double layer is most easily accomplished by using metal-solution interfaces because it is possible to vary the potential difference between the phases without varying their composition. If, on the application of a potential, no current flows across the interface of such a system, the double layer is electrically similar to a capacitor of large specific capacitance. The magnitude of the latter is a measure of the electronic charge on the metal surface and knowledge of this, in turn leads to further information about the double layer structure.

A detailed knowledge of the double layer is of fundamental importance, since it is the basis for the explanation of many natural phenomena. The electrokinetic ζ - potential is largely determined by double layer properties, and thus electrophoresis, electro-osmosis, streaming potentials and similar effects are dependent on double layer formation. Solid-liquid heterogeneous processes such as crystal growth and dissolution, electrode reactions and coagulation of colloids similarly require an intimate knowledge of double layer phenomena for their complete understanding. A biological effect that can be partly explained in terms of electrochemical disturbance of the double layer is the nerve impulse. Surrounding a nerve fibre there is a thin film which, in a rest state, is charged positively outside and negatively inside. An electric stimulus applied to the outside disturbs the equilibrium of the ions forming the double layer and thus changes the permeability of the film to ions. The local change in potential causes disturbance in adjacent areas and thus the initial impulse propagates itself along the nerve.

While double layer behaviour is the basis of the phenomena described above, a fundamental study must first be completed for simple systems. The main methods of investigation are therefore concerned with the direct or indirect determination of the capacitance of the double layer at a metal-solution interface. Mercury is pre-eminently suitable as the metal, since a pure reproduceable surface is easily obtained and since its low chemical activity and high hydrogen

overvoltage enable it to be used over a large range of potentials in many solution systems.

An ideal polarised electrode may be described as a metal-solution system for which no finite amount of charge may cross the interface during re-establishment of equilibrium after a small change in the potential difference between the phases. Such an electrode behaves like an electrical capacitor without leakage. Unlike a simple capacitor however, the capacitance of an ideal polarised electrode varies with applied potential, since it depends on the relative position of charges which may alter under different conditions of electrical field.

Most theories of the detailed structure of the double layer between a metal and an electrolytic solution have been based on an electrostatic model of a planar, charged conducting wall and an assembly of charged particles in an adjacent structureless dielectric. More refined theories take into account such factors as the energies of interaction of ions with themselves and with solvent molecules and also the solvent structure in the neighbourhood of the interface. The majority of theories neglect the atomic structure of the metallic side of the interface, although consideration has been given to the effect of penetration of an electrical field into the metal.

The first quantitative approach to double layer structure was given in 1879 by Helmholtz (2) who regarded the interface as a simple parallel plate capacitor.

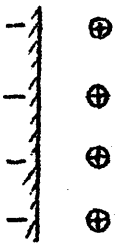

Thus $$C = \frac{q}{\psi} = \frac{DD_0A}{4\pi d} \quad \ldots\ldots\ldots\ldots\ldots 1.$$

where C is the capacitance, q the charge on the "plates", ψ the potential difference across the interface, D is the dielectric constant of the solvent, d is the distance apart of the plates, A is the area of the electrode and D_0 is a constant. This theory did not explain the experimentally demonstrated variation of capacitance with potential and required d $\simeq$ 0.3 Å, an unreasonably small value.

Gouy (3) and Chapman (4) independently considered that thermal motion would result in the solution side of the double layer being diffuse in character. Their approach was equivalent to that used by Debye and Hückel in their ionic atmosphere theory : the solution side of the double layer was regarded as being the ionic atmosphere of the electrode. This theory lead to an exponential fall in potential with distance from the electrode. It predicted values of capacitance of 200 - 300 μF / sq. cm. however, which were much larger than the measured double layer capacitances at the potentials concerned.

Stern (5) made allowance for the finite size of ions and considered the possibility of a specific interaction between ions

and electrode. This treatment may be regarded as a combination of the Helmholtz rigid layer interpretation with that of Gouy - Chapman diffuse layer. Thus the potential difference between the interface and solution is assumed to fall linearly across the "inner" layer and thereafter to decay exponentially across the diffuse layer. Stern considered, however, that both cations and anions would be adsorbed simultaneously at the electrode surface, and in equal numbers. Grahame and Whitney (6) observed disagreement between experimental results and values calculated by Stern's theory, and in his classic review (7), Grahame suggested that only anions could be specifically adsorbed.

Grahame's concept of the double layer structure, upon which all modern ideas are based, postulates the existence of two "Helmholtz planes" - an inner marking the closest approach of anionic centres and an outer marking the closest approach of cationic centres. Thus the double layer at a perfectly polarised electrode is considered to consist of

(i) a metallic phase on the surface of which there is generally an excess or deficit of electrons.

(ii) a region of solution phase immediately adjacent to the metal into which no electrical centres can enter because of the physical size of the ions.

(iii) a region accessible to the electrical centres of anions but not of cations.

(iv) an outer diffuse layer region of the Gouy - Chapman type.

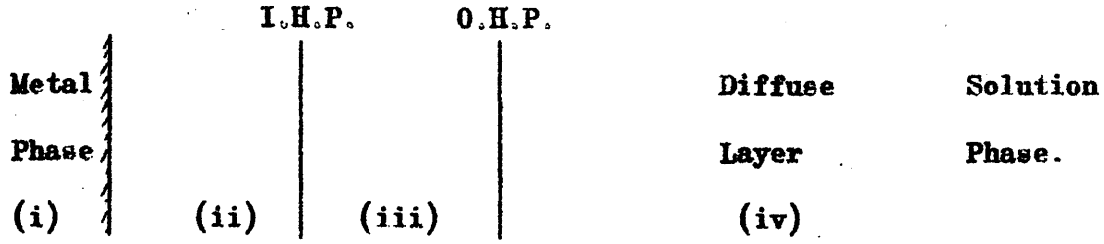

When anions are present at the inner Helmholtz plane (I.H.P.), they are held to the metallic phase by short range, covalent type forces. In this phenomenon, known as "specific adsorption", the distance between the metal and the I.H.P. is considered to be approximately equal to the radius of an unhydrated ion. Specific adsorption requires at least partial dehydration of the ion in question, and to make this process energetically favourable, the strength of the bond formed between metal and ion must be high. Thus in general only anions are specifically adsorbed, and adsorption becomes more likely for

(i) ions which are easily polariseable.

(ii) ions which have weakly bound hydration sheaths.

The following situations commonly occur;

(a) <u>Negative polarisation</u>.

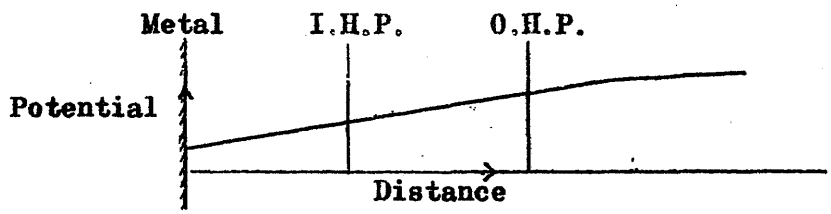

No ions at I.H.P.. Cations form diffuse layer starting at the outer Helmholtz plane (O.H.P.).

(b) Positive Polarisation

(i) No specific adsorption of anions.

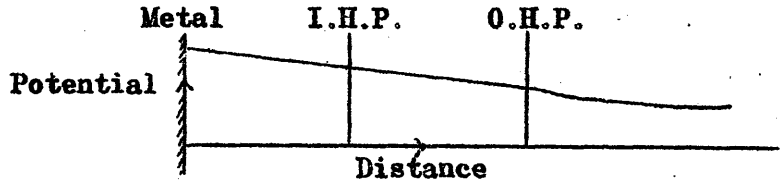

No ions at I.H.P.. Anions form diffuse layer.

(ii) Specific adsorption of anions

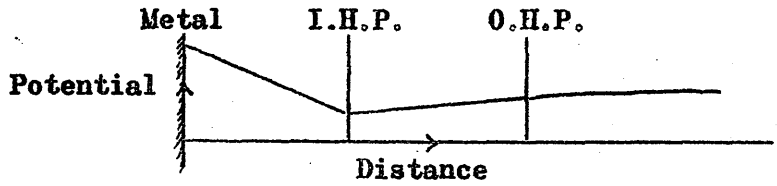

Anions present at I.H.P.. Diffuse layer of cations similar to that in (a).

If specific adsorption of anions is very strong, it may occur at the potential of the electrocapillary maximum where the metal is uncharged, or even at slightly cathodic potentials.

THEORY

It is the purpose of modern theories of the double layer to describe the behaviour of the various regions at the interface and hence to explain experimental capacitance / potential curves. The theory concerning the different parts of the double layer will now be discussed.

§1. THE DIFFUSE DOUBLE LAYER

The theory of the diffuse double layer has been well established by Grahame and others (7,8,9). In the absence of specific adsorption the capacitance of the double layer is considered to be made up of two series capacitances, C_i and C_d, where C_i is the differential capacitance of the "inner region" and C_d is that of the diffuse layer. C_o the observed total capacitance is given by

$$1/C_o = 1/C_i + 1/C_d \quad \ldots\ldots\ldots\ldots\ldots\ldots 2.$$

If w_i is the work required to bring an ion of type X_i and valency z_i from the interior of a solution to a given point in the double layer with potential ψ with respect to the interior of the solution,

$$w_i = z_i . e . \psi \quad \ldots\ldots\ldots\ldots\ldots\ldots\ldots\ldots\ldots 3$$

where e is the charge on an electron. Also if n_{oi} is the number of ions of type X_i per unit volume in the bulk of the solution and n_i is the number of similar ions per unit volume at the point where the potential is ψ,

$$n_i = n_{oi} \exp (- w_i / kT) \quad \ldots\ldots\ldots\ldots\ldots 4.$$

in which k is the Boltzmann constant. The charge in a region is

related to the potential by Poisson's equation:

$$\nabla^2\psi = -\frac{4\pi\rho}{DD_o} \qquad \ldots\ldots\ldots\ldots\ldots\ldots\ldots\ldots\ldots 5$$

where ρ is the charge density in the region, D is the dielectric constant of the medium and D_o is a constant equal to 1.112×10^{-12} coul. volt^{-1} cm^{-1}, and referred to as the diabattivity of free space. The latter is introduced to keep D a dimensionless quantity in terms of the equation. In the case of the diffuse double layer, only potential differences normal to the interface need be considered, so that if x is the distance of the region in question from the metal surface a simpler form of Poisson's equation may be used:

$$\frac{d^2\psi}{dx^2} = -\frac{4\pi\rho}{DD_o} \qquad \ldots\ldots\ldots\ldots\ldots\ldots\ldots\ldots\ldots 5'$$

Grahame has demonstrated that the potential at a "point" = the region containing a solvated ion = is not a wholly unambiguous quantity, but he regards equation 3 as a definition of ψ. This neglects other work terms such as the crowding effect and the energy required to displace polar solvent molecules from regions of high field strength. As this theory deals only with ions on the solution side of the O.H.P., the considerable work required to remove solvent sheath molecules from the side of an ion facing the metallic phase does not require consideration. The correctness of using the bulk dielectric constant in describing the structure of the diffuse double layer has been the subject of much discussion in the literature (10,11,12,13). Grahame (10) developed the theory for the case of a dielectric constant which varied with field strength, and was able to show that the onset of dielectric saturation would not greatly affect

the diffuse double layer. Watts-Tobin (13) has pointed out that the structure of the solvent is probably maintained in the diffuse double layer and thus the capacitance of the latter may be calculated accurately assuming the bulk value of solvent dielectric constant.

From equations 3 and 4 :

$$n_i = n_{o,i} \exp(-ze\psi / kT) \quad \ldots\ldots\ldots\ldots 6$$

Now the charge density in a lamina parallel to the electrode and with potential ψ, is given by the sum of the charge densities of all the ionic types ; viz

$$\rho = \Sigma n_i z_i e = \Sigma n_{o,i} z_i e . \exp(-z_i e\psi / kT) \quad \ldots\ldots 7$$

Substituting for ρ in equation 5' :

$$\frac{d^2\psi}{dx^2} = -\frac{4\pi e}{DD_o} \Sigma n_{o,i} z_i \exp(-z_i e\psi / kT) \quad \ldots\ldots\ldots\ldots 8$$

Now $$\frac{d^2\psi}{dx^2} = \frac{1}{2} \cdot \frac{d}{d\psi} \left(\frac{d\psi}{dx}\right)^2 \quad \ldots\ldots\ldots\ldots 9$$

Thus, substituting for $\frac{d^2\psi}{dx^2}$ in equation 8, and integrating, we have

$$\left(\frac{d\psi}{dx}\right)^2 = \frac{8\pi kT}{DD_o} \Sigma n_{o,i} \left(\exp\{-z_i e\psi / kT\} - 1 \right) \quad \ldots\ldots\ldots 10$$

since in the solution interior, $\frac{d\psi}{dx}$ is equal to zero and $\psi = 0$.

From Gauss' theorem, effectively an integrated form of the one dimensional Poisson equation, 5',

$$\frac{d\psi}{dx} = \frac{4\pi\eta}{DD_o} \quad \ldots\ldots\ldots\ldots\ldots\ldots\ldots 11$$

where $$\eta = \int_x^\infty \rho . dx \quad \ldots\ldots\ldots\ldots\ldots\ldots\ldots\ldots\ldots 12$$

η is the total charge in a column of liquid extending from the plane to which $\frac{d\psi}{dx}$ refers, into the body of the solution where $\psi = 0$.

From equations 10 and 11, η is given as a function of ψ :

$$\eta = \pm \left[\frac{DD_0 kT}{2\pi} \sum n_{0i} \left(\exp \left\{ - z_i e \psi / kT \right\} - 1 \right) \right]^{1/2} \quad \ldots\ldots 13$$

For a z-z valent electrolyte and where $A^2 = \frac{DD_0 kT n_{0i}}{2\pi}$, equation 13 can be simplified to

$$\eta = - 2 A \sinh z.e.\psi / 2 kT \quad \ldots\ldots\ldots\ldots 14$$

If the potential of the O.H.P., ψ°, is now substituted in equation 14, a value η_d is found for the entire diffuse double layer. Further, in the absence of specific adsorption, solvent dipole screening of the electrode and similar effects,

$$\eta_d = - q \quad \ldots\ldots\ldots\ldots\ldots\ldots\ldots\ldots\ldots\ldots 15$$

where q is the charge on the electrode. The differential capacitance of the diffuse double layer is defined in terms of ψ° as

$$C_d = - \frac{d\eta_d}{d\psi^\circ} \quad \ldots\ldots\ldots\ldots\ldots\ldots\ldots\ldots\ldots\ldots 16$$

and hence $$C_d = \frac{zeA}{kT} \cosh z.e.\psi^\circ / 2 kT \quad \ldots\ldots\ldots\ldots 17$$

The capacitance of the diffuse double layer can be given in terms of charge from equations 14 and 17 using the identity

$$\cosh^2 \phi - \sinh^2 \phi = 1 .$$

Hence $$C_d = \frac{ze}{2kT} \left(\eta_d^2 + 4A^2 \right)^{1/2} \quad \ldots\ldots\ldots\ldots\ldots 18$$

§ 2. THE INNER REGION

Let the inner region of the double layer be defined as that part lying between the metal surface and the O.H.P. There are four effects which must be considered:

(i) the specific adsorption of anions

(ii) the formation of adatoms or adions of the metal

(iii) the dielectric properties of the solvent in an electric field

(iv) compression of the region by an electric field.

(i) Specific adsorption of anions.

In Stern's theory of specific adsorption, consideration is made of the ratio of the probabilities, based on the Boltzmann distribution law, of an ion being either in solution or at the interface. Thus the number of specifically adsorbed anions per unit area is

$$m_i = 2r.m_{o_i}\exp\left(-w_i'/kT\right) \quad \ldots\ldots\ldots\ldots 19$$

where r is the radius of an ion, m_{o_i} the number of ions per unit volume in the body of the solution and w_i' is the work required to move an ion from the interior of the solution to a point on the I.H.P. Let β be defined as μ/e , where μ is the dipole moment produced by an adsorbed anion. The adsorbed anions produce a potential across the layer of $\frac{4\pi m_i e \beta}{D_1 D_o}$ where D_1 is the dielectric constant of the inner region. It is essential to note, however, that at points in the latter remote from an adsorbed anion, the lines of force are straight and normal to the metal so that further

anions may be attracted by an undiminished field. Under such conditions, if ψ is the potential difference between the metal and the O.H.P., or approximately the total rational potential difference between the two phases, the work done to bring up an ion from the interior of the electrolyte to an adsorbed site is

$$w_i' = H_i + e\lambda\psi \quad \ldots\ldots\ldots\ldots\ldots\ldots 20$$

where H_i is the difference between the partial molal free energy of an ion in solution and in an adsorbed site, and

$$\lambda = 1 - \frac{\mu}{e}(\beta+\gamma) = \frac{\gamma}{\beta+\gamma}$$

for $(\beta+\gamma)$ being the distance of the O.H.P. from the metal. Equation 20 assumes a constant electrical field between the metal and O.H.P. (Mott and Watts-Tobin have shown (9), however, that if the concentration of specifically adsorbed anions becomes high, this assumption of a linear potential drop in the inner region is no longer valid and equation 20 must be modified.) In dilute solutions, from equations 19 and 20:

$$m_i = 2r.m_{o_i}\exp\left(\{-H_i - \lambda e\psi\}/kT\right) \quad \ldots\ldots 21$$

According to this formula, the amount of adsorption increases rapidly with increasing anodic polarisation. Grahame and Parsons (14) have developed the theory of the inner region further, in the presence of specific adsorption, assuming a similar linear fall in potential. Their model, however, is only strictly correct when the field caused by the adsorbed ions does not penetrate into the diffuse region.

The present work is mainly concerned with the double layer in the absence of specific adsorption of anions and further discussion of this will not therefore be made.

(ii) Formation of adions by an electric field.

A sharp rise in electrode capacitance at anodic potentials is noted in almost all systems studied, even although they contain no specifically adsorbed anions. While suggestions have been made that the rise in aqueous solutions is caused by specific adsorption of hydroxyl ions, the existence of a similar rise in almost completely unionised solvents such as methanol and ethanol make this explanation unlikely. Austin and Parsons (15) have studied aqueous fluoride systems at various values of pH and their results also indicate that this theory is erroneous.

The idea of a liquid metal surface with adatoms of the same metal on it was postulated by Watts-Tobin (13). It is difficult to conceive of a planar surface of atomic dimensions: the thermal energy of the mercury atoms must result in their fluctuation about a mean plane. If there is an energy barrier to cross in pulling an adatom out of the surface, this might be reduced if the adatom was charged in the opposite sense to the ions in the double layer. While the charge on an adatom and the distance of the "adatom I.H.P." are unknown, the resulting dipole moment μ' will cause a voltage drop of $\frac{4\pi\mu'}{D_1 D_0}$ per adatom, i.e. a total voltage drop of $\frac{4\pi p\mu'}{D_1 D_0}$, where p is the number of adatoms. As in the case of specific adsorption of anions

$$p = y \exp(-w''/kT) \quad \ldots\ldots\ldots\ldots 22$$

where $$w'' = H_2 + \gamma\mu'/(\beta+\gamma) \quad \ldots\ldots\ldots\ldots 23$$

H_2 is the difference between the free energy of a mercury ion in the surface of the metal and as an adion, while y is the ratio of

adatom sites to surface sites. Here again a constant field is assumed in the inner region.

Gerischer has also suggested that if adatoms and adsorbed anions were present simultaneously, they would cluster round each other to form complexes which would contribute more to the potential drop than would the adsorbed anions or adions separately.

From energetic considerations it is unlikely that a significant quantity of negative adions would be present on cathodic polarisation. This is supported by the fact that the cathodic rise of differential capacitance is almost completely independent of temperature (16)

(iii) The dielectric properties of the solvent in an electric field.

Solvent molecules in the interface behave differently from those in bulk because of their proximity to the mercury surface and since they may be subjected to very large fields. Kirkwood (17) developed a theory expressing the dielectric constant for highly associated polar liquids in which it was explained that the high value of the constant for the latter is due to the fact that the effect of a group of associated dipoles in opposing a field is greater than that of the individual dipoles. Near the interface, however, the electric field is often so high that the orientation polarisation of the solvent is almost completely saturated, and the dielectric constant falls to a very low value. Only the solvent molecules which lie between the mercury surface and the O.H.P., have moments which contribute

to the capacitance. For if a solvent molecule on the solution side of the O.H.P. had any average moment, ions would move up to screen out the field.

Consider the inner region of the double layer in the absence of specific adsorption and under a small cathodic polarisation. The solvent in the cation hydration sheaths is dielectrically saturated, but the solvent is little affected by ions in the area between them. The dielectric constant of this part of the solvent is affected only by the constant field across the inner region. Lines of force travelling normal to the interface until they terminate on an ion in solution orientate the solvent dipoles, and a "chain" of dipoles may be considered to run from the metal to a plane, P, past which the field is of negligible magnitude and the solvent dielectric constant has its normal bulk value. If a molecule of solvent has a resultant dipole moment μ'' parallel or antiparallel to the field F and if a normal to the metal and P cuts s solvent molecules between them, then the dipole moment of the chain is $\pm s.\mu''$ F is approximately $\frac{\psi}{s.d}$, where d is the diameter of a solvent molecule and hence the interaction energy of the dipole chain with the field is

$$- Fs.\mu'' = \mp \mu''\psi / d \qquad \ldots\ldots\ldots\ldots\ldots\ldots\ldots\ldots 24.$$

Let L and M be the numbers of the dipole chains parallel and anti-parallel to the field respectively, and let C and D be the adsorption energies of a solvent molecule bonded to the mercury in directions corresponding respectively to parallel and anti-parallel

chains. From equation 24 the energies of the two types of chain are

$$A = C - \mu''\psi / d \qquad \ldots\ldots 25$$

and $$B = D + \mu''\psi / d \qquad \ldots\ldots 26$$

If N is the number of solvent molecules per unit area of the interface, then

$$N = L + M \qquad \ldots\ldots 27$$

and, taking the chains to be independent of one another, by Boltzmann's law

$$L/M = \exp\left(- \{A-B\} / kT \right) \qquad \ldots\ldots 28$$

The contribution of the solvent molecules to the potential is

$$\frac{-4\pi(L-M)\mu''}{D_1 D_0} = \frac{4\pi N \mu''}{D_1 D_0} \tanh\left(\{A-B\} / 2kT \right)$$

$$= \frac{-4\pi N \mu''}{D_1 D_0} \tanh \frac{\mu''}{d\,kT}\left[\psi - \frac{d(C-D)}{2\mu''}\right] \qquad \ldots\ldots 29$$

Since no specific adsorption is taking place, a charge η on the metal balances an equal and opposite charge, actually in the diffuse region, but here assumed to be on the O.H.P. Hence

$$\psi = \frac{4\pi\eta(\beta+\gamma)}{D_1 D_0} - \frac{4\pi\mu''}{D_1 D_0} \tanh \frac{\mu''}{d\,kT}(\psi - V) \qquad \ldots\ldots 30$$

where $V = d(C-D) / 2\mu$

From equation 30,

$$\eta = \frac{D_1 D_0 \psi}{4\pi(\beta+\gamma)} + \frac{N\mu''}{(\beta+\gamma)} \tanh \frac{\mu''}{d\,kT}(\psi - V) \qquad \ldots\ldots 31$$

Differentiating equation 31 with respect to ψ gives the differential capacitance of the inner region, C_i :

$$C_i = \frac{d\eta}{d\psi} = \frac{D_1 D_0}{4\pi(\beta+\gamma)} + \frac{N(\mu'')^2}{d(\beta+\gamma)kT} \operatorname{sech}^2 \frac{\mu''}{d\,kT}(\psi - V) \qquad \ldots\ldots 32$$

The second term in equation 32 gives the contribution to the capacitance of the solvent dipoles, provided that two assumptions

are correct:

(a) there is a linear potential drop across the inner region

(b) D is constant.

Since $\operatorname{sech}\phi$ increases as ϕ decreases, it is seen that this contribution is a maximum when $\psi = V$. Thus only if the adsorption energy of a solvent molecule bonded with the positive end of the dipole towards the metal was equal to that with negative end towards the metal, would this maximum occur at the position of least applied field, i e at the potential of the electrocapillary maximum.

Mott and Watts-Tobin point out (9) that in the presence of specific adsorption of anions, the field vanishes when

$$N_i \beta = N_o (\beta + \gamma) \qquad \ldots\ldots\ldots\ldots\ldots\ldots 33$$

where N_o and N_i are respectively the number of cations at the O H P and of absorbed anions. Since $q = -(N_i - N_o)e = -N_o \gamma e / \beta$ a positive quantity, the maximum value of the solvent contribution must occur on the anodic side of the electro-capillary maximum potential when $V = 0$.

Two points may be made from inspection of equation 32. Firstly the "hump" in capacitance/charge curves noted with aqueous solutions, and its behaviour at different temperatures can be explained (13). Secondly the capacitance due to the dipoles of a polar solvent is seen to decrease rapidly with increasing field strength.

It has recently been suggested (18) that in aqueous systems, the dielectric constant of the solvent may increase to a high value in the second monolayer next to the metal due to the structure of water

enabling molecules in this layer to be comparatively free to rotate. Thus if P lies between the metal and the O.H P., the field will not extend to the latter. The capacitance of the inner region in this case must depend only on the region from the metal to P, since the solution side of P behaves almost as a conductor. While this concept explains the relative constancy of the capacitance for different cations, since solvent between the metal and P is almost completely orientation polarised, it is possible to derive a low enough capacitance to correspond to the minimum aqueous value of approximately 16 μF / sq cm. For a parallel plate capacitor:

$$C_i = D_1 D_0 A / 4\pi d \qquad \ldots\ldots\ldots\ldots\ldots\ldots\ldots\ldots 1$$

Taking A = 1 sq cm, and $D_1 = 4$, if d, here the distance between the interface and P, is 2.2 Å then

$$C_i = \frac{4 \times 1.11 \times 10^{-12} \times 1 \times 10^{6}}{4 \times 3.141 \times 2.2 \times 10^{-8}} \ \mu F / \text{sq cm}$$

$$= 16.05 \ \mu F / \text{sq cm}$$

(iv) Compression of inner region by an electric field.

A high electric field strength would cause compression of the inner region. The thickness of the layer under cathodic polarisation is approximately equal to the sum of the ionic radius of the cation plus the diameter of one or more solvent molecules. If the force between the cation and the electrode is increased, the solvent molecules between the two must be flattened and the shape of the cations may be distorted.

Macdonald (19) considered that the compression might be linear for relatively small pressures with a gradual transition to a much smaller dependence on pressure for larger values. For P, the pressure across the double layer, having a small value

$$d / d_o = (1 + 8\pi P\alpha)^{-1} \quad \ldots\ldots\ldots\ldots\ldots\ldots 34$$

where α is a constant and d_o is the distance of the O.H.P. from the metal at zero field strength Macdonald concludes that

$$P = D_1 D_o F^2 / 8\pi \quad \ldots\ldots\ldots\ldots\ldots\ldots 35$$

where F is the field strength, approximately equal to ψ / d Thus

$$d = d_o(1 + \frac{\alpha D_1 D_o \psi^2}{d^2})^{-1}$$

$$\simeq d_o(1 + \frac{\alpha D_1 D_o \psi^2}{d_o^2})^{-1} \quad \ldots\ldots\ldots\ldots\ldots\ldots 36$$

Equation 36 is not simple, however, since ψ and hence the field strength is affected by dielectric saturation In previous discussion D_1 has been assumed to have a constant value of 2 - 4 corresponding to the dielectric constant of the solvent when completely orientation polarised and the contribution of the dipoles to the potential and hence to the field has been calculated This procedure would be required here since ψ and F in equations 36 and 35 should in fact be the <u>resultant</u> potential and field respectively Substitution of a form of equation 36 into equation 30 results in a very complex expression for C_i Macdonald, after Grahame (10), assumes ψ to be the <u>applied</u> potential and replaces D_1 by an empirically calculated value of total dielectric constant (including orientation effects) corresponding to a given field.

The following important deduction can be made from either treatment of the theory. If the rate of increase of compression of the inner region at any given field strength is great, the capacitance is expected to rise with increasing applied potential. If, however, the dielectric orientation saturation is not complete, the capacitance will tend to fall with increasing applied potential as solvent in the interface becomes more and more orientation polarised. Thus the capacitance minimum in aqueous solutions is explicable in terms of a fall caused by dielectric polarisation in the inner region, which is balanced out and then superseded by a rise due to the compression of the inner region. Macdonald has noted that the sharp cathodic rise observed by Grahame (20) for methanol solution is presumably due to the higher compressibility of the methanolic layer compared with the aqueous system. It is possible, however, that in methanolic solutions the solvent approaches complete orientation polarisation at much lower field strength than for water, and hence the compressional cathodic capacitance rise is unimpeded by further solvent polarisation.

§ 3. THE ELECTRIC FIELD IN THE METAL

In 1928, Rice (21) postulated a model of the double layer in which he suggested that a field would penetrate into a metal to produce a diffuse layer of electrons, which would result in a capacitance of not more than 16μF/ sq.cm. in series with any solution capacitance. Taking mercury as a medium of mercuric ions with two free electrons per atom, he showed that the field would penetrate to approximately 0.5 Å. The small capacitance of this region was explained by its having a low dielectric constant, as suggested by Pauling (22).

While Grahame (7) stated that there would be no potential drop in the metal, Mott and Watts-Tobin (9) supported Rice's view. They pointed out, however, that the field does not rise sharply at the interface and that hence the only effect of the penetration is to add approximately 0.5 Å. to the inner region.

The remainder of this thesis is divided into three sections. The first describes the construction and development of an electronic system for the accurate measurement of the impedance of a dropping mercury electrode; in the second a study is made of the mode of growth of a mercury drop in aqueous potassium chloride solutions, establishing an accurate relationship between drop are and time of growth. These two sections enable a highly reproduceable measurement of double layer capacitance to be made.

In the final section, measurement of the differential capacitance of the double layer in solutions of alkali metal chlorides in formamide are described. The results of this work are discussed and interpreted in terms of general double layer theory.

PART 1

APPARATUS AND EXPERIMENTAL PROCEDURE

The three most accessible parameters of the electrical double layer are the interfacial tension, the charge and the capacitance at the interface. Much of the earliest data on the mercury/solution interface was collected by Lipmann (23) who measured interfacial tension with a capillary electrometer. In this instrument, contact is made between mercury and solution in a narrow glass capillary. Variation of the potential difference between the mercury and the solution alters the interfacial tension and hence the position of the mercury meniscus. The change in height of the mercury reservoir required to restore the meniscus to its original position is a measure of the change in interfacial tension. The classical research of Gouy (24, 25) was carried out using such an arrangement, as was the more recent work of Parsons and Devanathan (26, 27). The drop weight method for determining surface tension has been used at various times since 1935 (28, 29). A rigorous theoretical relationship between drop weight and interfacial tension has been developed by Smith (30). While inconsistent results are sometimes obtained because of solution creep within the capillary of the dropping mercury electrode, the method is particularly suitable for non-aqueous solvents which do not wet glass sufficiently for them to be used with the capillary electrometer. Accurate data on interfacial tension have also been derived from measurements of the dimensions of sessile mercury drops (31). While the above methods are applicable primarily to mercury, gallium, amalgam and melt systems, techniques have also been developed for the measurement of interfacial

tension at a solid metal surface. Frumkin (32) devised a method based on the variation of the angle of contact of a gas bubble and a metal electrode with the polarisation of the latter.

There are several methods of estimating the charge of the electrical double layer. For an electrode of constant area, the amount of electricity required to change the potential by a given amount is measured. Provided that the electrode is perfectly polarised, current flow is restricted to the charging of the double layer. Measurement techniques using either high current density (33) or low density "equilibrium" charging (34) have been used.

If a charging curve is obtained at constant current, the capacitance of the double layer can be evaluated from the slope of the linear portion (35), since

$$C_o = \frac{dq}{dE} = \frac{dq}{dt} \cdot \frac{dt}{dE}$$

$$= i \cdot \frac{dt}{dE} \quad \ldots\ldots\ldots\ldots\ldots\ldots\ldots\ldots\ldots\ldots 37$$

where i is the constant current flowing. Using equivalent circuit analogues of electrode impedances, McMillan and Hackerman (36) compared their charging and discharging curves with those of test electrodes and were thus able to measure capacitances which were too large for easy measurment with conventional a. c. bridges.

For a dropping mercury electrode (hereafter D.M.E.), if the rate of formation of the new interface is known, the magnitude of the charge density can be determined directly from the current flowing to maintain the electrode at a constant potential with

respect to the solution. At the potential of the electrocapillary maximum, this current is zero. Philpot (37), Frumkin (38) and others allowed mercury to drop through an electrolytic solution into a mercury pool and measured the current flowing between the latter and the D.M.E. reservoir. If the area of the drops was known, the charge per unit area could be calculated.

Loveland and Elving (39) devised an electronic circuit for the direct display of differential capacitance/potential curves on a cathode-ray oscilloscope. For a linear variation of applied potential with time, $dE / dt = K$, for K a constant.

Thus $C_o' = dq / dE = \{1 / K.\}\{dq / dt\} = 1 / K. i$ ...38

for C_o' the total electrode capacitance.

Capacitance per unit area is thus

$C_o = i / K.A$ where A is the area of the electrode at the time of measurement. In this instance, a display of charging currents against time is equivalent to a graph of differential capacitance against applied potential.

Using a high input impedance amplifier and an oscillograph, Proskurnin and Frumkin (40) measured the voltage produced across a test cell by a known alternating current. On the assumption that the impedance of the test cell was solely due to the capacitance of the test electrode, this quantity, being inversely proportional to the output voltage, could be measured. Randles (41) improved on this idea by making a phase sensitive instrument which gave data about both the resistive and reactive parts of the impedance.

The most accurate method of determining the differential capacitance of an electrode is the direct measurment of impedance using an a.c. bridge network. The first such measurement was made by Wien in 1896 (42). The electrode impedance was determined with a Wheatstone bridge, the capacitance being balanced off with a variable inductance in series with the cell. The a.c. bridge method employs a cell containing the test electrode together with an auxiliary electrode of such large area that its impedance may be neglected in comparison with that of the test electrode. The solution resistance is subtracted vectorially from the total cell impedance to give the test electrode impedance. Many authors have included the double layer impedance in a Wheatstone bridge network (15,43,44,45,46). In the classical work of D.C. Grahame the equivalent circuit used to balance the cell impedance was a series combination of resistance and capacitance.

The conventional Wheatstone networks suffer from a number of disadvantages, the most important being that the accuracy is entirely dependent on a large number of impedance standards and that some form of Wagner earthing is necessary for precise bridge balancing. It is also very difficult to measure large capacitances on a conventional bridge (36). Nancollas and Vincent (47) showed that the transformer bridge, on the other hand, is much more suitable. Only one resistive and one reactive standard are involved, no special earthing is required and the impedance of the test leads can easily be eliminated.

THE TRANSFORMER RATIO-ARM BRIDGE

The basic circuit of the transformer ratio-arm bridge (48) (henceforth referred to as "T.R.A. bridge") is shown in figure 1 and, in simplified form, below:

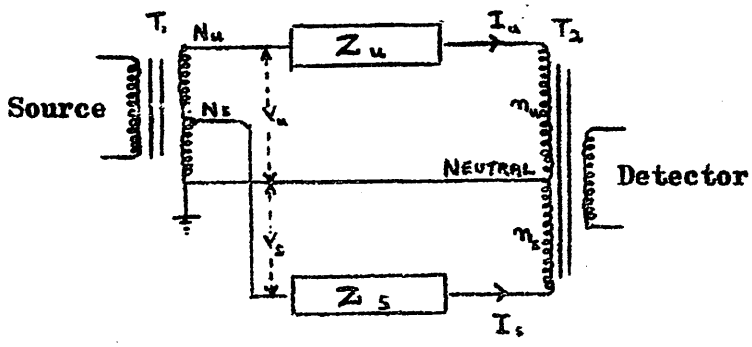

Let z_u and z_s be the unknown and standard impedances respectively. T_1 is a voltage transformer, to the primary of which the source of a.c. is connected. The secondary winding is tapped to give N_u and N_S turns. T_2 is a current transformer whose primary is tapped at n_u and n_s turns, the secondary coil being connected to the detector.

Assuming that the transformers are ideal, if impedance z_s is adjusted to give a null indication on the detector, zero flux is produced in the current transformer and there is therefore no voltage-drop across its windings. The detector sides of both the unknown (z_u) and standard (z_S) impedances are therefore at neutral potential.

If the voltages across z_u and z_s are V_u and V_s respectively then the currents through them are given by

$$I_u = V_u/z_u \quad ; \quad I_s = V_s/z_s$$

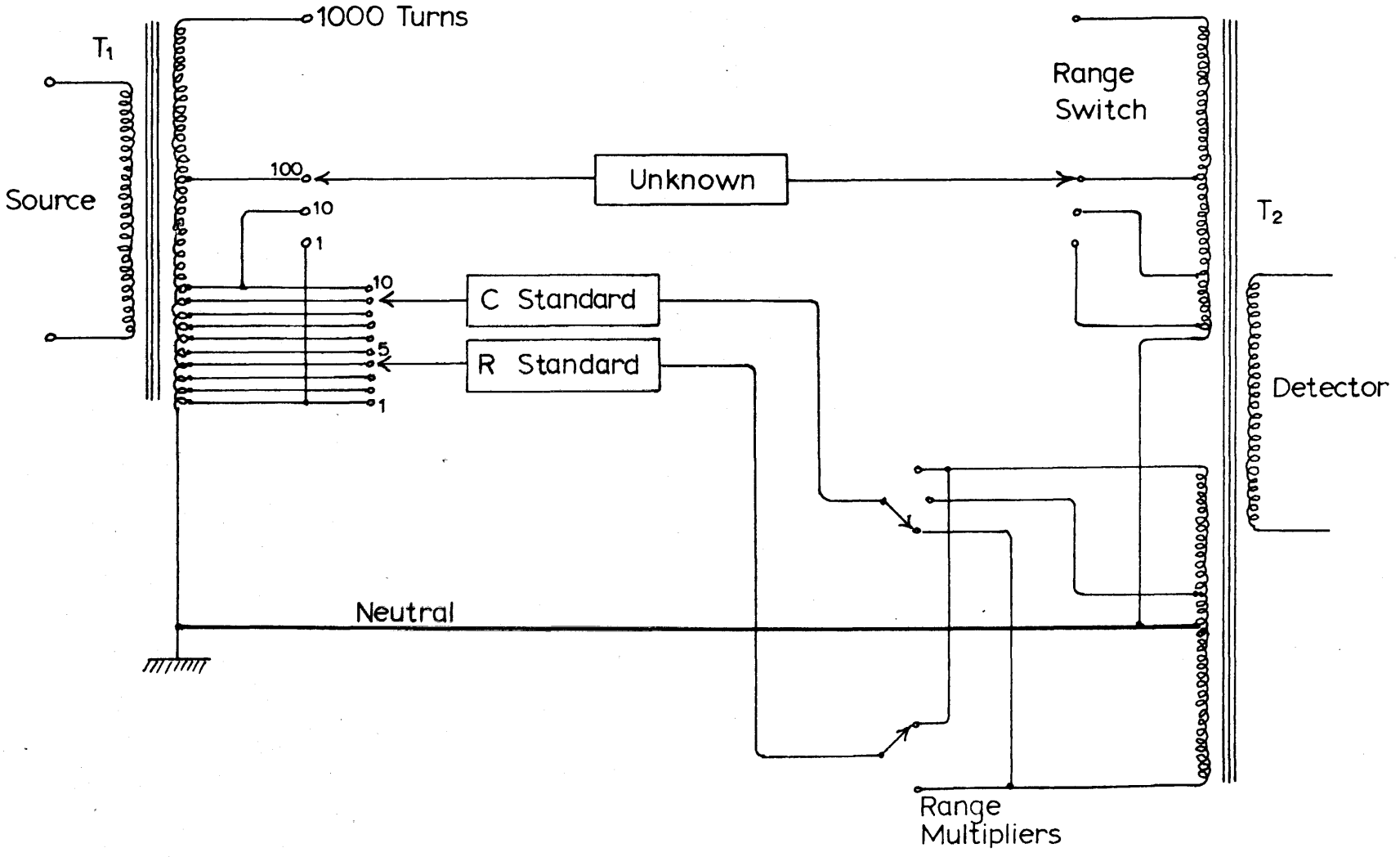

FIG. 1 TRANSFORMER BRIDGE

Now for zero core flux in T_2, the algebraic sum of the ampere turns must be zero:

$$\text{i.e.} \quad I_u . n_u = I_s . n_s$$

$$\text{or} \quad (V_u/z_u) n_u = (V_s/z_s) . n_s$$

$$\text{and hence} \quad z_u = (V_u/V_s) . (n_u/n_s) . z_s$$

For an ideal transformer, the voltage ratio is equal to the turns ratio, and therefore

$$z_u = \frac{N_u . n_u}{N_s . n_s} . z_s \quad \ldots\ldots\ldots 40$$

Thus with suitable tappings on the two transformers, a wide range of measurements can be carried out. Although transformers are not ideal in practice, transmission losses merely reduce the sensitivity. Provided that the coils are precision wound, and that their effective self-resistance is small compared with that of z_u or z_s, all the turns embrace the same flux and hence the ratio of induced voltages is accurately equal to the turns ratio.

Standard impedances are divided into resistive and reactive components. At balance, it is necessary for both the "in phase" and "quadrature" ampere turns to sum algebraically to zero, and thus the resistive and reactive standards must be capable of being connected to different tappings to balance out the currents of the unknown impedance (figure 1). The independance of components is useful in that impurities in the standards can be balanced out by compensating trimmers in the unknown side of the bridge. Thus an impure capacitor is equivalent to a pure capacitance shunted by a resistance. The effect of the latter can be cancelled by feeding a

current, equal to that produced by the resistance impurity, through a fixed trimming resistor into the opposite side of the transformer.

In the Wayne Kerr, B221 Universal Bridge, used in the present work, transformer tappings are arranged to give two decades, each requiring one resistive and one reactive standard. With a T.R.A. bridge it is possible to add continuously variable controls without detracting from the accuracy of the decade standards. A continuously variable reactance is provided by an air-dielectric capacitor whose residual capacitance is balanced by a pre-set trimmer connected to a transformer winding of opposite sense:-

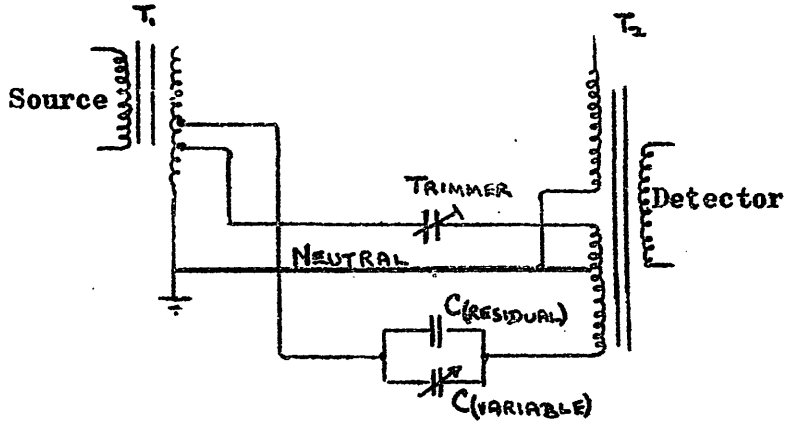

A continuously variable conductance is obtained by connecting a linear potential divider across a few turns of T_1 to produce a variable voltage across a close-tolerance resistor:-

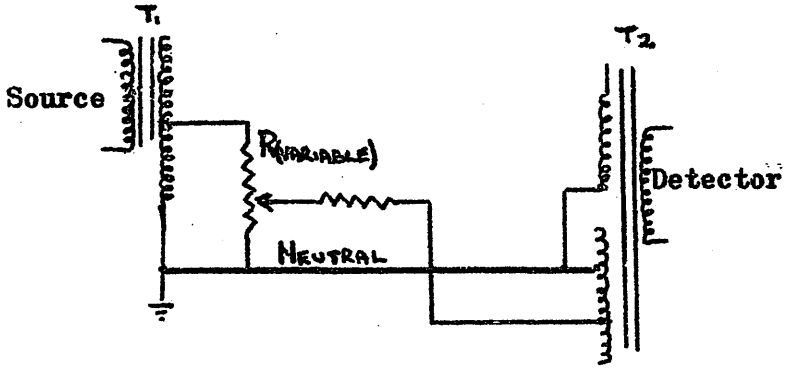

While the voltage transformer is tapped to provide the decade adjustment of each standard, the current transformer is tapped to allow the relative ranges of resistive and reactive standards to be altered; by connecting the unknown to different tappings on both voltage and current transformers, the range of the bridge can be extended above and below that of the standards (figure 1). It may be noted that although one resistive and one reactive standard is required per decade, the transformer ratio may be used to set those in one decade against those in another, so that only one resistive and one reactive fixed standards of known accuracy are required. Finally, in a similar method to that whereby the standards are purified, compensation can be made for any impedance in the external test leads. An excellent feature of the Wayne Kerr bridge is the "set zero" controls which enable small external impedances in series with the unknown to be trimmed out.

Because the T.R.A. bridge sums currents, it can only measure impedance as a parallel combination of in-phase and quadrature components. Grahame (49) has proposed however, that the equivalent circuit of the double layer at a polarised D.M.E. is best represented by a resistance and capacitance in series. (With such an analogue circuit the measured double layer capacitance was, within experimental error, independent of bridge a.c. frequency between 240 c.p.s. and 5000 c.p.s.)

It is possible to derive an expression relating series and parallel networks:

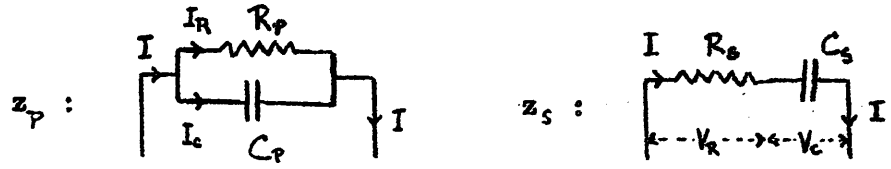

(i) (ii)

Impedance as parallel network Impedance as series network

Let the a.c. frequency be $\omega / 2\pi$

Then for (i) :-

$$1/z_p = 1/R_p + j\omega C_p$$

$$\therefore z_p = \frac{R_p}{1 + j\omega C_p R_p}$$

$$= \frac{R_p(1 - j\omega C_p R_p)}{1 + \omega^2 C_p^2 R_p^2}$$

$$= \frac{R_p}{1 + \omega^2 C_p^2 R_p^2} - j\frac{\omega C_p R_p^2}{1 + \omega^2 C_p^2 R_p^2} \quad \ldots\ldots\ldots\ldots\ldots 41$$

Also for (ii) :-

$$z_s = R_s + 1/j\omega C_s$$

$$= R_s - j/\omega C_s \quad \ldots\ldots\ldots\ldots\ldots 42$$

Then since $z_s \equiv z_p$

$$R_s = \frac{R_p}{1 + \omega^2 C_p^2 R_p^2} \quad \text{and} \quad C_s = \frac{1 + \omega^2 C_p^2 R_p^2}{\omega^2 C_p R_p^2}$$

Now if $Q = \omega R_p C_p$, then

$$R_s = R_p(1 + Q^2)^{-1} \quad \text{and} \quad C_s = C_p(1 + 1/Q^2).$$

In a similar manner, other transforms may be derived for different equivalent circuit analogues.

APPLICATION OF AN A.C. BRIDGE TO A DROPPING MERCURY ELECTRODE

A dropping mercury electrode consists essentially of a vertical glass capillary tube from which mercury, supplied from a reservoir under a pressure of about 30 cm. Hg, issues dropwise. A D.M.E. used as test electrode, has the great advantage over other electrodes, that its surface is being continually renewed, and it is therefore relatively simple to obtain and maintain a pure, reproducible surface. Two serious disadvantages of the D.M.E. are that a more elaborate electrical arrangement is necessary to detect bridge balance with an electrode whose impedance varies with time, and that a method must be sought for the determination of drop dimensions at the point of bridge balance. The latter are related to the time interval between drop birth at the capillary orifice and the instant of balance. Although this interval may be measured manually using a stop-watch, the sensitivity of the impedance bridge is such that a much more accurate determination is required. A number of methods have been described which incorporate a cathode-ray oscilloscope as balance detector. Grahame (44) impressed accurately timed pulses on the time base and thus indirectly measured the time of bridge balance by means of distance on the oscilloscope screen. A similar method was used by Parsons (15) who arranged that the bridge balanced at a fixed interval after the birth of a drop. The interval was measured by a crystal controlled electronic timer which emitted a pulse into a double beam cathode-ray oscilloscope. By displaying the

bridge output on the other beam, bridge balance could be made to coincide with the timer output pulse. Randles (46) used a tapping-off device to give drops of constant lifetime. The relative birth-balance interval, as compared to drop lifetime, was found by adjusting the time constant of a fixed capacitor in such a way that its discharge time could equal either the former or the latter. Here again, however, visual detection of balance was involved. Such procedures have inherent disadvantages in use, and the possible accuracies of systems employing visual indication of balance are severely limited. In the present work electronic circuits were developed which permitted the direct measurement of the birth-balance interval.

SELF-TIMING BRIDGE METHOD FOR DETERMINATION OF IMPEDANCE OF D.M.E.

A block diagram is given in figure 2 illustrating the arrangement of circuit components used in the present work to measure differential capacitance of the electrical double layer. A d.c. polarising voltage was applied between the D.M.E., A, and a reference electrode, C. A large blocking capacitor prevented d.c. from entering the T.R.A. bridge which was connected to the D.M.E. and a platinum net sphere electrode of large area which acted as anode. The T.R.A. bridge was used in conjunction with a variable frequency audio frequency generator, an amplifier and a "balance detector", a device which emitted a pulse whenever the bridge was balanced. Another unit, the "birth detector" gave out a pulse at the birth of each mercury drop. The pulses were fed to an "interval timer" which accurately measured the period of time between them.

INTERVAL TIMER.

The Ericsson interval timer, type 103 C, was essentially a device for counting the number of cycles of a known reference frequency occuring during the time interval being measured. Since the design of the circuit was such that an error of not more than ±one cycle could occur during the counting process, the accuracy of the instrument was determined by the accuracy of the reference frequency. This was provided by a 100 Kc./sec. crystal oscillator with an error of less than 0.005%, so that a time interval of one second could be measured

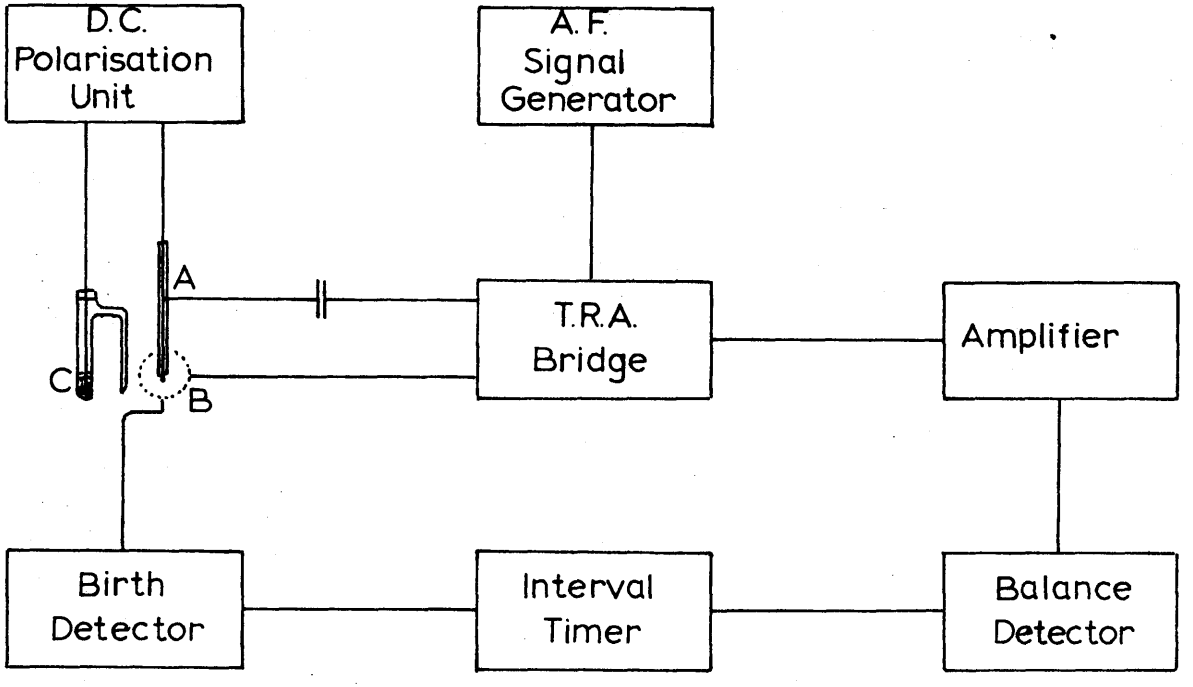

FIG. 2 BLOCK DIAGRAM

to within approximately 0.1 milliseconds. The start and stop electronic switches were Eccles-Jordan trigger circuits which were activated by positive or negative pulses of minimum amplitude 10 volts, and minimum mean duration 20 μ-seconds.

BALANCE DETECTION

The capacitance of a sphere can be expressed in terms of its radius, and it is shown below that for two concentric spheres of almost equal radii, the capacitance is directly proportional to the surface area. Let two hollow evacuated spheres of radii r_1 and r_2 be arranged concentrically and let a charge $+q$ be placed on the inner sphere, and $-q$ on the outer. The potential of the inner sphere by itself would be $V_1 = q/r_1$ and that of the outer sphere $V_2 = -q/r_2$. But the latter is also the potential of all points within the outer sphere. Hence the total potential of the inner sphere is

$$V = V_1 + V_2 = \frac{q(r_2 - r_1)}{r_1 r_2} = \frac{q\,d}{r_1 r_2} \quad \ldots\ldots\ldots 43$$

Where d is the distance between the spheres. Thus since $V = q/C$, $C = r_1 r_2/d \doteq r^2/d = K.A$, if $r_1 \doteq r_2 \doteq r$.

Here A is the area of a sphere of radius r, and K is a constant. This result, showing that the capacitance is proportional to the area, would also hold if the space between the spheres was filled with a medium whose dielectric constant was uniform or varied in an identiaal manner along any radius.

If the thickness of a spherical shell of material is small compared with the radius, the resistance across the shell is

$$R_o = \sigma \cdot \delta r / \pi r^2 \quad \ldots\ldots\ldots\ldots\ldots\ldots 44$$

where σ is a constant and δr is the thickness of the shell. Thus the resistance between two spheres of radius r_1 and r_2 is

$$R = \frac{\sigma}{\pi} \int_{r_1}^{r_2} \frac{dr}{r^2} = \frac{\sigma}{\pi} \left(\frac{1}{r_1} - \frac{1}{r_2} \right) \quad \ldots\ldots 45$$

If r_2 is very large compared with r_1, it is seen that the resistance is proportional to the radius of the smaller sphere.

Since during the life of a mercury drop its radius increases as a characteristic function of time, the capacitative component of the double layer impedance increases, while the resistive part decreases as monotonic functions of time. Thus as is shown in figure 3, any given balance point can occur at one and only one instant during the life of a drop, while at any one instant the impedance of the double layer has a unique value.

The bridge source frequency was provided by an Advance, model H 1, variable frequency audio signal generator whose output was controlled so that not more than 10 mV were impressed across the unknown. When the T.R.A. bridge was out of balance a sinusoidal waveform was emitted from the detector, the secondary winding of T_2 (figure 1). As the bridge was brought into balance, the amplitude of this signal decreased from approximately 0.5 volts to a "null" of about 5 μ-volts. Because of the time variation of the electrode impedance, the bridge gave out an amplitude modulated wave having minima at the instants at which the electrode impedance was closest

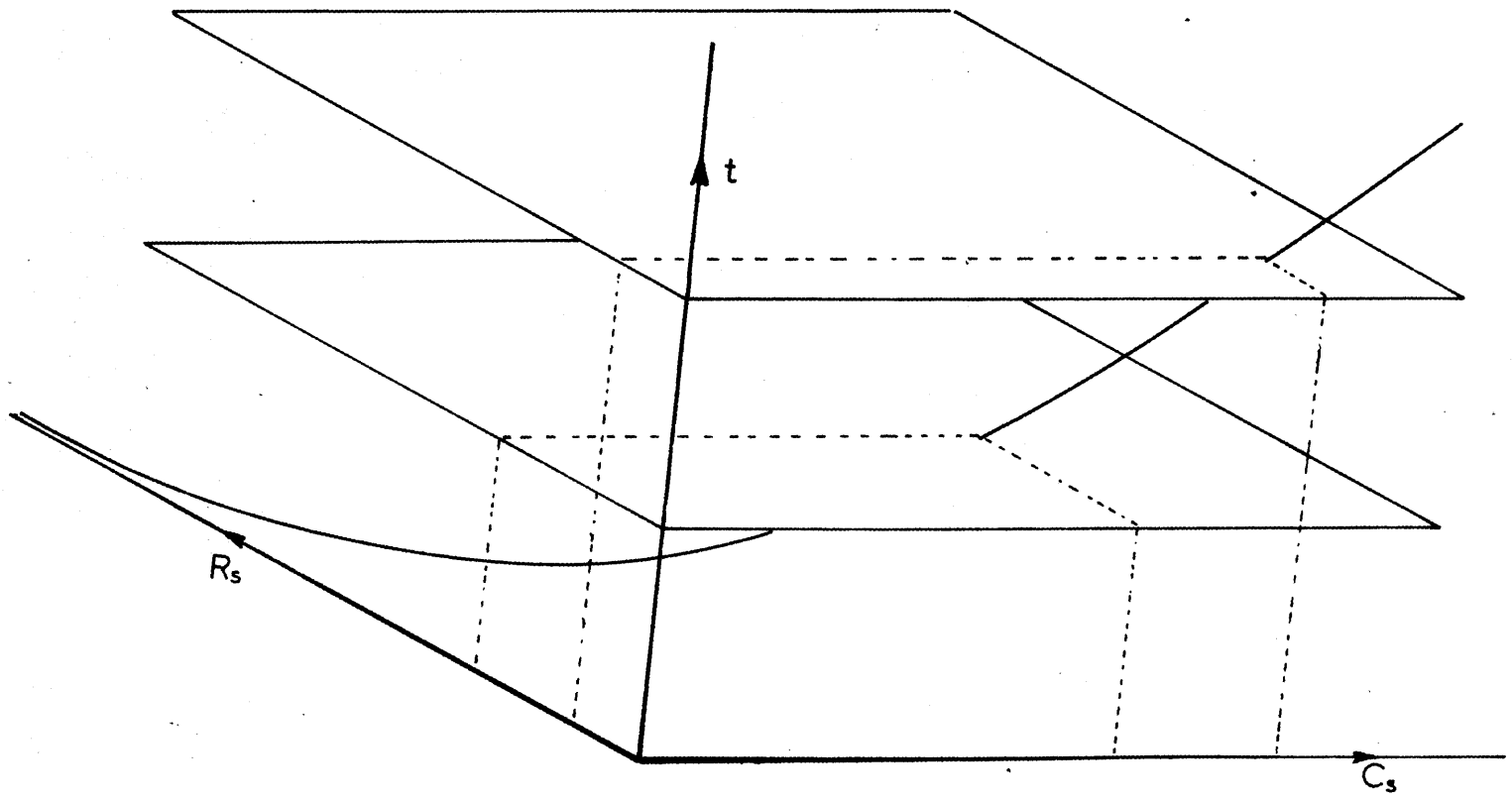

FIG. 3 VARIATION OF ELECTRODE IMPEDANCE WITH TIME

to that of the bridge standard impedance. If the bridge was exactly balanced, resistively and reactively, at a point during the life of a drop, the minimum had an amplitude value equal to that of the null signal.

It was originally intended to rectify the bridge output signal and to detect the a.c. minimum with a unit similar to the Hickling thyratron potentiometer (50), a device originally used to measure the amplitude of a transient. In this circuit the control grid of a thyratron was held just past the critical conducting potential by an applied voltage. The external signal was applied in series with the latter in such a manner as to oppose it and thus to stop the valve conducting. The potential divider controlling the applied voltage could be set so that the thyratron struck only at a predetermined minimum in the external signal voltage.

Two modifications to this scheme became immediately apparent. First, because of the relative insensitivity of the thyratron critical point, it was necessary to amplify the bridge output in such a way that any out-of-balance signal would retain the thyratron in a non-conducting condition. Second, a smoothing circuit was required between the rectifier and the thyratron to prevent the latter from firing in between the signal cycles (B in figure 4). This phenomenon was liable to occur at low values of signal frequency or even at quite high values before the original rectifier, a single crystal diode, had been replaced by a full-wave bridge rectifier of four diodes.

A Sullivan logarithmic amplifier was used at first. With a fixed external impedance of similar value to the cell impedance, it was found that the thyratron struck over a range of ±8% of the impedance around the correct balance point. When a Mullard "3-3 Audio Amplifier" was put in series with the Sullivan to act as a pre-amplifier, and with both amplifiers working at maximum gain the balance range was reduced to±0.4% of the impedance. The total gain of the combined amplifiers was approximately 10^6, and because of this, very adequate screening of leads and components was required as well as careful elimination of earth loops. To minimise 50 c. p. s. mains hum, a high-pass filter was incorporated in series with the amplifier output:

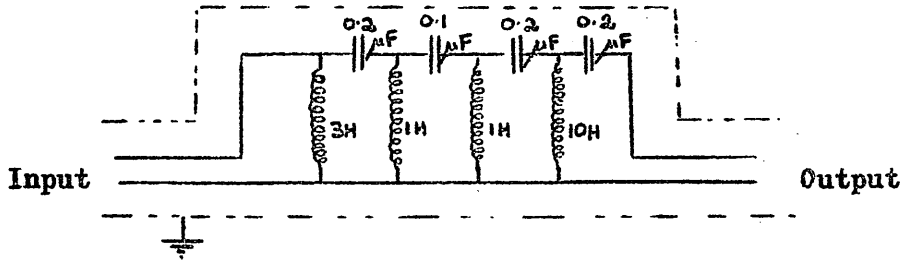

It was still difficult to obtain a "clean" balance signal, however, due to the presence of harmonics of the signal generator frequency which became apparent when the fundamental was suppressed.

An amplifier, which could be sharply tuned to the signal frequency and having a maximum overall gain of more than 10^7, was built by Elesco Electronics (Development) Ltd. This incorporated

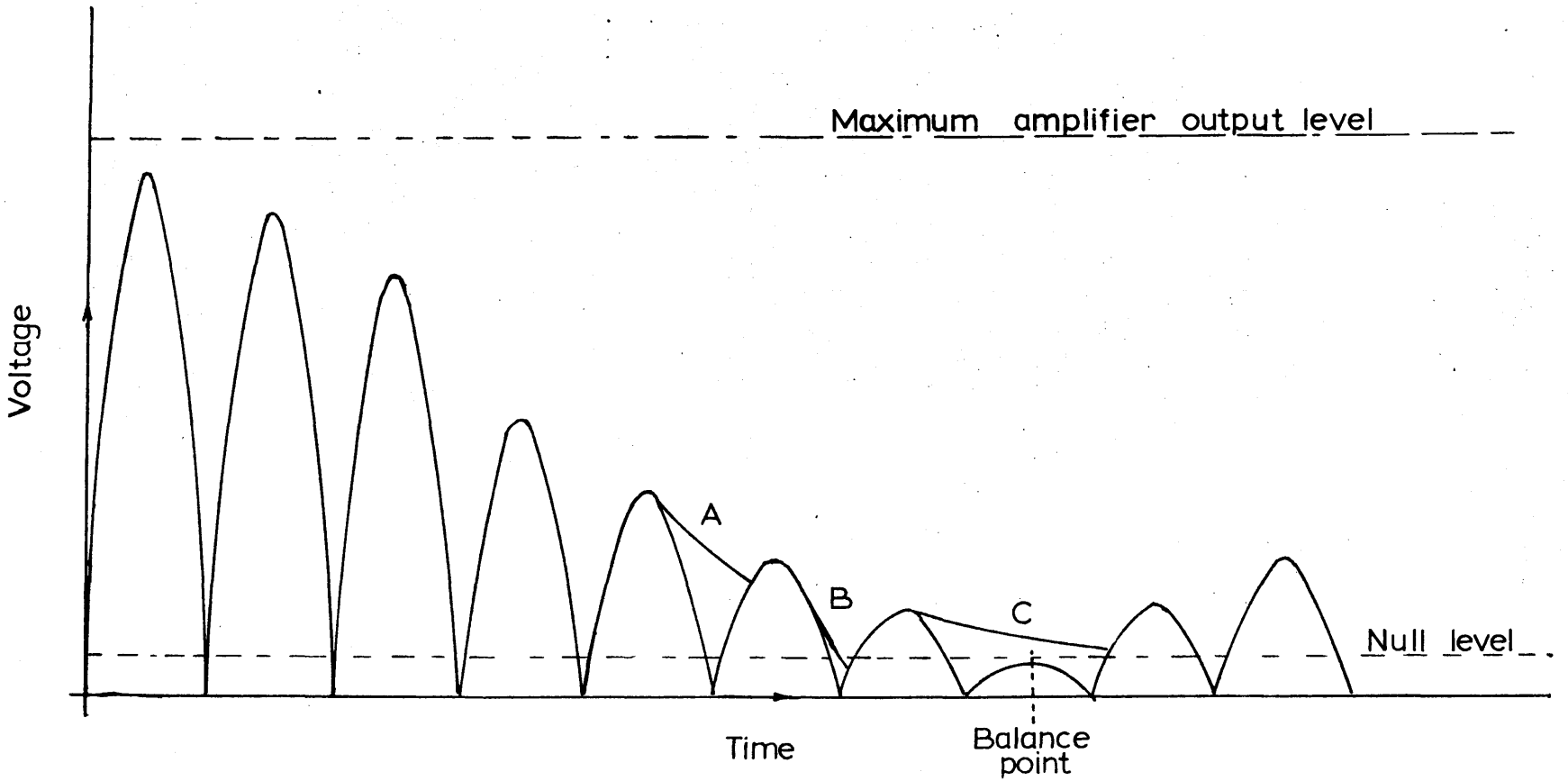

FIG. 4 RECTIFIED AMPLIFIER OUTPUT NEAR BRIDGE BALANCE

automatic gain control (A.G.C.), the threshold of which was made variable in order to facilitate coarse balancing of the bridge. When the A.G.C. was operative, a high bridge output biased the valves in such a manner that their gain was reduced, while with a lower bridge output, the attenuation was less. By withholding the A.G.C. bias until the signal had attained a certain level, the region around the balance point could be strongly amplified. The A.G.C. unit consisted of four variable-mu stages with two "straight" stages providing the feed-back. To make the amplifier highly frequency selective, the A.G.C. amplifier output was fed into a three stage amplifier, tuned to the measuring signal frequency by means of feed-back through bridged-T networks. A separate cathode follower input stage and head amplifier were connected by a short coaxial cable to the T_2 secondary of the T.R.A. bridge to ensure minimum loss of bridge output. The output from this unit was then fed into the A.G.C. amplifier. The amplifier was set up by use of an A.G.C. threshold level control, filter selector and tuners, and a feedback control. Two outputs were incorporated, consisting of a high level limited output, for use as trigger potential in the balance detector, and a low level output for monitoring purposes.

The final circuit of the balance detector is shown in figure 5. The out-of-balance voltage from the amplifier was fed to a full-wave diode bridge rectifier by way of a 1:1 balanced and screened transformer (Sullivian, 856) which eliminated any

d.c. level in the signal. The crystal diodes were G.E.C. type GEX 34 in the first version of the unit, and Mullard type OA 81 in the final form. The rectified signal was collected in one of four reservoir capacitors, C_1 - C_4, selected to have a suitable discharge time constant through VR_1. The discharge rate was chosen as in A (figure 4) so that it was not so great that the d.c. level fell to the null value between signal cycles (B in figure 4) giving a false indication of balance, nor so small that the real balance point was missed. (C in figure 4). The selection of the time constant using VR_1 and S_1 (figure 5) was governed by:

(i) the frequency of the bridge measuring signal, and

(ii) the rate of change of electrode impedance with time.

The d.c. signal was now applied in series with a backing potential provided by potential divider VR_2 connected across a 6 volt dry battery to the thyratron control grid. R_i was a grid stopper of 10 KΩ, the relatively small value having been chosen to sharpen the critical point of the valve. A characteristic of a thyratron is that once it has struck, the grid loses control and the discharge may be extinguished only by reduction of the anode voltage to below approximately 10 volts. This was accomplished by controlling the H.T. applied to the anode by an R-C combination of relatively long time constant (R_2-C_5 : 2.5 m.sec.). This part of the circuit was effectively that of a mono-stable multivibrator. The stable state occurred when the anode voltage was below the

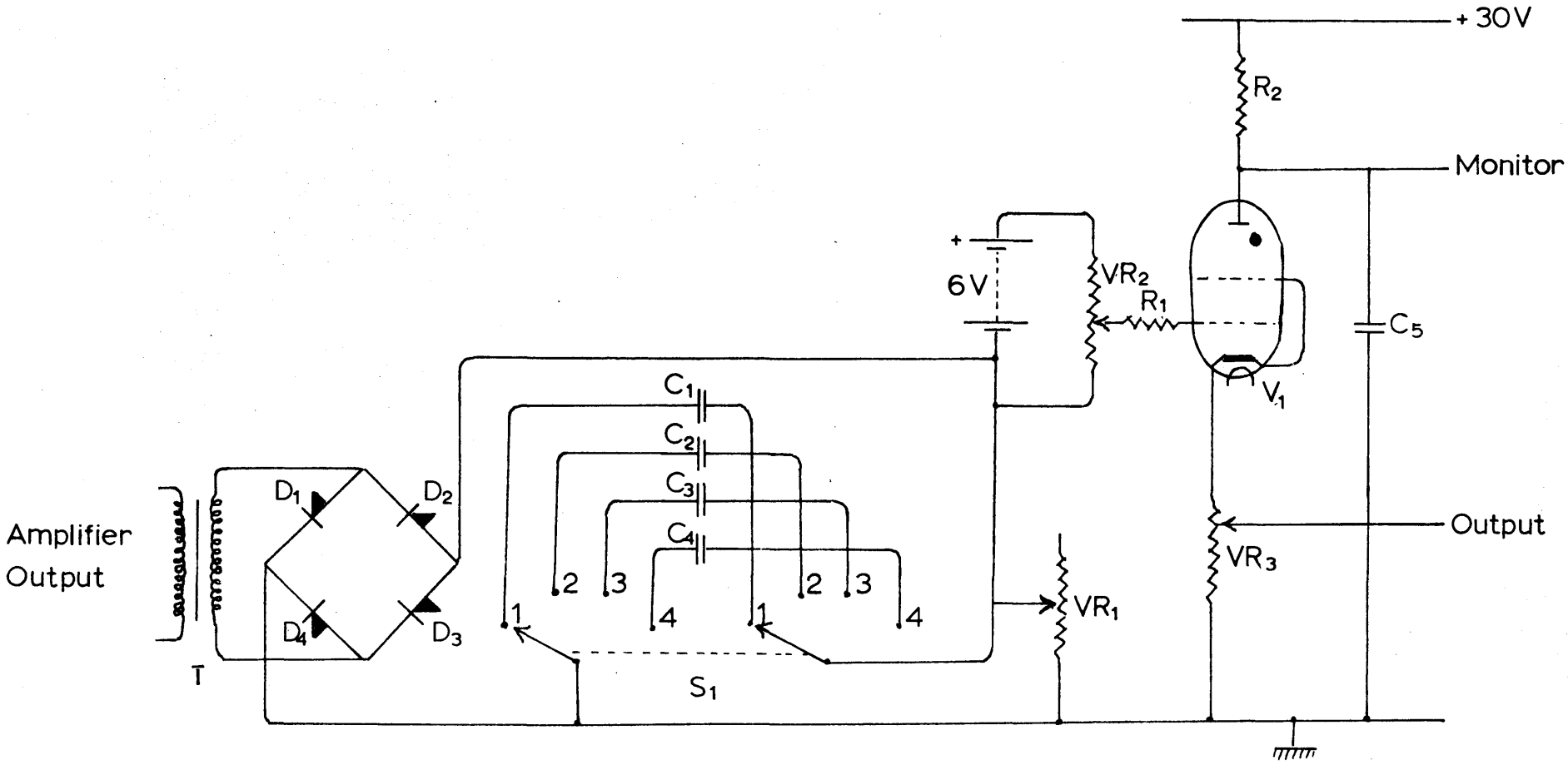

FIG. 5 BALANCE DETECTOR

Figure 5. BALANCE DETECTOR.

Components.

R_1	:	10 K Ω	C_1	:	700 pF
R_2	:	4.7 K Ω	C_2	:	0.002 μF
VR_1	:	152-506 K Ω	C_3	:	0.005 μF
VR_2	:	0-100 K Ω	C_4	:	0.01 μF
VR_3	:	0-100 Ω	C_5	:	0.5 μF

V_1 : CV 4018

D_1-D_4 : OA 81

T : 1:1 Sullivan (856)

striking value for the applied grid voltage and the capacitor C_5 was charged to H.T. voltage. When the grid potential was made more positive, the thyratron struck and rapidly discharged C_5 down to the thyratron maintenance voltage where the discharge was extinguished and the grid regained control. C_5 then recharged through R_2 to return the circuit to its stable condition. Since the discharge current was limited mainly by the small cathode resistor VR_3 of 100Ω, the time required to discharge C_5 was very short. Hence a sharp pulse could be obtained from VR_3 of suitable amplitude and duration to activate the stop gate of the interval timer. The thyratron used was a CV 4018 with the screen grid connected to the cathode. The H.T. voltage was 32 volts, although it is now suggested that a higher value would have been advantageous. The H.T. supply was obtained by transforming mains a.c., rectifying with a full-wave silicon rectifier and smoothing the rectified voltage with a π-filter to give less than 100 mV of 50 c.p.s. ripple.

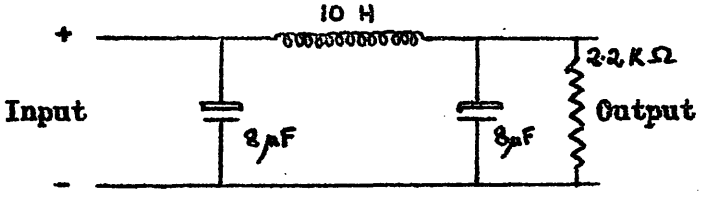

Bridge Standardisation

As it was required to polarise the D.M.E. with respect to the solution, it was necessary to prevent d.c. from entering the T.R.A. bridge. This was accomplished by placing a 1000 μF

blocking capacitor in one measuring arm, in series with the cell impedance (figure 6). The error introduced by this, approximately 0.2% at 1 Kc./sec., could be computed, but it was more convenient to compensate for the blocking capacitor and at the same time for the impedance of the coaxial leads, by using the bridge trimmers. An accurate standard parallel combination of resistance and capacitance (995.0 Ω and 0.1400 μF), maintained at 25°C ± 0.05°C in an oil bath, could be connected to the T.R.A. bridge through a 1000 μF capacitor and coaxial leads, identical to those of the cell (figure 6). The bridge readings were then set exactly to the value of the standard impedance, and a null was obtained by use of the bridge trimming controls. The potential divider, VR_2, of the balance detector (figure 5) was adjusted so that the thyratron just struck. By altering the bridge main controls in either direction, it could be confirmed that the thyratron ceased conduction on both sides of balance. It waspossible to confine the "in-balance" signal to a region smaller than 0.05% of the total impedance measured.

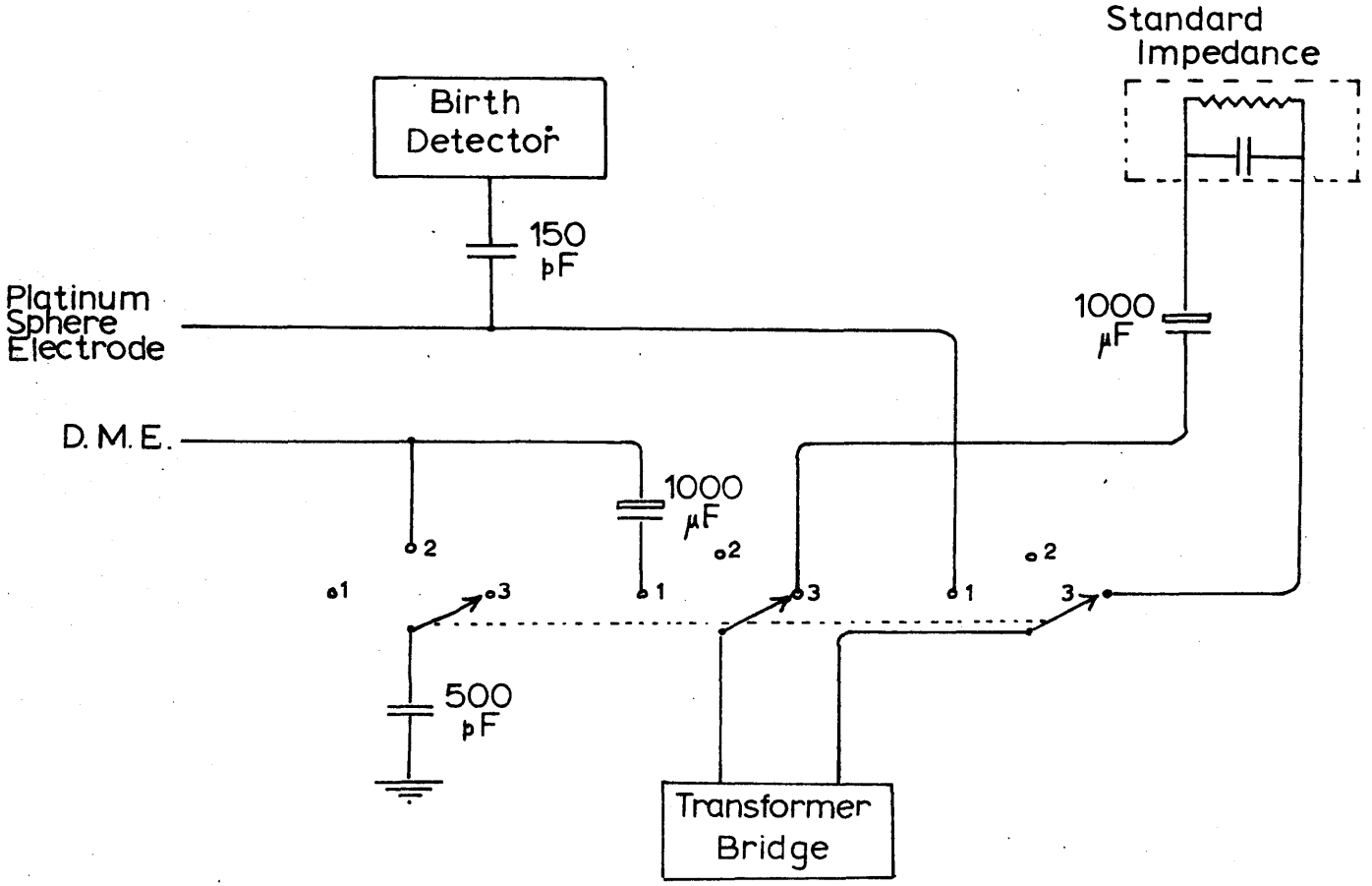

FIG. 6 BRIDGE STANDARDISATION

DROP BIRTH DETECTOR

A common method of detecting the birth of a drop (44), is to make use of the fact that when a drop falls, the cell impedance rises instantaneously to a very high value, thus causing an abrupt change in the amplitude of the signal representing the degree of unbalance of the bridge. With the present apparatus, the nature of the bridge amplifier was such that any increase in signal amplitude was severely limited, and thus no convenient signal was available for birth detection from this source. Also it was considered advantageous to have a birth detector independent of the bridge system, since it was intended to use it in the determination of drop lifetime and for drop counting.

To maintain a growing mercury drop at a constant potential, a small charging current must be supplied at all potentials except that of the electrocapillary maximum, when the charge on the electrode is zero. This current varies with time in a saw-tooth manner, a sharp increase occurring at the fall of each drop. On passing the current through a resistor, a rapid change in voltage could be detected through a capacitative coupling at this instant.

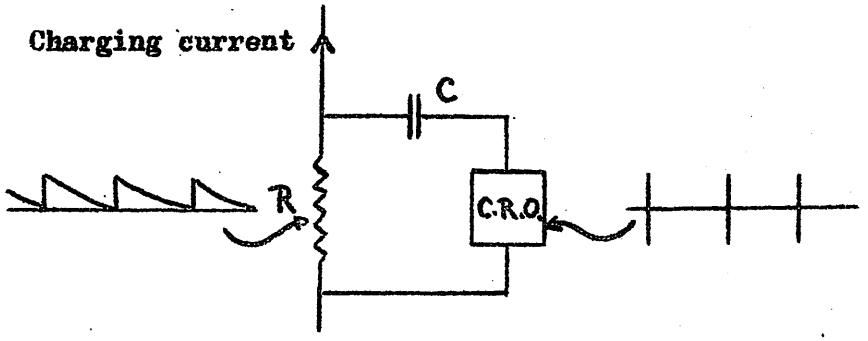

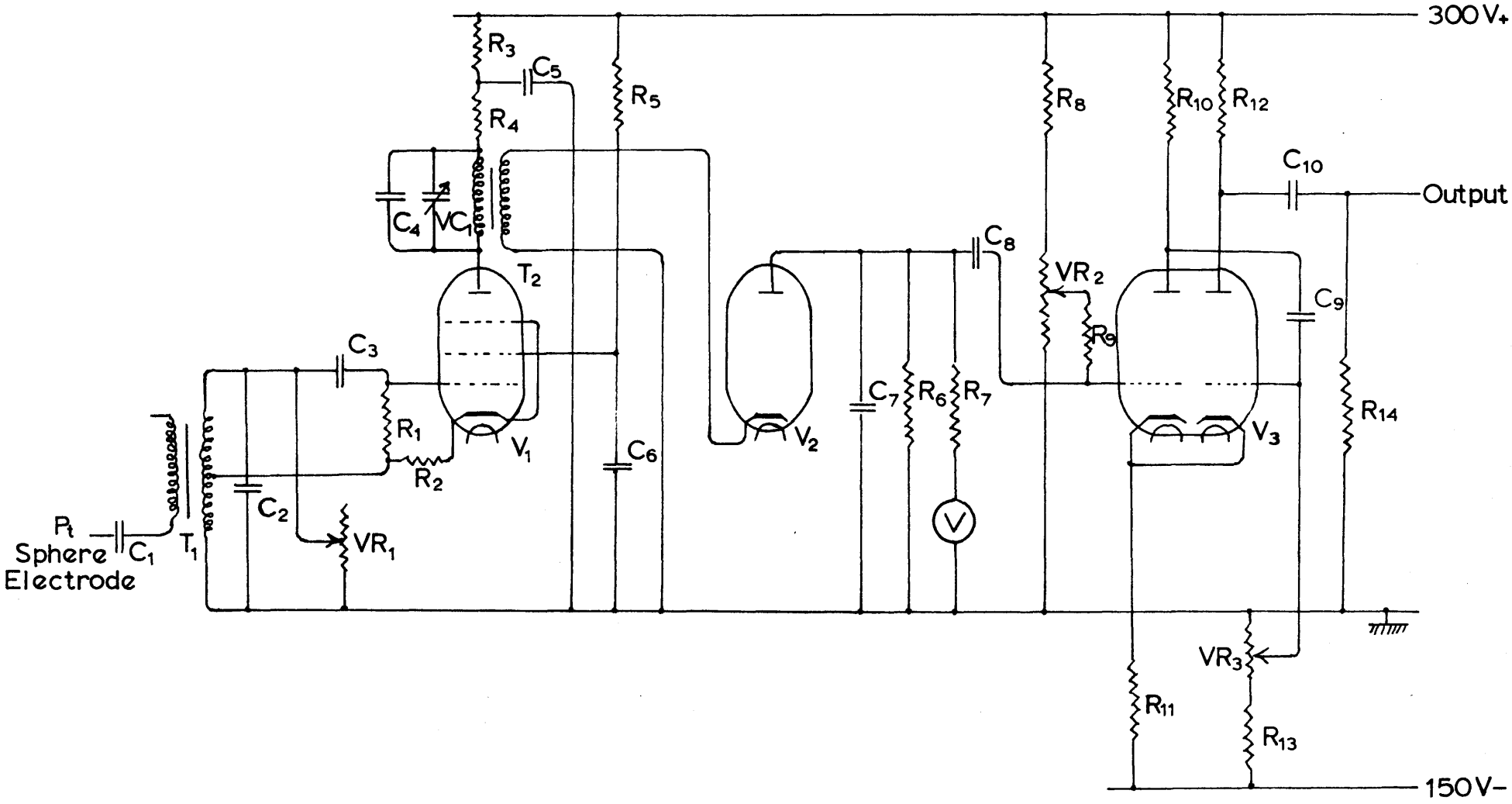

FIG. 7 DROP BIRTH DETECTOR.

Figure 7 **BIRTH DETECTOR**

Components

R_1	10 KΩ	R_7	33 KΩ	R_{13}	47 KΩ
R_2	330 Ω	R_8	560 KΩ	R_{14}	100 KΩ
R_3	100 Ω	R_9	33 KΩ	VR_1	0–550 KΩ
R_4	100 KΩ	R_{10}	1.2 KΩ	VR_2	0–100 KΩ
R_5	47 KΩ	R_{11}	20 KΩ	VR_3	0–50 KΩ
R_6	33 KΩ	R_{12}	10 KΩ		

C_1	150 pF	C_5	0.01 μF	C_9	0.47 μF
C_2	150 pF	C_6	0.005 μF	C_{10}	500 pF
C_3	100 pF	C_7	470 pF	VC_1	0–200 pF
C_4	100 pF	C_8	0.01 μF		

V_1	CV 4014
V_2	CV 4007
V_3	CV 4024

T_1	32 turns, ferrite core, 1 cm. diam. Polythene former.
T_2	32 " " " " " " "

The voltage pulses were fed into a pulse amplifier and the output was used to trigger the start gate of the interval timer. While this system was workable, it contained many disadvantages, the most serious being instability caused by extraneous pulses from any other switching taking place in the near vicinity. Also it was impossible to use the detector at or near the potential of the electrocapillary maximum, and it was necessary to increase the d.c. impedance of the polarisation circuit.

It was decided to use a method involving a special detecting signal of radio frequency, similar in principle to that described by Barker (51). The drop birth detector (figure 7) consisted of a 4.5 Mc./sec. Hartley oscillator, the coil of which had a secondary winding connected through a 150 pF capacitor to the platinum gauze electrode in the cell. While the mercury drop was growing, the oscillatory circuit was damped by the relatively low internal impedance of the cell. At the moment of drop detachment, however, a rapid burst of oscillations occurred due to the impedance in the damping circuit rising instantaneously to a very high value. A radio frequency path to earth was provided by a 500 pF capacitor connected to the D.M.E. (bridge selector switch position 2 in figure 6), which was disconnected when the electrode impedance was being measured (switch position 1 in figure 6). When the bridge selector switch

was in position 2, the T.R.A. bridge was disconnected from the electrodes. This was a necessary precaution during birth detection, since otherwise there was a low impedance path to earth for the R.F. signal through the bridge. The oscillation surge was amplified by a pentode with tuned anode, the anode coil being transformer coupled to the diode V_{2a}. C_5 and R_3 acted as a decoupling circuit. The signal, after rectification by V_{2a}, had its R.F. component filtered out by the C_7-R_6-R_7 network and was applied by C_8 to one control grid of the double triode V_3. This valve acted as a monostable multivibrator and gave out a sharp pulse. A final differentiation circuit, C_{10}-R_{14}, then limited the pulse width to 50 μ sec., ensuring that it would only activate the start gate of the interval timer if both start and stop gates were linked. In this latter condition, the timer was used to measure accurate drop lifetimes by utilising two successive pulses from the birth detector. A three-position switch enabled selection of stop signals to be made:

Stop Signal Selector

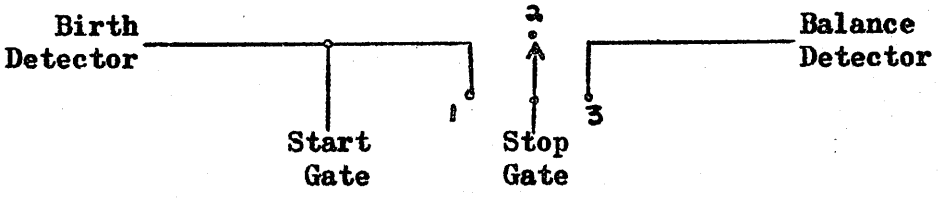

Switch position		1	Drop lifetime
"	"	2	Stop small gate open
"	"	3	Birth-balance interval

VR_1 acted as an internal oscillator damping control, and was set according to the impedance of the cell solution. The incorporation of a voltmeter facilitated the setting of VR_1 and was also useful for checking that the D.M.E. was functioning regularly. H.T. supplies for the birth detector were taken from the external output socket of the interval timer.

D. C. POLARISATION UNIT

The circuit used to charge the growing mercury drops to a fixed static potential with respect to a reference electrode is shown in figure 8. A 12 volt bank of lead accumulators was connected to a linear 1000 Ω Helipot in series with a linear 50 Ω potential divider. Two 150 H chokes were placed between the electrodes and the charging circuit to isolate bridge a.c. from the latter. While the error in measured electrode impedance caused by neglecting this parallel d.c. circuit was less than 0.05% at a bridge frequency of 1 Kc./sec., measurements at lower frequencies would require allowance to be made for it. The circuit also incorporated a microammeter so that any deviation from perfect polarisation, caused by an electrode reaction such as the reduction of ions or solvent decomposition could be detected; the maximum charging current was of the order of 1 μA. Because it had a large inductive impedance, it was necessary to ensure that the microammeter was not in circuit while the electrode impedance was actually being measured. It was possible to apply the polarisation potential between the D.M.E. and either a reference electrode or a mercury pool anode. Accurate adjustment of potential was made by switching in a potentiometer as shown in figure 8. The potentiometer was a Tinsley type 3387B instrument and this was used in conjunction with a Scalamp galvanometer or with an Electronic Instruments Ltd. Vibron Electrometer (model 33B) as null detector. The latter was especially useful if the internal impedance of the cell was high.

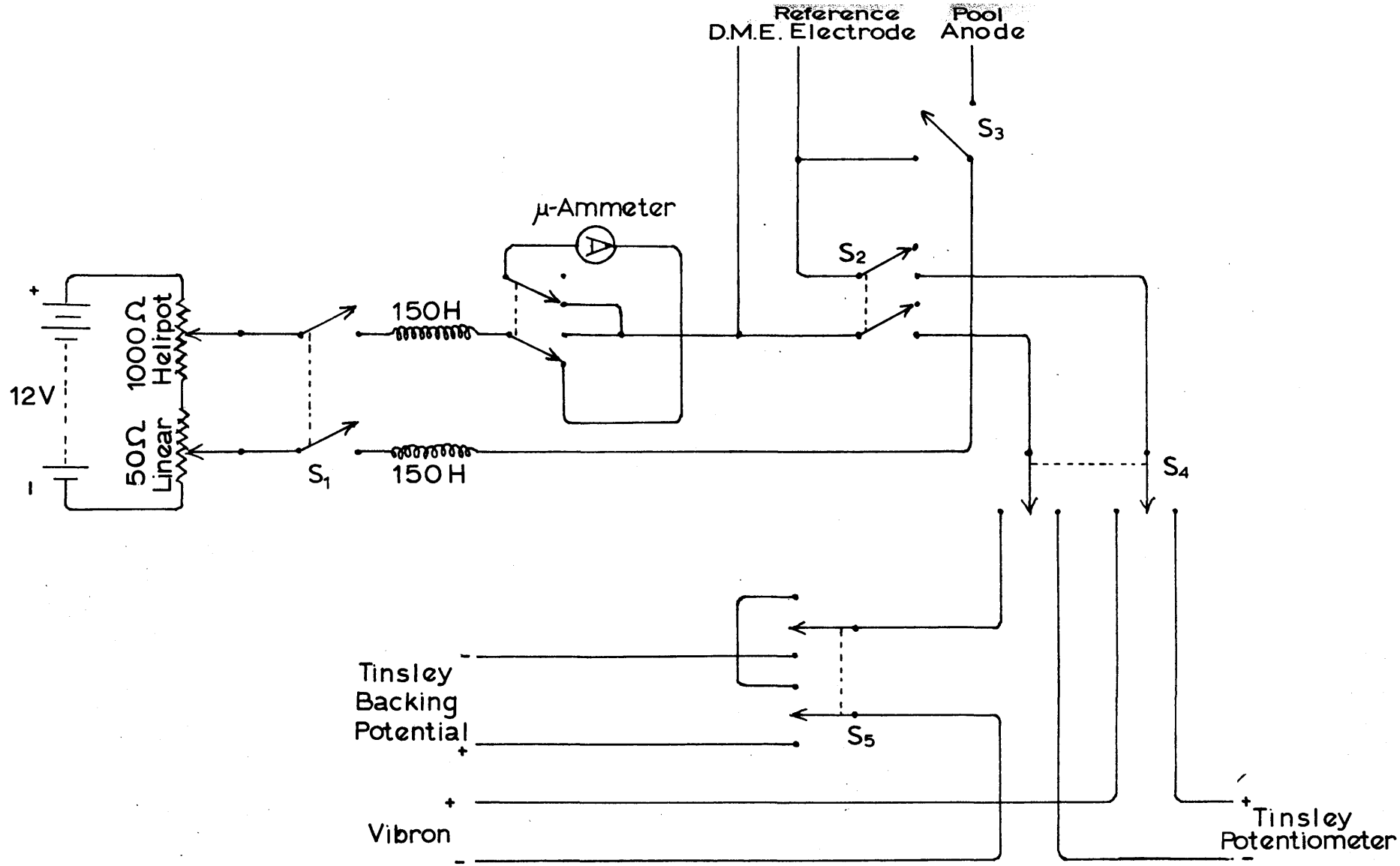

FIG. 8 D.C. POLARISATION UNIT.

Although it could be used directly for measuring potentials of 0.0 - 1.0 volts on its most insensitive scale, the Vibron electrometer was normally used as a null instrument, with a sensitivity of 100 mV or 300 mV for full scale deflection, in conjunction with a "backing potential" provided by the Tinsley potentiometer. The latter was standardised with a saturated Weston cell (Sangamo Weston Ltd., model S134) of internal resistance 600Ω and mean E.M.F. 1.0186 volts at 20°C.

Since the a.c. voltage impressed across the cell by the T.R.A. bridge never exceeded 10 mV, there was effectively no interference with the applied polarisation potential.

AUDIO FREQUENCY STANDARDISATION

The frequency of the audio signal generator, which must be accurately known for the parallel to series conversion, was standardised by comparing it with the sub-standard frequencies generated by the crystal oscillator in the interval timer. The latter produced pulses at repetition rates of 10^n p.p.s., where n is an integer between -1 and +5. Initially a generator frequency was selected close to 10^n c.p.s. and fed together with the appropriate timer signal into the X and Y plates respectively of a cathode-ray oscilloscope. The generator fine frequency control was then adjusted until a stationary Lissajous figure was obtained. A more effective method was to display both the generator output and the interval timer signal on a double beam oscilloscope, and to synchronise the time base of the latter with the timer pulses. In the Cossor model 1035 oscilloscope the one time base serves both beams and thus both traces appear stationary when the generator frequency is identical to the pulse repetition rate of the timer signal. Since the Advance signal generator became very stable after running for several hours, it was possible to obtain a frequency accurate to better than 0.01% with respect to the standard frequency. The long term frequency stability could be checked by feeding the generator output into the "External Frequency" channel of the interval timer, and thus counting the number of cycles over a long period. Although such tests verified the stability of the generator it was normal practice to check the frequency periodically during measurements, as outlined above.

PULSE COUNTER

It proved necessary to construct a device which would count pulses with a low repetition frequency:

(i) to extend the range of the interval timer above 10 seconds, by making use of the fact that the instrument gave out a pulse every 10 seconds.

(ii) to enable a drop count to be made, using the 'one pulse per drop' produced by the birth detector.

The circuit of the counter (figure 10) consisted of a thyratron trigger unit, a Post Office electromechanical relay and associated power supplies. The counter was able to add up to 9999 drops and extended the range of the interval timer by a factor of 10^4. The trigger circuit was activated by positive pulses such as those produced by the interval timer. Since the birth detector emitted negative pulses, however, (as opposed to balance detector pulses which were positive) it was necessary to invert the phase before using them to activate the counter. A complete circuit of the phase invertor and pulse switching unit is given in figure 9.

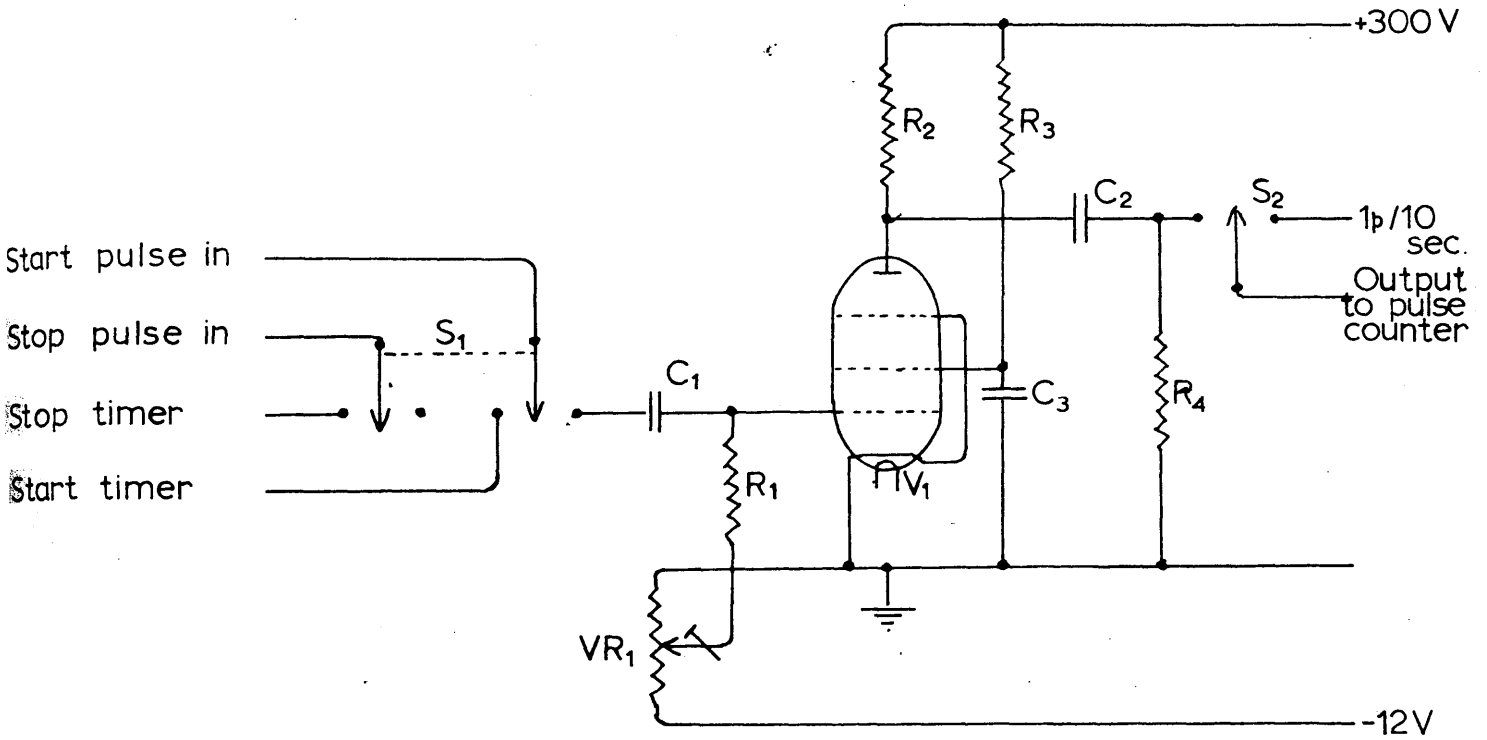

FIG. 9 PHASE INVERTOR AND PULSE SELECTOR

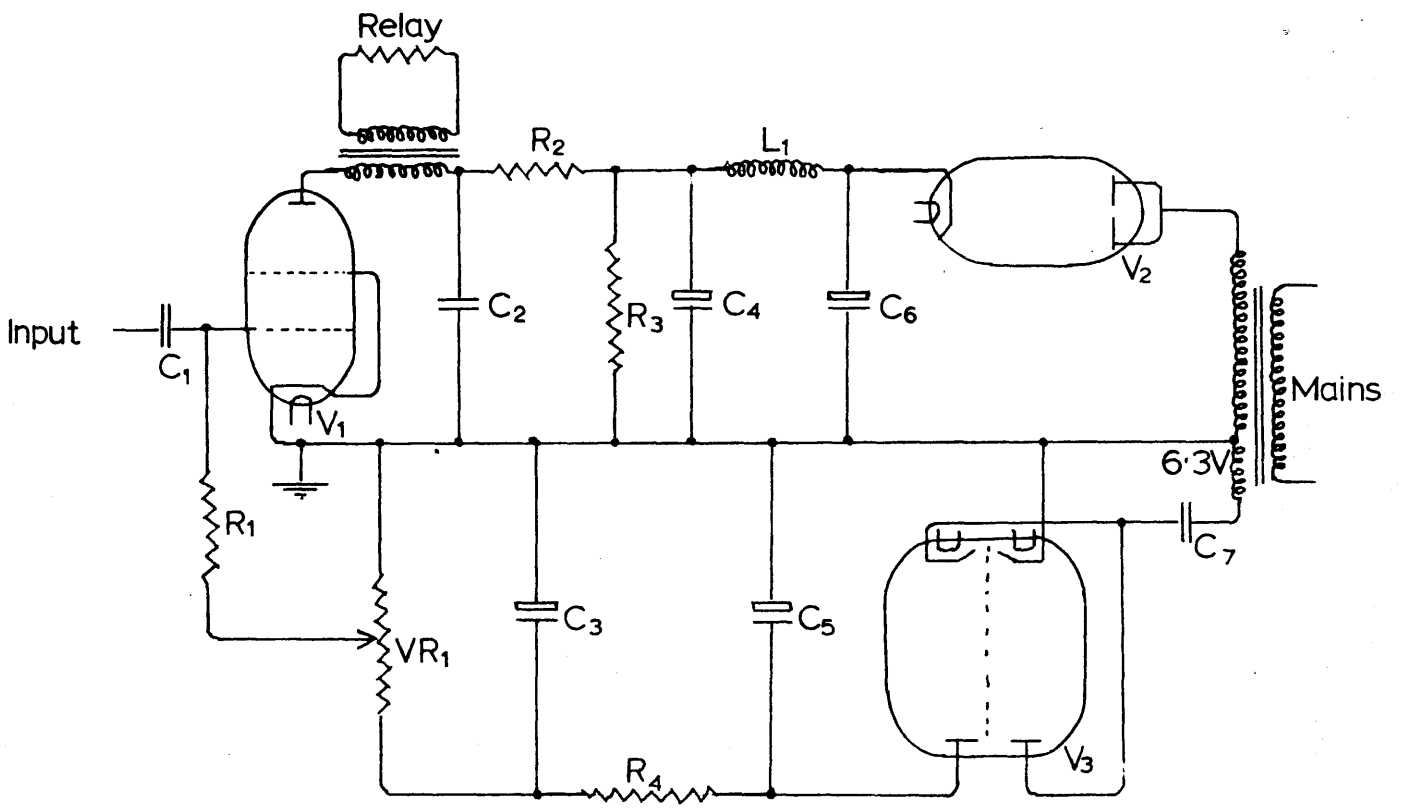

FIG. 10 PULSE COUNTER

Figure 9 PHASE INVERTOR AND PULSE SELECTOR

Components

R_1	:	470 KΩ	C_1	:	0.1 μF
R_2	:	22 KΩ	C_2	:	0.047 μF
R_3	:	120 KΩ			
R_4	:	100 KΩ	V_1	:	CV 4014
VR_1	:	5 KΩ			

Figure 10 PULSE COUNTER

R_1	:	100 KΩ	C_1	:	0.15 μF
R_2	:	1.5 MΩ	C_2	:	0.5 μF
R_3	:	47 KΩ	C_3	:	25 μF
R_4	:	2 KΩ	C_4	:	24 μF
VR_1	:	2 KΩ	C_5	:	25 μF
V_1	:	CV 4018	C_6	:	16 μF
V_2	:	CV 4005	C_7	:	25 μF
V_3	:	CV 140(283)	L_1	:	10 H.

MONITORING

During an experiment the amplifier output and balance detector signal voltages were monitored continuously on a Solartron double beam cathode-ray oscilloscope (type CD 1014.2), It was also found convenient to monitor certain other signals periodically. This was done on a Cossor (type 1035) cathode-ray oscilloscope, and an input selector was built for this to facilitate rapid checking (table 1). A selection of typical oscillographs are shown on plate 1.

Table 1 COSSOR C.R.O. INPUT SELECTOR

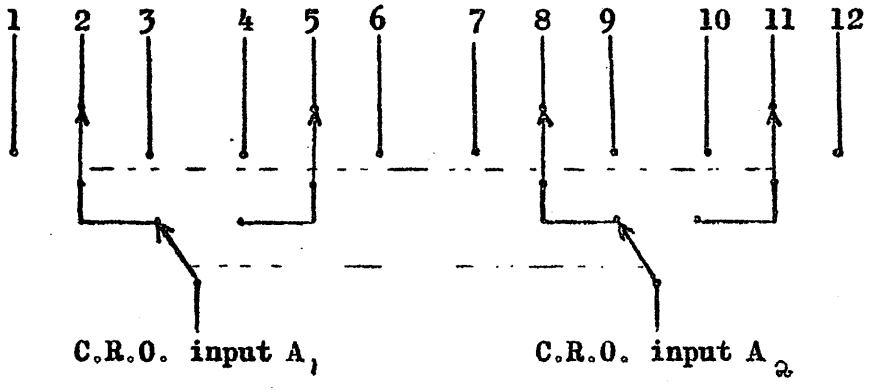

1	10^3 p.p.s.	7	A.F. signal generator output
2	-	8	-
3	10^4 p.p.s.	9	A.F. signal generator output
4	Start pulse (birth detector)	10	-
5	-	11	Unlimited amplifier output
6	Unlimited amplifier output	12	-

PLATE 1

OSCILLOGRAPHS

1 **Frequency Standardisation**

A.F. Generator 1 Kc./sec.

Interval Timer 1000 p.p.s.

2 **T.R.A. bridge out of balance by 0.2%**

Amplifier output (limited)

Balance detector.

3 **T.R.A. bridge in balance.**

Amplifier output (limited).

Balance detector

4 **Amplifier output**

T.R.A. bridge balanced.

Mush 10v.

5 **Amplifier Output**

T.R.A. bridge out of balance by 0.2%

Peak height 45 v.

6 **Amplifier output**

T.R.A. bridge fully out of balance

Peak height 90 v.

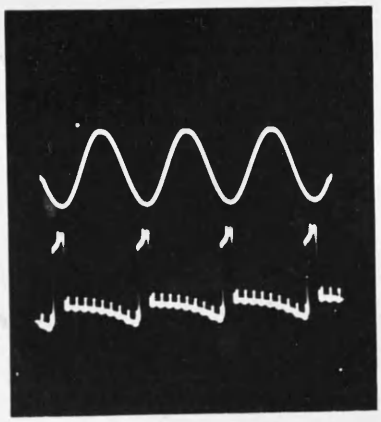

1

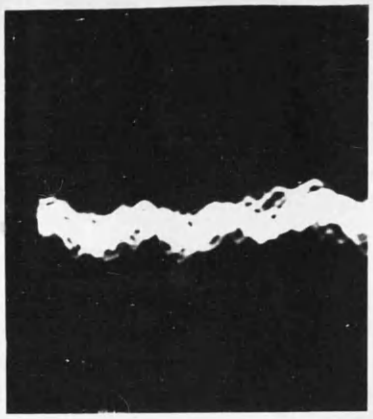

4

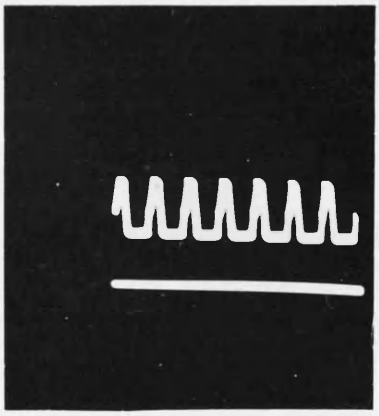

2

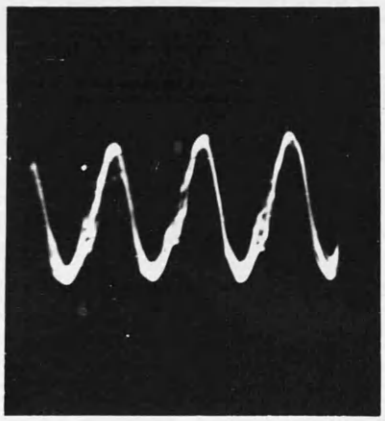

5

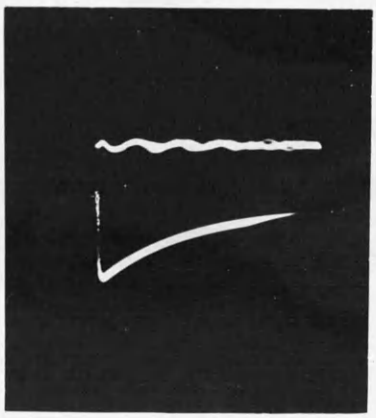

3

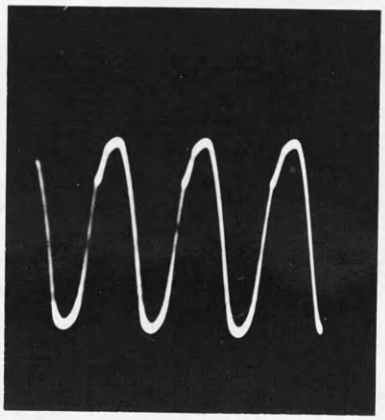

6

PLATE 1.

THE CELL.

The cell, illustrated in figure 11 and plate 2 was constructed of Pyrex glass and had a capacity of about 75 ml. The cathode was a fine glass capillary from which mercury dropped at the centre of a hollow spherical anode of platinum gauze. The latter made contact with the exterior by means of a platinum wire sealed into the glass and extending into side arm E (figure 11) which was filled with mercury. Two small holes in the sphere, 180° apart, allowed for the insertion of the capillary at the top and the escape of mercury at the bottom. The mercury fell into cup H, which could be emptied into the collection vessel I by turning the Teflon tap J. The mercury collection vessel was attached to the main part of the cell by a B 10 joint and was held in position by two springs attached at one end to a brass collar, and at the other to the outside of the tap. Mercury in the collection vessel could be transferred to weighing bottle G_2 by pumping air down side arm F. Solutions in the cell were de-oxygenated by bubbling pre-treated oxygen-free nitrogen through the cell from arms A or B and allowing the gas to escape via a conventional bubbler attached to side arm C. Provision was made for the use of a mercury pool anode: the mercury occupied the annular region around cup H and electrical contact was made with it by way of a glass-sealed platinum wire inserted in arm A. Side arm D was used to house the reference electrode or salt bridge, and all side arms terminated in B 10 sockets. Fine capillaries (external

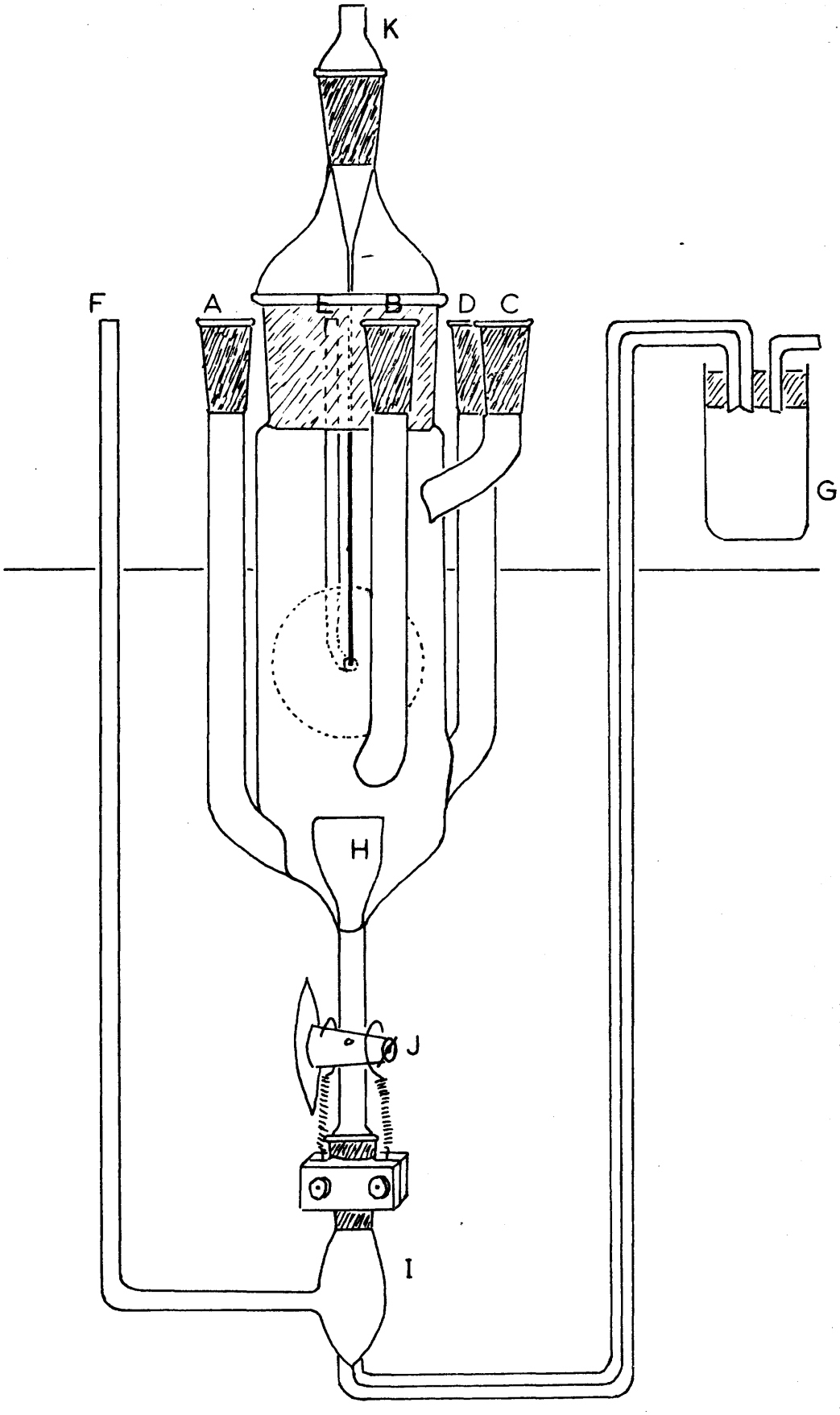

FIG. 11 THE CELL

radius ≑ 3 x 10^{-2}cm; internal radius ≑ 2 x 10^{-3}cm.) were drawn from thick walled Pyrex tubing joined to a B 14 air-bleed. A B 29 - B 14 adaptor completed the connection to the top of the cell and the mercury reservoir (capacity ≑ 4000 gm.) was attached to the capillary at K by means of a short length of carefully cleaned Polythene tubing to facilitate the insertion and withdrawal of the capillary. The reservoir was connected to a long vertical tube of bore 1 cm. to enable the height of the mercury head to be determined. An illuminated screen was placed behind this tube and the mercury level was observed by a cathetometer reading to ± 0.001 cm. In order to maintain the mercury level at a constant height, a special clamp was designed for attaching the reservoir to a clamp-stand.

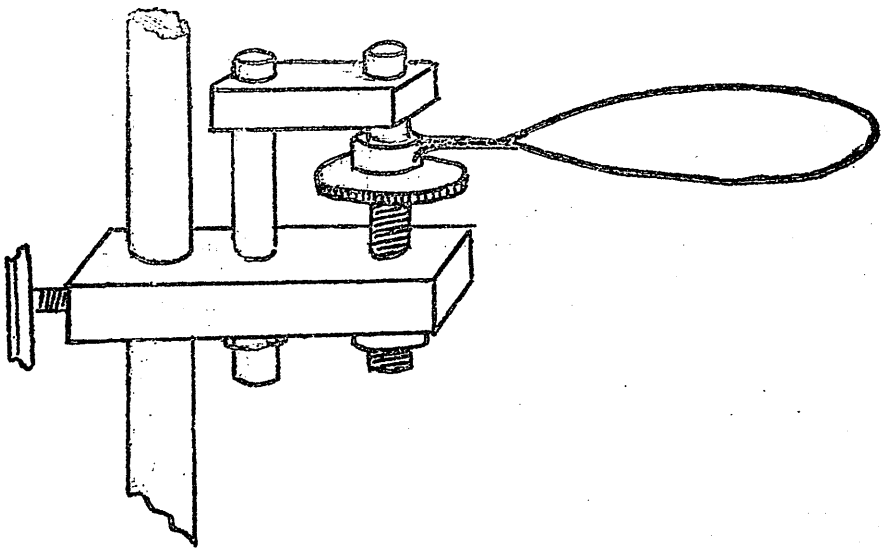

A very fine screw control allowed minute adjustments to be made to the mercury level. Electrical contact was made with the mercury in the reservoir by means of a glass-sealed platinum wire.

Plate 2 **THE CELL**

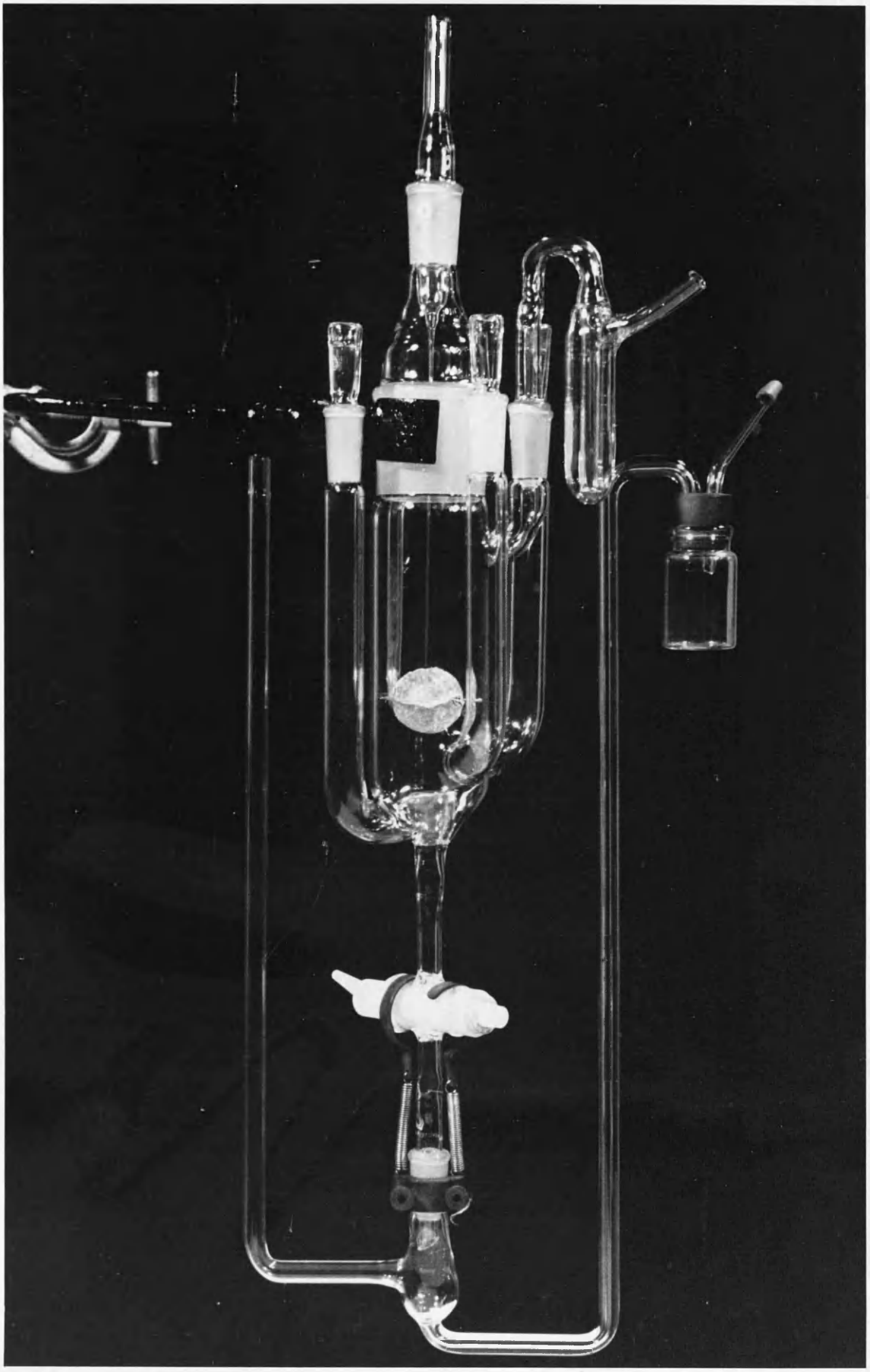

TEMPERATURE CONTROL

The cell was immersed in a tank of water fitted with a "Circotherm" thermostating unit which maintained the tank at a temperature of 25°C ± 0.05°C. Because the room temperature was at times above this level, a copper coil, through which cooling water could be passed, was immersed in the tank. Although the Circotherm motor was clamped to a different table from that holding the cell and tank in order to minimise the effect of vibrations, the thermostat was switched off during an actual measurement to prevent any vibration of the cell caused by the movement of water in the tank, or any electrical interference.

MERCURY PURIFICATION

Mercury was thoroughly washed with water by vigorous shaking and decantation. It was then filtered through a filter paper pierced with a small hole, and washed with acetone. It was sprayed down a 100 cm. column of 10% nitric acid and then allowed to stand under concentrated sulphuric acid for 24 hours. After another thorough wash with water and drying with acetone, the mercury was distilled three times under vacuum, with stringent precautions being taken to prevent the entries of impurities into the distillation system. The best method for storing purified mercury was under pressure in an atmosphere of nitrogen. It was difficult to assess the purity of the mercury, although it has been found (52) that a pure specimen, on shaking with conductivity water gives rise to a "foam" lasting for over 15 secs., while impure samples give foams lasting for shorter periods.

TEST OF APPARATUS FOR CAPACITANCE MEASUREMENT

Once a balance position has been found, the birth-balance interval should be constant, provided that the mercury flow rate is unaltered and the static polarisation potential is maintained constant. A small scatter in results was expected as a result of minor irregularities in drop formation and other random errors. The relative accuracy of the apparatus was tested

(i) by polarising the D.M.E. to a fixed potential, finding a balance position and checking that over a long period the bridge always balanced during the life of every drop; and

(ii) by maintaing the mercury flow rate constant by ensuring a constant mercury head and then measuring a large number of birth-balance intervals at a constant polarising voltage.

By investigating the statistical distribution of results, it was possible to estimate the number of readings required to give the desired accuracy.

Series of 50 to 300 birth-balance intervals were measured using different capillaries, flow rates and polarisation voltages so that the mean values of birth-balance times ranged from 0.5 seconds to 13.6 seconds. The percentage root mean square deviation decreased

for long birth-balance periods, but the actual deviation increased. A typical result had a mean of 0.5769 sec. and a standard deviation of± 0.0011 sec. or ± 0.2%. With 50 results, the standard deviation of the mean was ± 0.00002 sec. while with 10 results it was ± 0.0001 sec. It was normal practice to take ten birth-balance readings at each potential, although this was reduced to five if the standard deviation was very low.

DETERMINATION OF POTENTIAL OF ELECTROCAPILLARY MAXIMUM

In consideration of the potential difference between a D.M.E. and an electrolytic solution, the "electrocapillary maximum" (hereafter E. C. maximum) forms one of the most convenient reference points. At this potential, the electrode carries zero electronic charge. Since it was important to know this voltage for the calculation of the charge in the double layer from capacitance data, apparatus was constructed for its measurement.

Even in the presence of specific adsorption of ions, mercury issuing from an isolated D.M.E. will be uncharged provided that all traces of oxygen are removed from the cell solution. Thus the potential of the electrode under such conditions is that of the E.C. maximum. Newcombe (52,53) has recently described apparatus for the measurement of this potential, in which the cell voltage was compared with a standard voltage using a very high impedance valve voltmeter, and a similar method is used in the present work. The circuit, shown in figure 13, consisted of a ME 1400 electrometer valve acting as a d.c. amplifier (54). The anode load resistor and H.T. battery were interchanged from their usual positions in order to obtain an output near earth potential. Adjustment of the output level was made by a 1 MΩ potential divider. The 90 V H.T. battery was isolated from the chassis, since it changed potential with respect to earth by an amount equal to the amplified signal. Heater current was provided from a bank of lead accumulators through a heavy duty variable resistance.

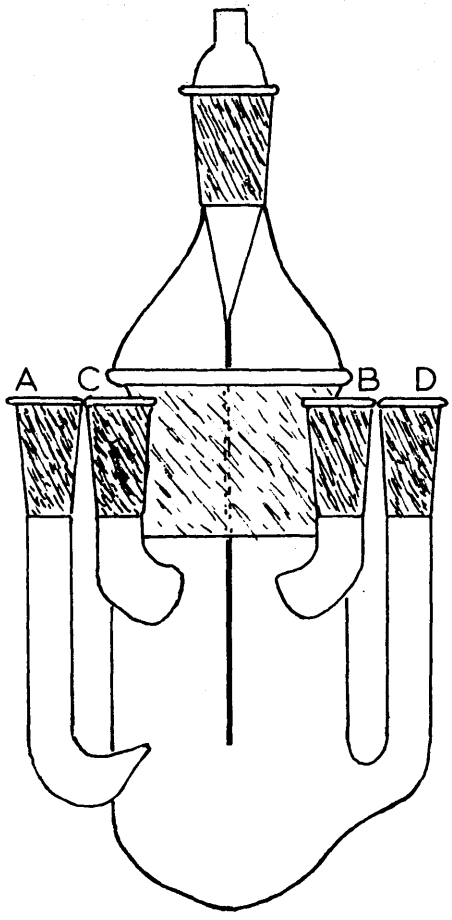

FIG.12 THE E.C. MAX. CELL

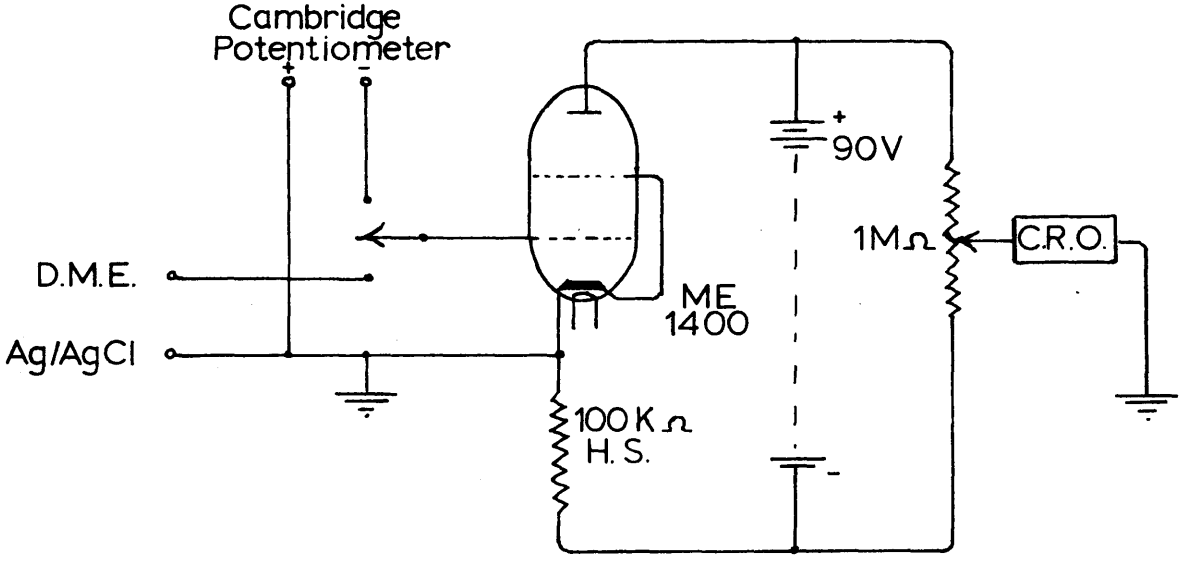

FIG13 E.C. MAX. VALVE VOLTMETER

The output was detected on one beam of a double beam cathode-ray oscilloscope, while the other beam was used as strobing device to mark the position of the E.C. maximum voltage on the screen. The control grid of the electrometer valve was then connected to a Cambridge slide-wire potentiometer which was adjusted until its output voltage caused the same deflection on the oscilloscope as the D.M.E. E.C. maximum. The potentiometer was standardised using the saturated Weston cell described previously. As it was required to determine potentials to the nearest millivolt, it was found necessary to incorporate a d.c. amplifier (Cossor, model 1434) in series with the electrometer to give an extra gain of x15.

The cell is illustrated in figure 12. Solutions could be blown out by passing pure nitrogen down side arm A, and allowing it to escape through a bubbler fitted at B. Arm D housed the reference electrode, and C enabled nitrogen to be passed over the cell solution during measurements.

It was essential to ensure the complete absence of oxygen from the solutions (52) and they were therefore blown out for 2-3 hours before an experiment. The cell was rinsed in a solution of sodium sulphide prior to every run. Ag / AgCl electrodes were used as reference, since it had been suggested by Newcombe that "paste electrodes" such as the calomel electrode might occlude oxygen.

Determinations of the potential were made over 1-2 hours to ensure that no drift occurred. A small amount of 50 c.p.s. mains hum present in the signal, did not seriously interfere with the measurement.

PART 2

THE DROPPING MERCURY ELECTRODE IN AQUEOUS POTASSIUM CHLORIDE SOLUTIONS

INTRODUCTION

Early workers considered that the rate of flow, m , of a D.M.E. was independent of time. Thus for a spherical growing drop, the area-time relationship was given by

$$A = Km^{2/3}t^{2/3} \qquad \ldots\ldots\ldots\ldots\ldots\ldots\ldots\ldots\ldots\ldots 46$$

where A is the area of the electrode at time t , and $K = (4\pi)^{1/3}\left(\frac{1}{D_T}\right)^{2/3}$, for D_T the density of mercury at a temperature of T°C. This approximate relationship was used both in the study of the perfectly polarised electrode (55,56) and in polarographic research.

The rate of flow of mercury is not constant, however, because of the action of back pressure exerted by interfacial tension. The back pressure at time t is $2\gamma/r_t$, where r_t is the radius of the growing drop at time t. The effect is thus greater when r_t and hence t is small. The calculation of instantaneous m_t values is quite simple, but it is completely erroneous to use such a value in the determination of drop area as is done by some workers (57), since what is required is the instantaneous surface area at time t, which is a function of average flow rate, $\bar{m}_t$, up to time t. It is seen that in all cases, $\bar{m}_t < m_t$ since m_t increases with time.

Several theoretical treatments of flow rate of a D.M.E. have been proposed recently, which all results in a similar form of equation (30,58,59). The relationships developed by Los and Murray

are the most rigorous. In all cases, w_t, the mass of a drop at time t is given by an integration process, which eliminates the doubtful calculation of an "average back pressure" (29).

The main demand for accurate mercury flow equations has been from polarographic workers wishing to test theoretical relationships such as the Ilkovic equation. There are, however, three main difficulties in the use of current-time curves for mercury flow analysis:

(i) The type of equation is

$$i_t = AnD^{1/2}m^{2/3}t^{1/6}c.(1 + BD^{1/2}m^{-1/3}t^{1/6} + CDm^{-2/3}t^{1/3} + \ldots) \quad \ldots\ldots 47$$

where i_t is the current at time t, and n, c, A, B, C and D are constants. Evaluation of this expression is dependent on an exact knowledge of D, the diffusion coefficient, a parameter very difficult to estimate.

(ii) The depletion effect must be allowed for, since otherwise successive drops grow in solution low in depolarisar.

(iii) Lingane has shown (60) that convection and stirring effects disturb the diffusion layer and hence affect the current.

A suitable method of testing area-time relationships is to investigate the charging curve for a perfectly polarised D.M.E. Newcombe (53,61,62,63) has given examples of voltage-time curves but has not attempted an area-time analysis of them.

If a constant static potential is applied to a perfectly polarised D.M.E., the differential capacitance per unit area of the

electrical double layer at the electrode will remain at a constant value. Thus the total series capacitance of the electrode is directly proportional to the electrode area. Measurement of the differential capacitance of a D.M.E. at different times during the life of a mercury drop is thus an excellent method of testing area-time relationships.

The main purpose of this section of the thesis was to investigate the growth of a mercury drop by making impedance measurements at various times during its lifetime. An expression was derived for area at time t, A_t, in terms of t such that $(C_s)_t/A_t$ was always constant, where $(C_s)_t$ is the series capacitance of the D.M.E. at time t. Consideration was also given to the effect on double layer capacitance measurements of varying the bridge frequency. The series resistance of the D.M.E. was then examined under diverse conditions. Finally a new method of obtaining double layer capacitance of a D.M.E. was investigated in which knowledge of mercury flow rate, time of measurement or area of electrode surface was not required.

EXPERIMENTAL

1. Preparation of Reagents

Potassium chloride. "AnalaR" quality potassium chloride was recrystallised three times from conductivity water. Before being used to make up solutions it was dried in a platinum crucible at about 300°C.

Conductivity water. Conductivity water was initially prepared by mixed-bed deionisation as described by Davies and Nancollas (64). The resins used were Amberlite IR 120(H) acid resin and Amberlite IRA 140 basic resin, intimately mixed in a proportion of 1 : 2 by volume.

It was not realised until seventeen experiments had been completed that such water contained appreciable traces of surface active organic material which had been eluted from the matrix of the ion exchanger. The discovery was made after experiments had been done with solutions made up with water prepared by Bourdillon still (65). Results of these showed that the differential capacitance was lowered by more than 1%. Boiling down a litre of "resin water" to dryness left a tarry brown mass. It is also noted that if resin water is passed through a column of dextrin, a brown band appears which gradually covers the whole column. Organic impurities present in resin water have been shown to inhibit crystal growth (66).

A distillation process was developed whereby distilled water, to which small quantities of potassium permanganate and potassium

hydroxide had been added, was boiled in a three litre Quickfit flask attached to a 60 cm. fractionating column. A water-cooled Quickfit condenser was attached to the top of the latter, and the distillate was slowly collected in well-cleaned steamed-out flasks. Any organic impurities in the original water were oxidised by the permanganate, probably to carboxylic acids, and at the high pH of the solution, these were present as salts.

As a final precaution, all potassium chloride solutions were passed down a column of activated charcoal, after the method of Barker (67). The charcoal was purified by refluxing on alternate days with normal hydrochloric acid and distilled water until the supernatent liquid became clear. This process took more than a month to complete. The charcoal was then washed and stored in conductivity water. Any surface active materials were removed from solutions by passing the latter through a 5 cm. x 1½ cm. column of the pre-treated activated charcoal at a very slow rate. Since it was probable that initially the charcoal would adsorb part of the solute, the first 40-50 ml. of the eluant were discarded.

Solutions were kept in stoppered Pyrex stock flasks with ground glass joints. Flasks were cleaned by rinsing with alcoholic potassium hydroxide solution, washing with water and standing in chromic acid. After further thorough washing with water they were steamed for thirty minutes. When not in use they were filled with distilled water. Samples of the reagents were weighed out in stoppered Pyrex weighing bottles using a Stanton semi-micro balance

with calibrated weights. All solutions were made up by weight using a large Sartorius balance.

2. Reference Electrode.

The reference electrode used with 0.1 M aqueous potassium chloride solutions was a 0.1 M calomel electrode with 0.1 M potassium chloride salt bridge, shown in figure 14. Approximately 0.5 ml. of distilled mercury was placed at the bottom of vessel A and this was covered by a layer of calomel paste prepared by rubbing together in a mortar, "AnalaR" mercurous chloride, mercury and a small quantity of 0.1 M potassium chloride solution. Tube B, which had a platinum wire sealed into it was fixed in position by a B 10 joint. The vessel and salt bridge were filled with solution from reservoir C. When not in use, the salt bridge was protected by a guard tube.

3. General Run Procedure.

Before an experiment, a thirty minute discharge was given to all accumulators to stabilise their E.M.F. It was important to start the mercury flow from the capillary before immersing it in the test solution. After the cell had been placed in the thermostat, the solution was deoxygenated with pre-saturated oxygen-free nitrogen for one hour; the D.M.E. was then polarised cathodically, to a voltage just below that of solvent decomposition, to remove any reducible material. The birth detector was now set up using VR_1 and VC_1 (figure 7) with the impedance selector switch at "Off" (position 2,

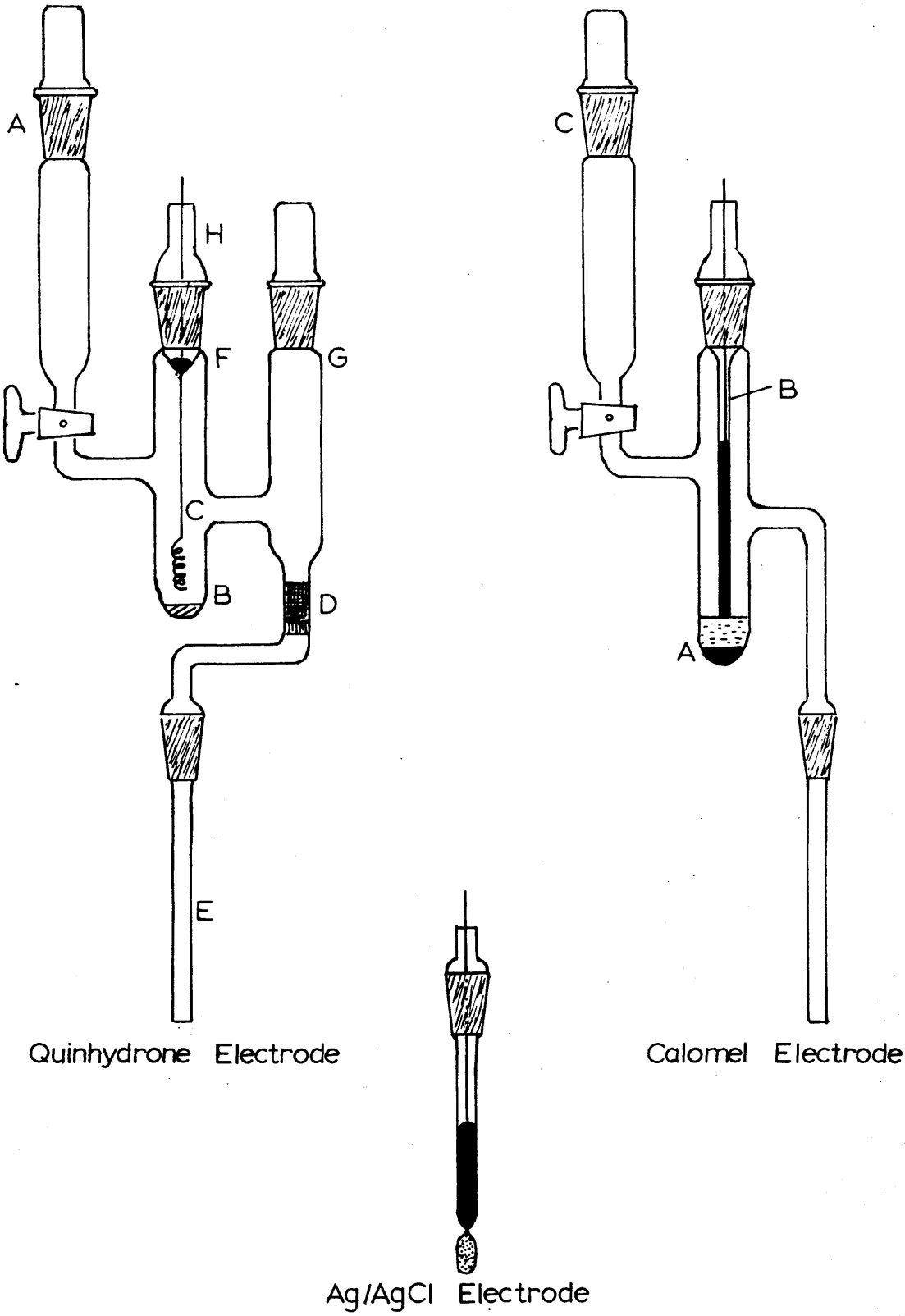

FIG. 14 REFERENCE ELECTRODES

figure 6) and the cathode-ray oscilloscope connected to "Start Pulse" (4, table 1). When the amplifier had been tuned to the bridge frequency in use, the balance detector was made ready as follows. With the impedance selector at "Standardise" (position 3, figure 6) and amplifier and signal generator outputs set to give maximum sensitivity, the T.R.A. bridge was adjusted to read the correct value of the standard impedance, and balanced by use of the trimmers. After the time constant for the reservoir capacitor discharge had been selected (VR_1, S_1), VR_2 could be set to allow the thyratron to strike (figure 5). It was essential to check that the thyratron ceased conduction within the prescribed limits on both sides of bridge balance.

For a given polarisation voltage, a birth-balance interval could be determined once a balance position had been accurately found. With the interval timer stop signal selector set at "Birth-balance" and the impedance selector at "Off", the timer was reset and the birth detector was allowed to start it. The impedance selector was then turned to "Unknown" (position 1, figure 6) in time for the balance detector pulse to stop the timer. The reading on the latter was then noted together with those on the bridge.

When the stop signal selector was set at "Drop lifetime" and the impedance selector at "Off", successive pulses from the birth detector enabled the interval timer to record t_g, the length of time between the birth of successive drops.

At frequent intervals during a run, checks were made on the mercury level in the reservoir, the standardisation of the potentiometer and the frequency of the signal generator.

The mean mercury flow rate at a fixed polarisation potential was determined in the following manner. Tap J (figure 11) was opened to allow any mercury in H to fall into I, the interval timer was started manually at the birth of a drop and J was immediately closed. Mercury in I was blown over into G and discarded. After maintaining the applied potential and mercury head constant for 30-60 minutes, all the mercury in H was allowed to flow through J into I, the interval timer was stopped at the birth of a drop and tap J was closed. The mercury in I was then blown over into G and was subsequently washed, dried and weighed. Since the mass of mercury flowing in a fixed interval of time was known, the mean flow rate could be calculated.

After a run the capillary was washed with conductivity water, dried and enclosed in a glass guard tube before the mercury flow was stopped.

RESULTS AND DISCUSSION.

1. Area-Time Relationship

If one considers a growing spherical mercury drop of radius r_t, the back pressure at time t due to interfacial tension γ is $2\gamma/r_t$. This is equivalent to a height of mercury

$$h_b = \frac{2\gamma}{g \cdot D_r r_t}$$ where g is the gravitational constant.

Thus
$$1/h_b = \frac{g \cdot D_r}{2\gamma} \cdot \left(\frac{3}{4\pi D_r}\right)^{1/3} \left(w_t \cdot 10^{-3}\right)^{1/3}$$

$$= \frac{172.73\, w_t^{1/3}}{\gamma} \quad \ldots\ldots\ldots\ldots\ldots\ldots\ldots\ldots 48$$

where w_t is the mass of the drop in mgm. at instant t.

Let m_t mgm./sec. be the instantaneous flow rate at time t, and let M be the constant rate that would be obtained with the same mercury head, h, if there were no back pressure. Then, assuming that the rate of flow is proportional to the effective pressure,

$$m_t/M = (h-h_b)/h \quad \ldots\ldots\ldots\ldots\ldots\ldots\ldots\ldots 49$$

Also, since $m = dw/dt$,

$$dw/dt = M(1 - h_b/h) = M\left(1 - \gamma/\{172.73 h w_t^{1/3}\}\right) \quad \ldots 50$$

Smith (30) showed that this expression may be integrated easily if $h_b \ll h$, for then

$$dw/dt = \frac{M}{\left(1 + \frac{h_b}{h} + \frac{h_b^2}{h^2}\right)} = \frac{M}{\left[1 + \frac{\gamma}{172.73 h w_t^{1/3}} + \frac{\gamma^2}{(172.73)^2 h^2 w_t^{2/3}}\right]} \quad \ldots 51$$

Integration leads to

$$Mt = w_t + \frac{3}{2}\cdot\frac{\gamma . w_t^{2/3}}{172{\cdot}73\ h} + 3\cdot\frac{\gamma^2 . w_t^{1/3}}{(172{\cdot}73\ h)^2} \quad ..52$$

in which the integration constant is ignored (i.e. $w_t = 0$ at $t = 0$). Smith also showed that inversion of equation 52 by means of approximations in which terms in $(\gamma/h)^3$ are considered negligible yields:

$$w_t = Mt - \frac{1{\cdot}5\, M^{2/3} t^{2/3} \gamma}{172{\cdot}73\ h} - \frac{1{\cdot}5\, M^{1/3} t^{1/3} \gamma^2}{(172{\cdot}73\ h)^2} \quad ....53$$

It must be noted that this equation, and the equivalent formula of Los and Murray (59), are only valid for $t \geq 0{\cdot}05$sec., since terms which are important when t is small, namely the lumen volume correction and the inertia term, have been neglected.

Equation 53 was used to calculate w_t from t, provided that h, M and γ were known: these parameters were determined as follows -

(i) h, the height in cm. of the mercury head above the capillary tip was measured by a cathetometer, reading to $\pm 0{\cdot}001$ cm.

(ii) The constant M was found from equation 53 by substituting values for w_g and t_g the drop mass and drop time respectively of drops growing in an electrolytic solution of known γ. In this form equation 53 is a cubic in $M^{1/3}$ and solution of it was effected by means of Newton's "Principle of Approximations".

w_g was found by weighing a large number of drops formed at a constant potential, normally taken close to that of the E.C. maximum so that a small deviation did not produce a large error

in interfacial tension. The mercury drops were either counted using the pulse counter, or the total time of flow was determined and w_g calculated from the relationship $w_g = \bar{m}_E . t_g$ where $\bar{m}_E$ is the experimentally found mean flow rate at a potential of E Volts.

t_g was ascertained by measuring the interval between two successive pulses from the birth detector as explained in Part 1. By taking the mean of 10-20 readings an accurate value was determined.

For 0.1 M potassium chloride solution, the value of γ at the potential used for w_g/t_g determination was taken from Devanathan and Peries (27). For solutions for which interfacial tension data were not readily available, γ was calculated from a form of Tate's Law as described below.

(iii) Since the value of γ at a given potential was not always known, as was especially the case for non-equeous solutions, a method was developed for its calculation, which would give values of sufficient accuracy for use in equation 53.

The upwards force acting on a mercury drop consists of the interfacial tension acting round the circumference of the capillary orifice plus the upthrust of the displaced solution. Acting against this is the gravitational pull on the drop mass plus the excess pressure due to the curvature of the drop. At the moment of drop detachment the upwards and downwards forces are equal, and hence for a spherical drop:

$$w_g \cdot g \cdot 10^{-3} + \frac{2\gamma}{r_t} \cdot \pi\rho^2 = 2\pi\rho\gamma + w_g \cdot \left(\frac{d_T}{D_T}\right) \cdot g \cdot 10^{-3} \quad \ldots\ldots 54$$

where ρ is the capillary orifice radius in cm. and d_T is the density of the electrolytic solution in gm./ml. at T°C.

Substituting Δ for $(D_T - d_T)/D_T$ in equation 54:

$$w_g \cdot \Delta \cdot g \cdot 10^{-3} = 2\pi\rho\gamma(1 - \rho/r_t)$$

$$= 2\pi\rho\left(1 - \frac{10\left\{\frac{4}{3}\pi D_T\right\}^{1/3}\rho}{w_g^{1/3}}\right) \quad \ldots\ldots\ldots 55$$

since $r_t = r_2 = \left(\frac{3}{4\pi D_T}\right)^{1/3} \cdot \left(w_g \cdot 10^{-3}\right)^{1/3}$ as in equation 48.

Thus on rearrangement equation 55 gives

$$\gamma = \frac{w_g \cdot \Delta \cdot g \cdot 10^{-3}}{2\pi\rho\left(1 - \frac{10\left\{\frac{4}{3}\pi D_T\right\}^{1/3}\rho}{w_g^{1/3}}\right)} \quad \ldots\ldots 56$$

at a given potential w_g may be found by substitution of t_g in equation 53. Since γ is not known initially, an approximate value is chosen and the resulting value of w_g is substituted into equation 56 in order to derive a better value. A new value of w_g is now determined using the latter in equation 53 and the whole process of successive approximations is continued until constant values of w_g and γ are produced. In the present work, this operation was carried out by Deuce computer using a tabular interpretative programme.

The capillary orifice radius, ρ, must be known for the calculation of γ from t_g by equation 53 and 56. There are several methods of estimating ρ from drop weights under conditions of known surface tension: e.g. ρ may be determined from equation 56

if w_g and Υ are known. Smith (30) has shown that one of the best relationships for the calculation of ρ is that of Harkins and Brown (68) who define a function

$$F = \frac{\gamma . \rho}{V_g . g (D_T - d_T)}$$ where V_g is the total drop volume.

Thus for $\beta = \alpha . g . 10^{-3}$, $\Upsilon = \beta w_g F / \rho$.

These authors showed that for $\rho \ll r_g$,

$F = a + b.(\rho / r_g)$, where a and b are constants.

Hence $$\Upsilon = \frac{\beta . w_g}{\rho} . \left(a + b . \frac{\rho}{r_g} \right)$$

$$= \frac{\beta w_g}{\rho} . \left(a + \frac{b \rho}{\left\{ \frac{3}{4 \pi D_T} \right\}^{1/3} . w_g . 10^{-1}} \right)$$

From the data of Harkins and Brown,

$$\Upsilon = \frac{\beta w_g}{\rho} . \left(0.159 + \frac{5.706 \rho}{w_g^{1/3}} \right)$$ and thus

$$\rho = \frac{0.159 \beta . w_g}{\Upsilon - 5.706 \beta w_g^{2/3}} \qquad \ldots\ldots\ldots\ldots\ldots\ldots 57$$

Equations 56 and 57 gave almost identical values for ρ. It may be noted that Corbusier and Gierst (29) suggest replacing w_g in equation 56 by w_g' where $w_g' = w_g (1+\delta)$ and $\delta = k' \rho / w_g^{1/3}$ for k' an empirical constant. This correction is intended to allow for the part of the drop left behind after the drop has been detached from the capillary. No such correction was made here.

h, M and Υ having been determined as explained above (i, ii, iii), w_t could be calculated from t using equation 53.

In all the present calculations, the growing mercury drop was assumed to be spherical. It is probable that this condition does not hold during the first few instants after drop birth, nor towards the end of drop life when the drop becomes pear-shaped. It has been shown, however, by Smith (30) and by MacNevin and Balis (69) using high speed photographic techniques that the area of a drop during the period in which measurements are made, is almost exactly equal to that of a sphere of equal mass. Hence $A_t = (4\pi)^{1/3} \cdot (3/D_T)^{2/3} \cdot w_t^{2/3} \cdot 10^{-2}$ 58

where A_t is the area of the sphere in sq.cm.

Results of impedance /time measurements from Runs 23, 24(a) and 38 are given in tables 2, 3 and 4. In table 5, values of series capacitance, C_s , are given (in μF) together with five estimates of capacitance/unit area which were obtained using areas (in sq.cm.) obtained by five different methods of calculation.

TABLE 2 RUN 23

Ref.	E volts	C_p μF	G_p mMho	t sec.	t_g sec.
1	-1.250	0.1571	0.3020	0.78558	3.82475
2	-1.250	0.1980	0.4200	1.13374	3.82475
3	-1.250	0.2517	0.6000	1.67087	3.82475
4	-1.250	0.3036	0.7950	2.29299	3.82475
5	-1.250	0.3300	0.9000	2.64458	3.82475
6	-0.400	0.2351	1.0080	0.59870	4.16309
7	-0.400	0.3119	1.6000	1.09362	4.16309
8	-0.400	0.3356	1.8000	1.28707	4.16309

Potential is given with respect to a 0.100 N calomel electrode.

h	31.908 cm.
$\bar{m}$	1.8454 mgm./sec.
w_g	7.7842 mgm.
ρ	2.7715×10^{-3} cm.
M	1.95782 mgm./sec.
$d_{25°C}$	1.0034 gm./ml.
f	1.0000 Kc./sec.
T	25°C

Equation for M :-

$$4.21805\ M - 0.30287\ M^{2/3} - 0.014450\ M^{4/3} - 7.78420 = 0$$

$\gamma_{-1.250} = 392.0$ dynes/cm.; $\gamma_{-0.400} = 419.0$ dynes/cm.

TABLE 3 RUN 24(a)

Ref.	E volts	C_p μF	G_p mMho	t sec.	t_g sec.
9	-1.200	0.1699	0.3400	0.89189	3.81777
10	-1.200	0.1878	0.4000	1.05092	3.81777
11	-1.200	0.2481	0.6000	1.65380	3.81777
12	-1.200	0.2984	0.8000	2.26795	3.81777

Potential is given with respect to a 0.100 N calomel electrode.

h	32.090 cm.
$\bar{m}$	1.8319 mgm./sec.
w_g	7.7168 mgm.
ρ	2.7468×10^{-3} cm.
M	1.94750 mgm./sec.
$d_{25°C}$	1.0034 gm./ml.
f	1.0000 Kc./sec.
T	25°C

Equation for M :-

$$4.21254\ M - 0.30089\ M^{2/3} - 0.01434\ M^{1/3} - 7.71684 = 0$$

$\gamma_{-1.200} = 392.6$ dynes/cm.

TABLE 4 RUN 38

Ref.	E volts	C_p μF	G_p mMho	t sec.	t_g sec.
13	-1.400	0.1485	0.3000	0.71914	3.60347
14	-1.400	0.1811	0.4000	0.98960	3.60347
15	-1.400	0.2092	0.5000	1.25493	3.60347
16	-1.400	0.2680	0.7000	1.87552	3.60347
17	-1.400	0.2948	0.8000	2.20006	3.60347
18	-1.400	0.3415	1.0000	2.83619	3.60347

Potential is given with respect to a 0.100 N calomel electrode.

h	32.209 cm.
$\bar{m}$	1.8048 mgm./sec.
w_g	7.7702 mgm.
ρ	2.7664×10^{-3} cm.
M	1.91794 mgm./sec.
$d_{25°C}$	1.0034 gm./ml.
f	1.0000 Kc./sec.
T	25°C

Equation for M :-

$$4.30535\ M - 0.30411\ M^{2/3} - 0.01432\ M^{1/3} - 7.77021 = 0$$

$\gamma_{-1.400} = 366.5$ dynes/cm.

1. A_1

In this calculation the flow rate was assumed to be independent of time - i.e. the effect of back pressure was neglected.

$$A_1 = K.\bar{m}^{2/3}.t^{2/3} \quad \ldots\ldots\ldots\ldots\ldots\ldots\ldots\ldots 59$$

where $K = (4\pi)^{1/3}(3/D_T)^{2/3}.10^{-2}$

$= 8.52833 \times 10^{-3}$ from equation 58.

Calculation of C_o using A_1 gave rise to a series of values of capacitance, which, for any one polarisation potential, increased as the birth-balance interval of the reading increased. The difference in C_o in a typical case was approximately 1.6% for birth-balance intervals of 0.7sec. and 2.8sec.

2. A_2

The trend experienced above could be eliminated by adding an empirical constant, c, to the expressin for A_1:

$$A_2 = K.\bar{m}^{2/3}t^{2/3} + c \quad \ldots\ldots\ldots\ldots\ldots\ldots\ldots\ldots 60$$

This constant was derived by plotting A_1 vs. C_s or $\bar{m}.t$ vs. $C_s^{3/2}$ and extrapolating to zero. In all cases the required constant was negative (table 7) and this result might imply that the mercury was breaking inside the capillary at the fall of a drop. There was no justification for using this method of calculation however, even although a constant set of capacitance values were obtained for unit area, since the action of back pressure had not been considered.

3. A_3

The areas of this series were derived from equivalent w_t values, using equation 53 which made allowance for back pressure.

$$A_3 = K.w_t^{2/3} \quad \text{.....61}$$

Calculated values of C_o again showed a trend however; in this instance, a decrease was observed as the birth-balance interval became longer.

4. A_4

In the integrated expressions giving w_t as a function of t, boundary conditions must be applied to give constants of integration corresponding to $t = 0$, and this is difficult because of the uncertainty about the physical mechanism of drop detachment. In the expression of Smith (30) used to derive equation 53, $w_{t=o} = 0$, whereas Los and Murray (59) put $w_{t=o} = \frac{2}{3}\pi\rho.D_T^3$.

Writing $$f(t) = Mt - \frac{1.5M^{2/3}t^{2/3}\gamma}{172.73h} - \frac{1.5M^{1/3}t^{1/3}\gamma^2}{(172.73h)^2}$$

and taking $$w_t = w_o + f(t) \quad \text{.....62}$$

Since by definition

$$C_s = C_o.A \text{ , then}$$

$$A_4 = K.\left\{w_o + f(t)\right\}^{2/3} \quad \text{.....63}$$

and $$C_s = C_oK\left\{w_o + f(t)\right\}^{2/3} \quad \text{.....64}$$

Therefore $$C_s^{3/2} = (C_oK)^{3/2}.w_o + (C_oK)^{3/2}.f(t) \quad \text{....65}$$

By plotting $C_s^{3/2}$ vs. $f(t)$, a straight line was produced with gradient $(C_oK)^{3/2}$ and intercept $(C_oK)^{3/2}.w_o$.(table 6)

In the above expression it was assumed that the area of the electrode was equal to the total area of the mercury sphere. This was erroneous since there was a small "screened area" where the mercury column in the capillary joined the drop, given by

$$A_s' = 2\pi r\,(r_t - \sqrt{r_t^2 - \rho^2}) \quad \ldots\ldots\ldots\ldots 66$$

It is seen that

$$\lim_{r/\rho \to \infty} A_s' = \pi\rho^2 = A_s \quad \ldots\ldots\ldots\ldots\ldots\ldots 67$$

In making allowance for A_s, the original approach was to calculate a mean "mass equivalent" of the screened area and to assume this to be independent of time. Values of A_4 were thus determined by finding w_o from a $C_s^{3/2}/f(t)$ plot and thence using it in equation 63.

5. A_5

While the calculation of A_4 and C_{o_4} was reasonably successful, a better approach was made by considering A_S, the screened area, in the construction of equations 63.

As before, $w_t = w_o + f(t)$

Writing $A' = Kw_t^{2/3}$, where A' is the total area of the mercury sphere, it is seen that the area of the electrode surface is given by

$$A_5 = K\left\{w_o + f(t)\right\}^{2/3} - A_s \quad \ldots\ldots\ldots 68$$

and hence $$C_s = C_o\left[K\left\{w_o + f(t)\right\}^{2/3} - A_s\right]$$

and $$(C_s + C_oA_s)^{3/2} = (C_oK)^{3/2}.w_o + (C_oK)^{3/2}.f(t) \quad \ldots\ldots\ldots 69$$

Equation 69 was solved by initially neglecting the term in A_s and determining an approximate C_o from a $C_s^{3/2}$ vs. $f(t)$ gradient as above. This approximate C_o value was used to calculate $(C_s + C_oA_s)^{3/2}$, as in table 6, which was then plotted against $f(t)$ (figure 15) to give a better value of C_o. This process was repeated until there was no further appreciable change in gradient or intercept and final values of these are included in table 7. The A_5 values of table 5 were calculated using equation 68 together with a mean w_o derived from four $(C_s + C_oA_s)^{3/2}$ vs. $f(t)$ plots.

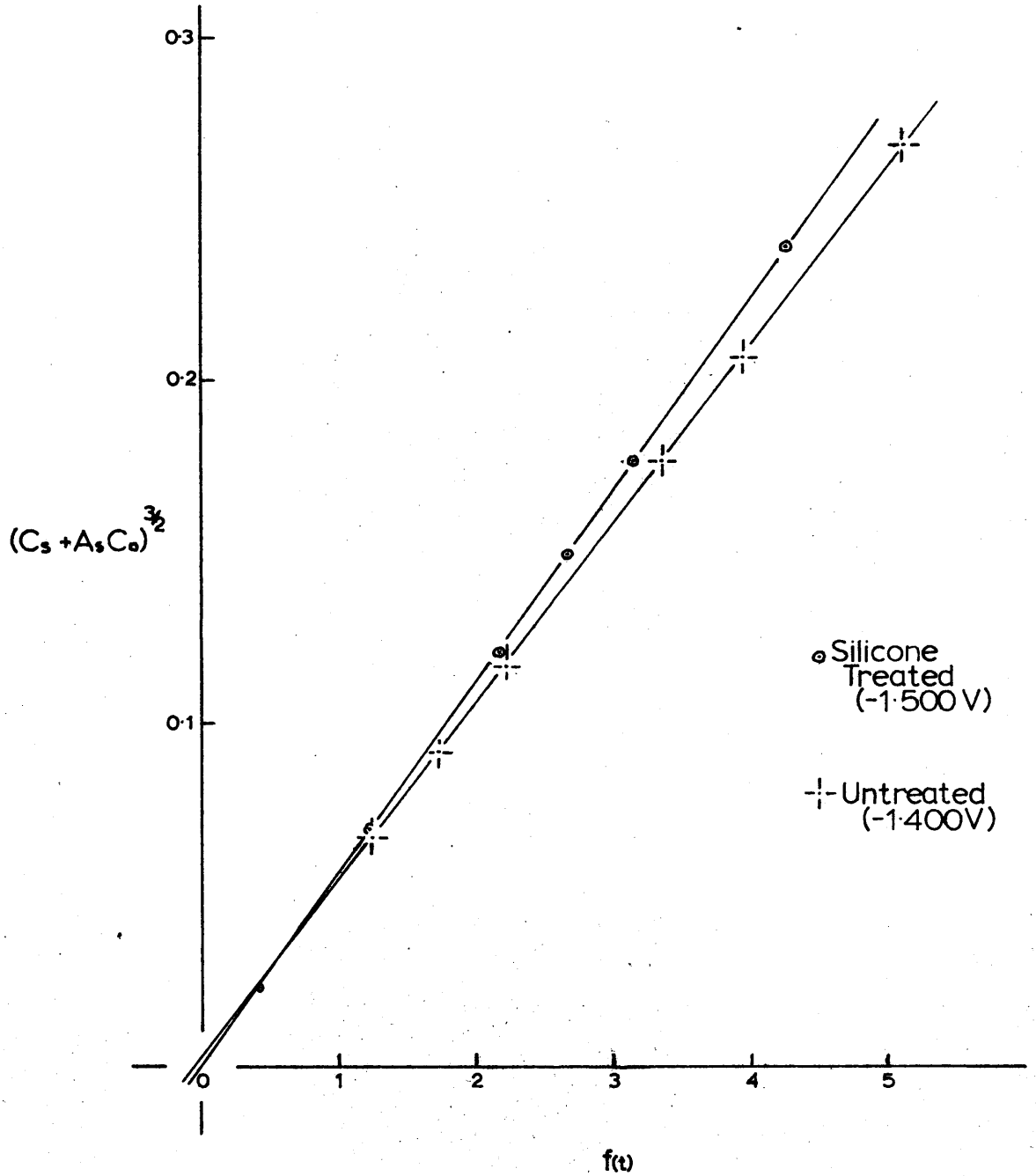
0·3
0·2
0·1
$(C_s + A_s C_o)^{\frac{3}{2}}$
0
1
2
3
4
5
f(t)
Silicone Treated (-1·500 V)
Untreated (-1·400V)

FIG. 15

TABLE 5

Ref.	C_s	A_1	A_2	A_3	A_4	A_5
1	0.17181	0.010924	0.010660	0.010607	0.010740	0.010735
2	0.22057	0.013947	0.013714	0.013665	0.013782	0.013775
3	0.28793	0.018086	0.017870	0.017848	0.017952	0.017941
4	0.35634	0.022313	0.022129	0.022153	0.022245	0.022234
5	0.39218	0.024538	0.024363	0.024420	0.024507	0.024496
6	0.34457	0.009115	0.008935	0.008739	0.008885	0.008881
7	0.51980	0.013620	0.013464	0.013268	0.013387	0.013380
8	0.58015	0.015182	0.015043	0.014846	0.014959	0.014950
9	0.18713	0.011831	0.011606	0.011524	0.011651	0.011645
10	0.20938	0.013198	0.012986	0.012906	0.013026	0.013019
11	0.28485	0.017856	0.017674	0.017626	0.017728	0.017719
12	0.35273	0.022040	0.021876	0.021879	0.021971	0.021960
13	0.16385	0.010147	0.009899	0.009879	0.010016	0.010011
14	0.20348	0.012554	0.012345	0.012311	0.012435	0.012428
15	0.23947	0.014708	0.014516	0.014494	0.014608	0.014599
16	0.31431	0.019926	0.019057	0.019084	0.019183	0.019173
17	0.34979	0.021385	0.021225	0.021282	0.021376	0.021364
18	0.41567	0.025330	0.025183	0.025304	0.025390	0.025378

TABLE 5 CONT.

Ref.	C_{o1}	C_{o2}	C_{o3}	C_{o4}	C_{o5}
1	15.73	16.12	16.20	16.00	16.00
2	15.81	16.08	16.14	16.00	16.01
3	15.92	16.11	16.13	16.03	16.04
4	15.97	16.10	16.09	16.02	16.03
5	15.98	16.10	16.06	16.00	16.01
6	37.80	38.56	39.43	38.78	38.80
7	38.16	38.61	39.18	38.82	38.84
8	38.21	38.57	39.08	38.78	38.81
9	15.82	16.12	16.24	16.06	16.07
10	15.86	16.12	16.22	16.07	16.08
11	15.95	16.12	16.16	16.07	16.07
12	16.00	16.12	16.12	16.05	16.06
13	16.15	16.55	16.58	16.36	16.37
14	16.21	16.48	16.53	16.36	16.37
15	16.28	16.50	16.52	16.39	16.40
16	16.35	16.49	16.47	16.38	16.39
17	16.36	16.48	16.44	16.36	16.37
18	16.41	16.51	16.43	16.37	16.38

TABLE 6

Ref.	C_s	$C_s^{3/2}$	$C_s+C_oA_s$	$(C_s+C_oA_s)^{3/2}$	$\bar{m}.t$	$f(t)$
1	0.17181	0.071215	0.17220	0.07146	L.44975	1.38715
2	0.22057	0.10359	0.22096	0.10387	2.09226	2.02827
3	0.28793	0.15450	0.28832	0.15482	3.08720	3.02762
4	0.35634	0.21272	0.35673	0.21306	4.23160	4.18650
5	0.39218	0.24560	0.39257	0.24597	4.88044	4.84528
6	0.34457	0.20227	0.34551	0.20309	1.10487	1.03724
7	0.51980	0.37478	0.52074	0.37578	2.01822	1.94047
8	0.58015	0.44190	0.58109	0.44296	2.37522	2.29686
9	0.18713	0.08095	0.18752	0.08120	1.63384	1.57079
10	0.20938	0.09581	0.20977	0.09607	1.92517	1.86158
11	0.28485	0.15203	0.28524	0.15234	3.02958	2.97115
12	0.35273	0.20949	0.35312	0.20984	4.15463	4.10909
13	0.16385	0.06632	0.16425	0.06656	1.29789	1.24671
14	0.20348	0.09179	0.20388	0.09206	1.78601	1.73447
15	0.23947	0.11719	0.23987	0.11748	2.26487	2.21558
16	0.31431	0.17621	0.31471	0.17655	3.38490	3.34746
17	0.34979	0.20688	0.35019	0.20723	3.97062	3.94195
18	0.41567	0.26799	0.41607	0.26837	5.11870	5.11078

TABLE 7

		Run 23 E=-1.250V	Run 23 E=-0.400V	Run 24(a) E=-1.200V	Run 38 E=-1.400V
$C_s^{3/2}$ vs. $\int t$	Gradient	0.05088	0.18808	0.05098	0.05277
	Intercept	-0.002657	-0.006156	-0.002361	-0.002348
	Mean Deviation	-	-	-	-
	w_o	-0.0326mgm	-0.0326 mgm	-0.0463mgm	-0.0445mgm
	C_o*	16.10	35.58	16.12	16.50
$C_s^{3/2}$ vs. $\int(t)$	Gradient	0.05049	0.190382	0.05063	0.05217
	Intercept	0.001348	0.004915	0.001508	0.001394
	Mean Deviation	2.203×10^{-4}	3.107×10^{-4}	0.744×10^{-4}	1.448×10^{-4}
	w_o	0.0267mgm	0.0258mgm	0.0297mgm	0.0267mgm
	C_o*	16.01	38.80	16.05	16.37
$(C_s+C_oA_s)^{3/2}$ vs. $\int(t)$	Gradient	0.05050	0.190460	0.05067	0.052205
	Intercept	0.001549	0.005539	0.001702	0.001602
	Mean Deviation	2.240×10^{-4}	3.098×10^{-4}	0.754×10^{-4}	1.501×10^{-4}
	w_o	0.0307mgm	0.0291mgm	0.0335mgm	0.0307mgm
	C_o*	16.02	38.82	16.06	16.38

* μF/sq.cm.

Significance of w_o

Four independent determinations of w_o are given in table 8 (a). It is significant that for the one capillary, w_o is reasonably constant and is not greatly affected by changing interfacial tension and differential capacitance. It is, however, very unlikely that w_o represents the actual mass of mercury at t =0. The constant which has been added to Smith's equation is not the integration constant which would have been derived if the initial boundary conditions were changed to that of a drop of mass w_o, since the other terms in equation 53 would also have been affected. While certain further corrections would be necessary in order to use equation 53 below t = 0.5 seconds as was noted above, the experimental value of w_o is too large to be explained by this alone.

The high speed photographic observations of Newcombe (63) and of McNevil and Balis (69) were of interest. The former seemed to agree with the existence of an actual "rest mass". Graphical integration of enlarged photographs gave values for w_o/w_g of up to 1.4%, compared with a value of 0.5% in the present work. Newcombe, however, used a very fast flow rate which caused the new drop emanating from the capillary orifice to catch up and re-unite with the previous drop. This process was repeated after several successive breakaways for each drop and each time w_o became larger. At the first breakaway, the rest mass was very small and might well be considered

TABLE 8(a)

Ref.	E volts	$(C_oK)^{3/2}.w_o$ Intercept	$(C_oK)^{3/2}$ Gradient	w_o Mgm.
1- 5	-1.250	0.005539	0.190460	0.0291
6- 8	-0.400	0.001549	0.050494	0.0307
9-12	-1.200	0.001702	0.050668	0.0335
13-18	-1.400	0.001602	0.052205	0.0307

$\bar{w}_o$ = 0.0304 mgm.

TABLE 8(b)

Ref.	$(C_s+C_oA_s)^{3/2}$ vs. $f(t)$ Intercept	$(C_s+C_oA_s)_{t=o}$ μF	$(C_oA_s)_{t=o}$ μF	$(C_s)_{t=o}$ μF	C_o μF/sqcm	A_o sq.cm.
1- 5	0.005539	0.03130	0.00094	0.03036	38.82	7.82×10^{-4}
6- 8	0.001549	0.01339	0.00038	0.01301	16.02	8.12×10^{-4}
9-12	0.001702	0.01425	0.00039	0.01386	16.06	8.63×10^{-4}
13-18	0.001602	0.01370	0.00040	0.01284	16.38	8.13×10^{-4}

$\bar{A}_o$ = 8.17×10^{-4} sq.cm.

to be equal in volume to $\frac{2}{3}\pi\rho^3$ as suggested by Los and Murray. It was improbable that a re-uniting effect occurred with the relatively slow flow rates used in the present works. In the photographs of MacNevin and Balis, some very curious phenomena were apparent in which the drop remained attached to the capillary by a long thread of mercury. Such situations, howevr, were only detected in cases of anodic polarisation.

The most probable explanation for the existence of w_o in equation 63 and 68 is that it represents a "wetted area" caused by creep of solution up the capillary between the glass wall and the mercury column. Determinations of the wetted area, A_o, from the results of Runs 23, 24(a), and 38 are given in table 8(b), and it is seen that the height of creep would be approximately 0.5m.m.

In order to test this theory, the bore of a capillary was treated with a water-repellant substance to reduce solution creep. A very pure dimethyl silicone fluid (F 111), kindly given by the Nobel Division of Imperial Chemical Industries Ltd., was dissolved in fifty times its volume of carbon tetrachloride and the tip of a capillary was placed in this solution. Excess solution was blown out by dust-free nitrogen and the capillary, still with gas passing through it, was baked in an oven for several hours. Although the temperature required to cross-link such a silicone and cure it onto the glass is very high, the temperature was not raised above 450°C

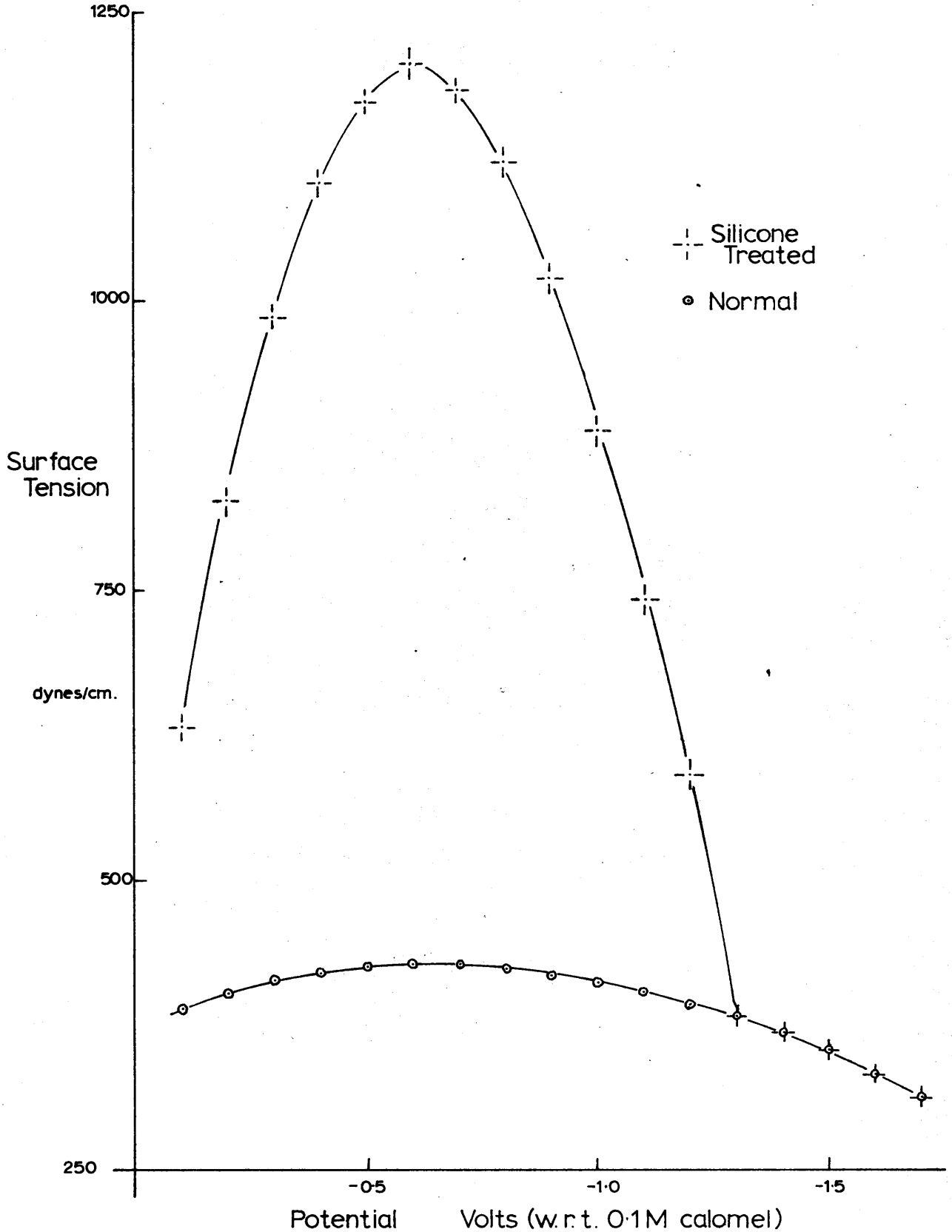

FIG. 16 0·1 M KCl ELECTROCAPILLARY CURVES

in case the thin Pyrex capiallary would become distorted or the silicone be destroyed. Surface tension and differential capacitance measurements in 0.1 M potassium chloride aqueous solutions showed that the film on the capiallary bore tended to strip off when the capillary was used as a D.M.E., and thus affect the ionic structure of the double layer (figure 16) . In further experiments, using "Araldite" epoxy resin as anti-wetting agent, the resin plus hardener were dissolved in a mixture of carbon tetrachloride and ethanol and a capillary treated as before. While a thin resin film was strongly bonded to the glass its water-repellant properties were not great, and it tended to roughen the interior of the capillary leading to erratic mercury flow. Tests were also carried out using a chlorsilane and a methyl hydrogen polysiloxane as anti-wetting agents, but it was found extremely difficult to achieve strong bonding to the glass with these substances.

At potentials more cathodic than -1.3 volts with respect to the 0.1 M calomel electrode, the interference to interfacial tension and differential capacitance of 0.1 M potassium chloride solution caused by the dimethyl silicone treatment of the capillary, was negligible (figure 16). Experiments were therefore carried out at -1.5 volts to investigate the effect of the silicone treatment on the area-time relationship.

TABLE 9 Run 42

Ref.	E volts	C_p μF	G_p mMho	t sec.	t_g sec.
19	-1.500	0.0789	0.1000	0.35527	3.52500
20	-1.500	0.1539	0.3000	0.99326	3.52500
21	-1.500	0.2151	0.5000	1.70280	3.52500
22	-1.500	0.2440	0.6000	2.08581	3.52500
23	-1.500	0.2685	0.7000	2.45341	3.52500
24	-1.500	0.3216	0.9000	3.30308	3.52500

Potential is given with respect to a 0.100 N calomel electrode.

h	28.746 cm.
$\bar{m}$	1.2973 mgm./sec.
w_g	4.5731 mgm.
ρ	1.9625×10^{-3} cm.
M	1.38761 mgm./sec.
d	1.0034 gm./ml.
f	f.0000 Kc./sec.
T	25°C

Equation for M :-

$$3.52500\ M - 0.24560\ M^{2/3} - 0.01141\ M^{1/3} - 4.57312 = 0$$

γ = 351.0 dynes/cm.

TABLE 10

Ref.	C_s	A_1	A_3	$*A_6$	C_{o1}	C_{o3}	C_{o6}
19	0.08211	0.005089	0.004779	0.004767	16.14	17.18	17.22
20	0.16871	0.010099	0.009817	0.009805	16.71	17.19	17.20
21	0.24454	0.014466	0.014244	0.014232	16.90	17.17	17.18
22	0.28137	0.016561	0.016376	0.016364	16.99	17.18	17.19
23	0.31473	0.018434	0.018304	0.018292	17.06	17.19	17.20
24	0.38540	0.022500	0.022435	0.022423	17.13	17.18	17.19

* Note :- $A_6 = A_3 - A_s$

Ref.	$C_s^{3/2}$	$C_s + C_oA_s$	$(C_s + C_oA_s)^{3/2}$	$f(t)$
19	0.02353	0.08232	0.02362	0.41948
20	0.06930	0.16892	0.06943	1.23501
21	0.12093	0.24475	0.12108	2.15850
22	0.14925	0.28158	0.14942	2.66083
23	0.17656	0.31494	0.17674	3.14454
24	0.23926	0.38561	0.23945	0.26670

TABLE 11

Run 42

	$C_s^{3/2}$ vs. $f(t)$	$(C_s+C_oA_s)^{3/2}$ vs. $f(t)$
Gradient	0.05609	0.05612
Intercept	zero	0.00009
Mean Deviation	0.977×10^{-4}	1.012×10^{-4}
w_o	zero	0.002 mgm.
C_o	17.18 μF/sq.cm.	17.19 μF/sq.cm.

Ref.	$(C_s+C_oA_s)^{3/2}$ vs. $f(t)$ Intercept	$(C_s + C_oA_s)_{t=o}$ μF	C_oA_s μF	$(C_s)_{t=o}$ μF	C_o μF/sq.cm.	A_o sq.cm.
19-24	0.000090	0.00199	0.00021	0.00178	17.19	1.03×10^{-4}

Results of a typical experiment, Run 42, are shown in table 9. In table 10, values of A and C_o are calculated, while table 11 gives the results of the $(C_s + C_oA_s)^{3/2}$ vs. f(t) plot which is is illustrated in figure 15. It is seen that the silicone treatment has reduced w_o by x15 and A_o by x8 as compared with an untreated capillary of similar bore. These calculations thus support the theory that the constant in the equations for w_o is introduced to make allowance for solution creep in untreated capillaries.

Conclusions.

The conclusion drawn from the area-time investigations is that the best possible method of calculating differential capacitance per unit area is to use equation 69 and hence find C_o from the gradient of a $(C_s + C_o A_s)^{3/2}$ vs. f(t) plot. This operation may be rapidly carried out using a least squares programme on the Deuce computer. The calculation is completely free from empirical or experimental constants, but requires that the electrode impedance is measured at several instants during the life of a drop.

A simpler and quite accurate method is to use equation 68 to calculate the area of the electrode at one instant. This assumes that for any given solution and capillary, w_o remains constant and needs to be determined only once. This method is sufficiently accurate for most purposes.

Tables 12-18 show the result of differential capacitance measurements in 0.1M potassium chloride over the range of potentials from -0.1 volts to -1.7 volts with respect to the 0.1 M calomel electrode. For purposes of comparison, A_1, A_3, A_4 and A_5 have been calculated as described above and the values of C_{o_1}, C_{o_3}, C_{o_4} and C_{o_5} are given.

TABLE 12 RUN 18

E volts	C_T μF	G_T mMho	t sec.	t_g sec.	C_s μF	γ dyne/cm
-0.800	0.1980	0.4950	0.86557	4.05559	0.22935	422.1
-0.900	0.2052	0.4950	1.02046	4.01777	0.23545	418.4
-1.000	0.2139	0.5000	1.16895	3.96886	0.24350	413.6
-1.100	0.2200	0.5000	1.28178	3.87812	0.24878	404.7
-1.200	0.2200	0.5000	1.33074	3.77578	0.24878	394.6

h	32.159 cm.
$\bar{m}$	1.86862 mgm./sec.
w_g	7.7128 mgm.
ρ	2.7450×10^{-3} cm.
M	1.98631 mgm./sec.
d	1.0034 gm./ml.
f	1 Kc./sec.
T	25°C

A_1 sq.cm.	A_3 sq.cm.	A_4 sq.cm.	A_5 sq.cm.	C_{o_1} μF/sqcm	C_{o_3} μF/sqcm	C_{o_4} μF/sqcm	C_{o_5} μF/sqcm
0.011749	0.011382	0.011506	0.011500	19.52	20.15	19.93	19.94
0.013118	0.012764	0.012881	0.012874	17.95	18.45	18.28	18.29
0.014360	0.014031	0.014142	0.014135	16.96	17.35	17.22	17.23
0.015266	0.014972	0.015080	0.015071	16.29	16.61	16.50	16.51
0.015654	0.015387	0.015494	0.015485	15.89	16.16	16.06	16.06

Equation for M :-

$$4.12755\ M - 0.29619\ M^{2/3} - 0.01417\ M^{1/3} - 7.71282 = 0$$

Potential with respect to 0.100 N calomel electrode.

TABLE 13 RUN 19

E volts	C_T μF	G_T mMho	t sec.	t_g sec.	C_s μF	γ dyne/cm
-1.700	0.2138	0.5000	1.04432	3.11300	0.24342	319.5
-1.600	0.2160	0.5000	1.13449	3.30200	0.24532	337.8
-1.500	0.2159	0.5000	1.21429	3.47660	0.24523	354.7
-1.400	0.2180	0.5000	1.28847	3.61952	0.24705	368.4
-1.300	0.2185	0.5000	1.33201	3.76308	0.24748	382.2
-1.200	0.2199	0.4990	1.33620	3.88712	0.24858	394.1
-1.100	0.2190	0.5000	1.31426	3.98161	0.25044	403.1

h	31.855 cm.
$\bar{m}$	1.8590 mgm./sec.
w_g	7.8472 mgm.
ρ	2.7948×10^{-3} cm.
M	1.96113 mgm./sec.
d	1.0034 gm./ml.
f	1 Kc./sec.
T	25°C

A_1 sq.cm.	A_3 sq.cm.	A_4 sq.cm.	A_5 sq.cm.	C_{o1} μF/sq.cm	C_{o3} μF/sqcm	C_{o4} μF/sqcm	C_{o5} μF/sqcm
0.013272	0.013067	0.013183	0.013176	18.34	18.63	18.46	18.47
0.014025	0.013787	0.013900	0.013892	17.49	17.79	17.65	17.66
0.014676	0.014405	0.014516	0.014508	16.71	17.02	16.89	16.90
0.015267	0.014970	0.015078	0.015070	16.18	16.50	16.38	16.39
0.015609	0.015282	0.015389	0.015381	15.85	16.19	16.08	16.09
0.015642	0.015286	0.015393	0.015385	15.89	16.26	16.15	16.15
0.015471	0.015092	0.015199	0.015199	16.18	16.59	16.48	16.49

Equation for M :-

$$4.22119\ M - 0.30400\ M^{2/3} - 0.01459\ M^{1/3} - 7.84719 = 0$$

Potential is given with respect to 0. 100 N calomel electrode.

TABLE 14 RUN 20

E volts	C_p μF	G_p mMho	t sec.	t_g sec.	C_s μF	γ dyne/cm
-1.700	0.2100	0.4995	1.00531	2.98770	0.24009	307.1
-1.600	0.2170	0.4995	1.14013	3.21027	0.24612	328.7
-1.500	0.2200	0.4995	1.23844	3.40965	0.24873	347.9
-1.400	0.2207	0.5000	1.30692	3.57796	0.24939	364.2
-01.300	0.2300	0.5210	1.43475	3.71740	0.25989	377.5
-1.200	0.2300	0.5210	1.45256	3.82649	0.25989	388.0

h	31.530 cm.
$\bar{m}$	1.83966 mgm./sec.
w_a	7.83404 mgm.
ρ	2.7899×10^{-3} cm.
M	1.95739 mgm./sec.
d	1.0034 gm./ml.
f	1 Kc./sec.
T	25° C

A_1 sq.cm.	A_3 sq.cm.	A_4 sq.cm.	A_5 sq.cm.	C_{o1} μF/sqcm	C_{o3} μF/sqcm	C_{o4} μF/sqcm	C_{o5} μF/sqcm
0.012850	0.012735	0.012853	0.012846	18.69	18.85	18.68	18.69
0.013974	0.013838	0.013943	0.013935	17.61	17.79	17.65	17.66
0.014766	0.014591	0.014700	0.014692	16.84	17.05	16.92	16.93
0.015306	0.015100	0.015207	0.015199	16.29	16.52	16.40	16.41
0.016288	0.016064	0.016168	0.016160	15.96	16.18	16.07	16.08
0.016423	0.016175	0.016278	0.016269	15.83	16.07	15.97	15.97

Equation for M :-

$$4.25842\ M - 0.30845\ M^{2/3} - 0.01489\ M^{1/3} - 7.83404 = 0 .$$

Potential is given with respect to 0.100 N calomel electrode.

TABLE 15 RUN 21

E volts	C_T μF	G_T mMho	t sec.	t_g sec.	C_s μF	γ dyne/cm
-1.700	0.2050	0.4600	0.96399	3.02270	0.23115	312.7
-1.600	0.2080	0.4600	1.05532	3.21609	0.23377	331.6
-1.500	0.2120	0.4600	1.14351	3.39503	0.23728	349.0
-1.400	0.2120	0.4600	1.20582	3.55226	0.23728	364.3
-1.300	0.2135	0.4600	1.25561	3.70077	0.23860	378.6
-1.200	0.2139	0.4600	1.26016	3.82084	0.23896	390.2
-1.100	0.2110	0.4600	1.20032	3.92341	0.23640	400.1
-1.000	0.2079	0.4600	1.11413	4.01811	0.23368	409.2
-0.900	0.2000	0.4600	0.97001	4.08879	0.22680	416.0
-0.800	0.1921	0.4590	0.82123	4.14876	0.21988	421.7
-0.700	0.1879	0.4590	0.67545	4.17800	0.21630	424.5
-0.600	0.2740	1.0000	0.95659	4.18865	0.36645	425.5
-0.554	0.2438	0.9000	0.66725	4.19496	0.32796	426.1
-0.500	0.2479	1.0000	0.65017	4.17992	0.35008	424.7
-0.400	0.2860	1.3000	0.84498	4.12645	0.43568	419.6
-0.350	0.2849	1.3000	0.86160	4.08372	0.43516	415.5
-0.300	0.2880	1.3000	0.87341	4.02996	0.43664	410.3
-0.250	0.2900	1.3470	0.84475	3.97961	0.44848	405.5
-0.100	0.2954	2.0000	0.75858	3.76739	0.63840	385.1

h	32.100 cm.
$\bar{m}$	1.86100 mgm./sec.
w_g	7.8068 mgm.
ρ	2.7799×10^{-3} cm.
M	1.96334 mgm./sec.
d	1.0034 gm./ml.
f	1 Kc./sec.
T	25°C

A_1 sq.cm.	A_3 sq.cm.	A_4 sq.cm.	A_5 sq.cm.	C_{o1} µF/sqcm	C_{o3} µF/sqcm	C_{o4} µF/sqcm	C_{o6} µf/sqcm
0.012591	0.012400	0.012519	0.012513	08.36	18.64	18.46	18.47
0.013375	0.013151	0.013267	0.013259	17.48	17.78	17.62	17.63
0.014410	0.013855	0.013967	0.013960	16.81	17.13	16.99	17.00
0.014618	0.014333	0.014443	0.014435	16.23	16.56	16.43	16.44
0.015018	0.014703	0.014812	0.014704	15.88	16.23	16.11	16.12
0.015054	0.014712	0.014821	0.014813	15.87	16.24	16.12	16.13
0.014597	0.014239	0.014340	0.014332	16.19	16.61	16.49	16.49
0.013867	0.013473	0.013587	0.013580	16.85	17.34	17.20	17.21
0.012644	0.012329	0.012349	0.012343	17.94	18.55	18.36	18.37
0.011315	0.010885	0.011013	0.011007	19.43	20.20	19.96	19.98
0.009933	0.009497	0.009634	0.009629	21.77	22.78	22.45	22.46
0.012527	0.012091	0.012211	0.012205	29.25	30.31	30.00	30.02
0.009853	0.009413	0.009551	0.009547	33.29	34.84	34.34	34.35
0.009684	0.009248	0.009386	0.009382	36.15	37.86	37.30	37.31
0.011533	0.011107	0.011233	0.011228	37.78	39.22	38.78	38.80
0.011683	0.011267	0.011392	0.011386	37.25	38.62	38.20	38.22
0.011790	0.011385	0.011509	0.011503	37.04	38.35	37.94	37.96
0.011530	0.011135	0.011261	0.011255	38.90	40.28	39.82	39.85
0.010732	0.010377	0.010507	0.010502	59.48	61.52	60.76	60.79

Equation for M :-

$$4.19496\ M - 0.29996\ M^{2/3} - 0.01430\ M^{1/3} - 7.80682 = 0$$

Potential is given with respect to 0.100 N calomel electrode.

TABLE 16 RUN 22

E volts	C_T μF	G_T mMho	t sec.	t_g sec.	C_s μF	$\mathcal{T}$ dyne/cm
-1.700	0.2021	0.4600	0.97366	3.02109	0.22862	309.8
-1.600	0.2049	0.4600	1.06466	3.29262	0.23106	336.0
-1.500	0.2080	0.4600	1.15936	3.46337	0.23377	352.5
-1.400	0.2100	0.4600	1.22808	3.63723	0.23552	369.2
-1.300	0.2108	0.4600	1.27505	3.78083	0.23623	383.0
-1.200	0.2121	0.4600	1.28804	3.89934	0.23737	394.3
-1.100	0.2102	0.4600	1.24086	4.00155	0.23570	404.0
-1.000	0.2062	0.4600	1.14447	4.08674	0.23220	412.1
-0.900	0.2019	0.4600	1.01924	4.16142	0.22845	419.2
-0.800	0.1955	0.4590	0.86866	4.21968	0.22280	424.7
-0.700	0.1839	0.4600	0.71532	4.25739	0.21304	428.3
-0.554	0.2590	1.2000	0.83873	4.26605	0.39983	429.1
-0.400	0.3450	1.8000	1.31597	4.20618	0.58288	423.4
-0.350	0.3475	1.8000	1.35424	4.16332	0.58367	419.4
-0.300	0.3500	1.8000	1.37572	4.11495	0.58449	414.7
-0.275	0.3468	1.8000	1.35437	4.08722	0.58345	412.1
-0.250	0.3440	1.8000	1.31774	4.06082	0.58258	409.6
-0.200	0.3058	1.6000	0.94966	3.99936	0.51785	403.8
-0.100	0.2550	1.6000	0.54295	3.85604	0.50930	390.1

h	31.496 cm.
$\bar{m}$	1.79405 mgm./sec.
w_g	7.6535 mgm.
ρ	2.7235×10^{-3} cm.
M	1.90995 mgm/sec.
d	1.0034 gm./ml.
f	1 Kc./sec.
T	25°C

A_1 sq.cm.	A_3 sq.cm.	A_4 sq.cm.	A_5 sq.cm.	C_{o_1} µF/sqcm	C_{o_3} µF/sqcm	C_{o_4} µF/sqcm	C_{o_5} µF/sqcm.
0.012370	0.012245	0.012365	0.012359	08.48	18.67	18.49	18.50
0.013129	0.012959	0.013076	0.013069	17.60	17.83	17.67	17.68
0.013896	0.013701	0.013814	0.013807	16.82	17.06	16.92	16.93
0.014440	0.014214	0.014325	0.014317	16.31	16.57	16.44	16.45
0.014806	0.014553	0.014662	0.014654	15.96	16.23	16.11	16.12
0.014906	0.014627	0.014736	0.014728	15.92	16.22	16.10	16.11
0.014540	1.014233	0.014344	0.014336	16.21	16.56	16.43	16.44
0.013777	0.013442	0.013556	0.013549	16.85	17.27	17.13	17.14
0.012753	0.012391	0.012510	0.012504	17.91	18.44	18.26	18.27
0.011464	0.011079	0.011206	0.011200	19.44	20.11	19.88	19.89
0.010071	0.009672	0.009807	0.009803	21.15	22.03	21.72	21.73
0.011199	0.010803	0.010931	0.010926	35.70	37.01	36.58	36.60
0.015121	0.014774	0.014882	0.014874	38.55	39.45	39.17	39.19
0.015413	0.015079	0.015186	0.015178	37.87	38.71	38.43	38.46
0.015575	0.015255	0.015561	0.015353	37.53	38.32	38.05	38.07
0.015414	0.015098	0.015205	0.015197	37.85	38.65	38.37	38.40
0.015135	0.014821	0.014929	0.014921	38 49	39.31	39.02	39.04
0.012166	0.011833	0.011955	0.011949	42.57	43.76	43.31	43.34
0.008380	0.008049	0.008198	0.008195	60.77	63.27	62.13	62.15

Equation for M :-

$4.26605\ M - 0.30915\ M^{2/3} - 0.01494\ M^{1/3} - 7.65351 = 0$

Potential is given with respect to 0.100 N calomel electrode.

TABLE 17 RUN 24(b)

E volts	C_p μF	G_p mMho	t sec.	t_g sec.	C_s μF	γ dyne/cm
-1.200	0.1878	0.4000	1.05392	3.81777	0.20938	391.1
-0.700	0.1680	0.4000	0.60428	4.21005	0.19212	428.9
-0.600	0.3215	1.2000	1.29830	4.22770	0.44153	430.6
-0.500	0.4530	1.8220	1.45699	4.21346	0.59121	429.2
-0.400	0.3455	1.8220	1.31914	4.16437	0.58888	424.5
-0.350	0.3468	1.8220	1.34955	4.12645	0.58927	420.8
-0.300	0.3488	1.8220	1.37166	4.07863	0.58988	416.2
-0.200	0.2950	1.5000	0.90701	3.95657	0.48820	404.5
-0.100	0.3598	3.0000	1.53204	3.81139	0.99341	390.5

h	32.090 cm.	M	1.94750 mgm.
$\bar{m}$	1.83189 mgm./sec.	d	1.0034 gm./ml.
w_g	7.7168 mgm.	f	1 Kc./sec.
ρ	2.7468×10^{-3} cm.	T	25°C

TABLE 18 RUN 39

E volts	C_p μF	G_p mMho	t sec.	t_g sec.	C_s μF	γ dyne/cm
-0.500	0.2363	1.0000	0.63318	4.29288	0.34350	424.5
-0.500	0.2781	1.3200	0.89586	4.29288	0.43681	424.5

h	32.142 cm.	M	1.91378 mgm./sec.
$\bar{m}$	1.80049 mgm./sec.	d	1.0034 gm./ml.
w_g	7.7456 mgm.	f	1 Kc./sec.
ρ	2.7353×10^{-3} cm.	T	25°C

A_1 sq.cm.	A_3 sq.cm.	A_4 sq.cm.	A_5 sq.cm.	C_{o1} μF/sqcm	C_{o3} μF/sqcm	C_{o4} μF/sqcm	C_{o5} μF/sqcm
0.013198	0.012906	0.013026	0.013019	15.86	16.22	16.07	16.08
0.009126	0.008730	0.008872	0.008869	21.05	22.01	21.65	21.66
0.015195	0.014836	0.014945	0.014937	29.06	29.76	29.54	29.56
0.016410	0.016068	0.016172	0.016163	36.03	36.80	36.56	36.58
0.015358	0.015015	0.015123	0.015114	38.34	39.22	38.94	38.96
0.015593	0.015262	0.015369	0.015360	37.79	38.61	38.34	38.36
0.015763	0.015445	0.015551	0.015542	37.42	38.19	37.93	37.95
0.011964	0.011633	0.011756	0.011770	40.81	41.96	41.52	41.55
0.016969	0.016730	0.016832	0.016823	58.54	59.37	59.02	59.05

Equation for M :-

$4.21254\ M - 0.30089\ M^{2/3} - 0.01434\ M^{1/3} - 7.71684 = 0$

Potential is given with respect to 0.100 N calomel electrode.

A_1 sq.cm.	A_3 sq.cm.	A_4 sq.cm.	A_5 sq.cm.	C_{o1} μF/sqcm	C_{o3} μF/sqcm	C_{o4} μF/sqcm	C_{o5} uF/sqcm
0.009307	0.008920	0.009064	0.009060	36.91	38.51	37.90	37.91
0.011730	0.011354	0.011481	0.011476	37.24	38.47	38.04	38.06

Equation for M :-

$4.30193\ M - 0.30458\ M^{2/3} - 0.01438\ M^{1/3} - 7.74558 = 0$

Potential is given with respect to 0.100 N calomel electrode.

TABLE 19

E volts	C_{o_1} μF/sqcm	C_{o_3} μF/sqcm	C_{o_4} μF/sqcm	C_{o_5} μF/sqcm	C_o* μF/sqcm
-1.700	18.46	18.69	18.52	18.53	-
-1.600	17.54	17.79	17.65	17.66	17.70
-1.500	16.80	17.08	16.93	16.95	16.96
-1.400	16.25	16.54	16.40	16.41	16.40
-1.300	15.91	16.21	16.10	16.10	16.10
-1.200	15.90	16.20	16.08	16.09	16.09
-1.100	16.19	16.57	16.47	16.48	16.46
-1.000	16.88	17.32	17.19	17.19	17.17
-0.900	17.93	18.47	18.30	18.31	18.30
-0.800	19.46	20.15	19.92	19.93	19.92
-0.700	21.46	22.26	21.94	21.95	21.93
-0.600	29.15	30.03	29.77	29.79	29.76
-0.500	37.1	38.5	37.9	37.9	37.9
-0.400	38.2	39.3	39.0	39.0	39.1
-0.300	37.3	38.3	38.0	38.0	38.1
-0.200	41.7	42.9	42.4	42.5	42.8
-0.100	59.6	61.4	60.6	60.7	-

* Interpolated results of D.C. Grahame

Potential is given with respect to 0.100 N calomel electrode

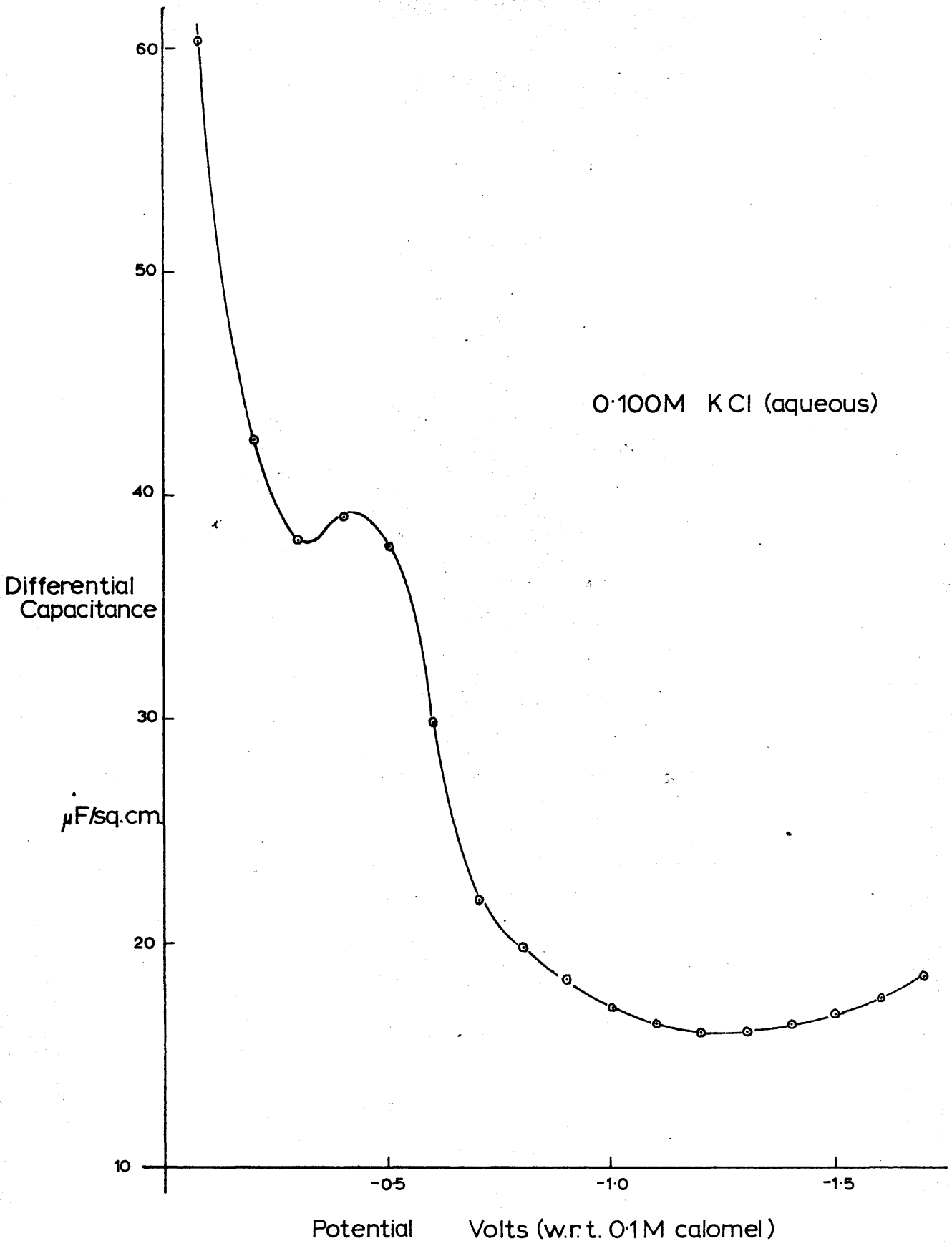
60
50
40
30
20
10
0·100M KCl (aqueous)
Differential Capacitance
μF/sq.cm.
-0·5
-1·0
-1·5
Potential Volts (w.r.t. 0·1M calomel)

FIG. 17

Table 19 includes the mean C_o values for all the experiments and figure 17 is a graph of $C_{o\frac{vs}{5}}$ polarisation potential. Table 19 also gives the interpolated results of unpublished data of Grahame, kindly made available by Dr. R. Parsons. While the method of calculation of these results is undisclosed, it is seen that they are almost identical to the $C_{o\,5}$ results of the present work. In subsequent calculations, equation 68 has been adopted for the determination of area.

Table 20 and figure 18 show the variation of interfacial tension with applied potential. In calculating γ by Tate's Law, using equation 56, w_g was taken to be equal to $f(t)$ and not to $f(t)+w_o$, since it was considered that the w_o term did not represent an actual rest mass. Also included in table 20 and figure 18 are interpolated results of electrocapillary measurements of Devanathan and Peries (27) and interfacial tension values derived by double integration of the C_o/E curve obtained in the present work. It is seen that all these sets of results agree well on the anodic branch of the curve, but that some deviation occurs for the Tate's Law values on the cathodic branch. This is believed to be due to irregularities in the mercury/solution boundary at the capillary orifice caused by solution creep. Comparison of the results shows sufficient agreement, however, for the Tate's Law values to be used in the back pressure corrections.

TABLE 20

E volts	γ_1 dynes/cm.	γ_2 dynes/cm.	γ_3 dynes/cm.
0.000	365.1	-	-
-0.100	387.7	388.5	388.0
-0.200	401.1	402.0	401.5
-0.300	413.3	413.7	413.6
-0.400	420.2	421.2	421.5
-0.500	424.5	425.0	425.5
-0.600	425.8	425.5	426.0
-0.700	425.3	423.3	424.0
-0.800	422.6	419.1	419.5
-0.900	417.7	412.4	413.1
-1.000	411.4	403.7	404.6
-1.100	403.0	394.0	395.0
-1.200	392.3	382.5	384.0
-1.300	380.3	366.6	371.0
-1.400	366.5	354.5	-
-1.500	351.0	334.0	-
-1.600	333.5	-	-
-1.700	312.3	-	-

γ_1 :- Tate's Law

γ_2 :- Interpolated data from double integration of C_o/E curve.

γ_3 :- Interpolated data of Devanathan and Peries. (27)

Potential is given with respect to 0.100 N calomel electrode.

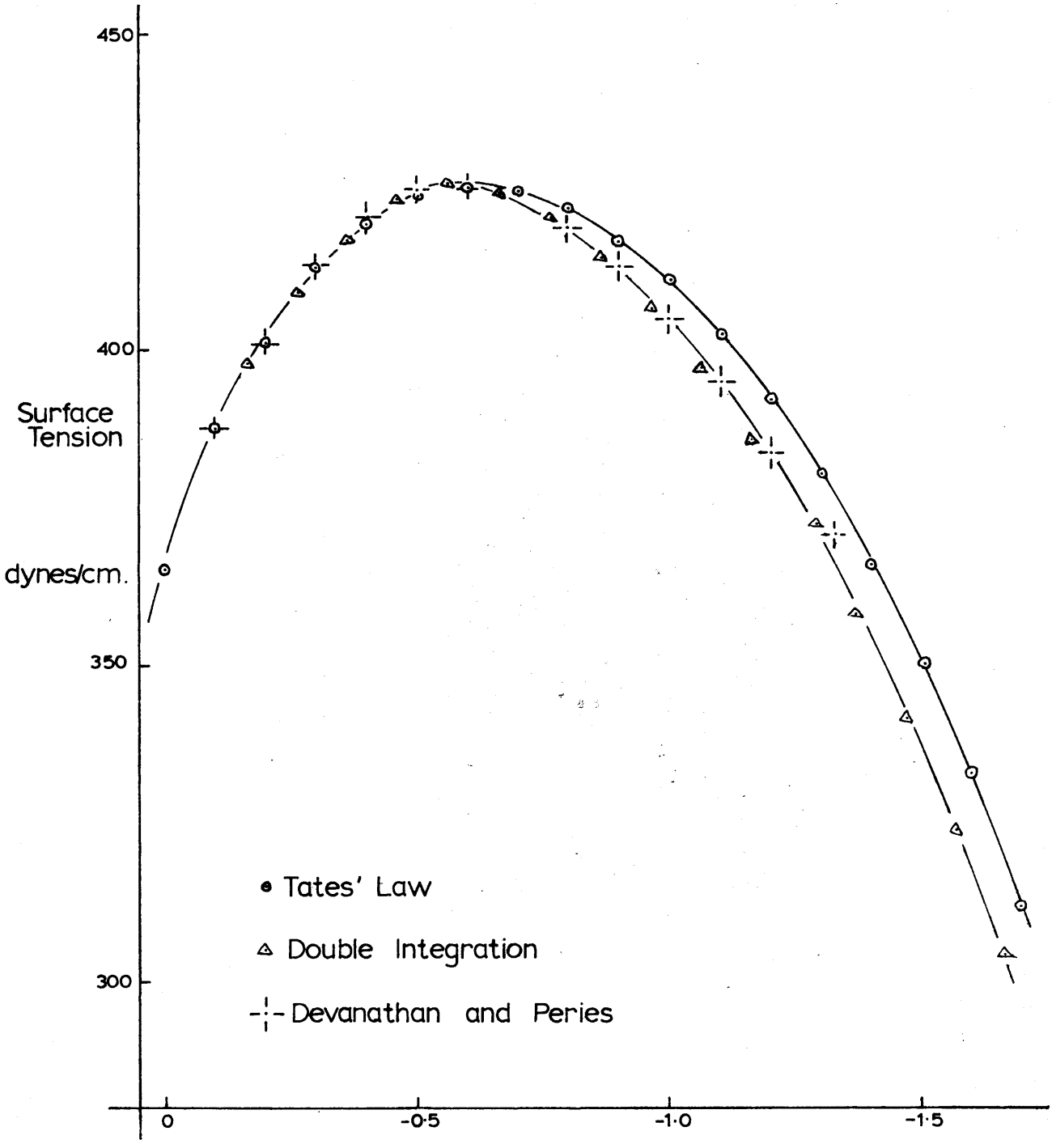

FIG. 18 0·100 M KCl ELECTROCAPILLARY CURVE

CAPACITANCE SHIELDING BY CAPILLARY TIP

While there is very little data on the subject, it is unlikely that capillaries as fine as those used in the present work would have much effect; Grahame (49) has noted that blunt capillaries gave abnormally high capacitance values. The double layer capacitance lies mainly within a few Å-units of the metal/solution interface, and thus the alteration in dielectric constant caused by the presence of the glass at a considerable distance from the O.H.P. is likely to have little effect. In support of this, it may be noted that Parsons (70) has shown that the shape of the Pt-gauze anode is not important, and Peacock (56) has pointed out that the position of the capillary tip within the gauze does not affect the electrode capacitance.

A different situation arises with an unpolarised electrode where the diffusion layer is relatively thick and is cut by the capillary tip. Thus Matsuda (71) made allowance for capillary shielding in applying boundary conditions to the diffusion layer in his consideration of polarographic processes.

THE EFFECT OF FREQUENCY.

Several experiments were carried out to measure differential capacitance at various frequencies of bridge measuring signal in order to confirm the equivalent circuit of the double layer at a perfectly polarised electrode.

Due to the difficulty of re-tuning the amplifier in a short time during an experiment, only few measurements could be made during any one run. At low frequencies, the accuracy of the measurements decreased due to the rate of amplitude modulation near the balance point approaching the rate of voltage alternation of the "carrier" signal. More accurate measurements at low frequencies could be achieved by using very long drop lifetimes and taking into account the parallel impedance of the d.c. polarisation circuit. Since the T.R.A. bridge measured parallel components of impedance, it was necessary to transform these to series equivalents by using the equations developed on page 32. It may be noted that for frequencies above 2-3 Kc./sec., this transformation becomes progressively less accurate. Hence results of high and low frequency measurements are less reliable than those obtained at 1 Kc./sec.

Results of Runs 17, 39 and 40 are given in table 21 and summarised in table 22. While these confirm that the equivalent circuit of

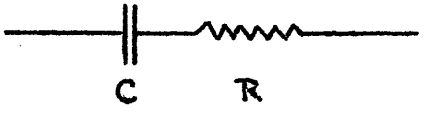

TABLE 21 RUN 17

E volts	f cps	C_P μF	G_P mMho	t sec.	γ dyne/cm	C_S μF	A_S sq.cm.	C_o μF/sqcm
-1.200	1000	0.2193	0.4960	1.52570	392.3	0.24771	0.015425	16.06
-0.400	1000	0.3000	1.4950	1.12116	420.2	0.48871	0.012504	39.08
-1.200	2000	0.1828	1.7200	1.85941	392.3	0.28528	0.017676	16.13
-1.200	5000	0.0779	5.5280	4.01975	392.3	0.47536	0.029814	15.95

h 30.123 cm. w_g 7.7925 mgm.

$\bar{m}$ 1.62054 mgm./sec. M 1.72969 mgm./sec.

Equation for M :-

$4.80856\ M - 0.35099\ M^{2/3} - 0.01699\ M^{1/3} - 7.79246 = 0$

Potential is given with respect to 0.100 N calomel electrode.

RUN 39

E volts	f cps	C_P μF	G_P mMho	t sec.	γ dyne/cm	C_S μF	A_S sq.cm.	C_o μF/sqcm
-1.450	500	0.4845	0.4000	3.84430	357.1	0.51796	0.031051	16.68
-1.250	1500	0.1021	0.4000	0.47336	386.3	0.11974	0.007502	15.96
-1.250	1500	0.1839	1.0000	1.33871	386.3	0.24512	0.015182	16.14
-1.250	2000	0.1248	1.0010	0.83542	386.3	0.17565	0.011022	15.95

h 32.142 cm. w_g 7.7456 mgm.

$\bar{m}$ 1.80049 mgm/sec. M 1.91378 mgm/sec.

Equation for M :-

$4.30193\ M - 0.30458\ M^{2/3} - 0.01438\ M^{1/3} - 7.74558 = 0$

Potential is given with respect to 0.100 N calomel electrode.

TABLE 21 (continued) RUN 40

E volts	f cps	C_p μF	G_p mMho	t sec.	γ dyne/cm	C_s μF	A_s sq.cm.	C_o μF/sqcm
-1.100	500	0.1180	0.0500	0.46286	403.0	0.12015	0.007298	16.46
-1.100	500	0.3010	0.1990	1.91510	403.0	0.31433	0.019155	16.41
-1.050	1000	0.1492	0.3000	0.70527	407.2	0.16448	0.009709	16.94
-1.050	1000	0.1787	0.4000	0.95769	407.2	0.20117	0.011953	16.83
-1.050	1000	0.2076	0.5000	1.21057	407.2	0.23810	0.014020	16.98
-1.050	500	0.2080	0.1173	1.04813	407.2	0.21470	0.012711	16.89
-1.050	500	0.2600	0.1600	1.47648	407.2	0.26998	0.016049	16.83
-1.050	300	0.5250	0.1820	4.09482	407.2	0.54276	0.032100	16.91

h 32.404 cm. w_g 7.4329mgm.

$\bar{m}$ 1.78280 mgm/sec. M 1.89025 mgm/sec.

Equation for M :-

$$4116924\ M - 0.28268\ M^{2/3} - 0.01278\ M^{4/3} - 7.43292 = 0$$

Potential is given with respect to 0.100 N calomel electrode.

TABLE 22

E	C_o 1 Kc/s	C_o 300cps	C_o 500cps	C_o 1.5 Kc/s	C_o 2.0 Kc/s	C_o 5.0 Kc/s	C_o 10.0 Kc/s
-1.050v	16.86	16.91	16.87	-	-	-	-
-1.100v	16.48	-	16.43	-	-	-	-
-1.200v	16.09	-	-	-	16.13	15.95	* 15.99
-1.250v	16.07	-	-	16.05	15.95	-	-
-1.450v	16.64	-	16.88	-	-	-	-

* Data from Run 16(b)

Capacitance values given in μF/sq.cm.

Potential given with respect to 0.100 N calomel electrode.

is probably correct, they do not entirely rule out the suggestion by Bockris (72) that the equivalent circuit may be

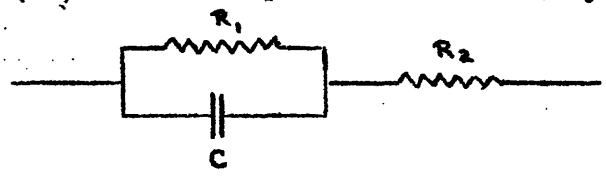

where R_1 is approximately 1MΩ. Since C is very large, it is difficult to detect R_1 unless very low frequencies are used. It may be pointed out, however, that the results of measurements by Grahame on potassium iodide solutions quoted by Bockris (73) do not in fact support his hypothesis (74).

THE RESISTIVE COMPONENT OF THE DOUBLE LAYER IMPEDANCE

The resistive component of the double layer impedance was investigated as a function of drop radius, signal frequency and the applied static polarisation potential. As has been shown on page 37 the resistance between two spheres is

$$R_s = \frac{\kappa}{4\pi}\left(\frac{1}{r_t} - \frac{1}{r'}\right)$$

where κ is the resistivity of the material between them and r_t and r' the radii. The series resistance of the double layer impedance was calculated together with the inverse of the drop radius, under different conditions. In table 23 data are given from Runs 17. 23 and 24 and in figure 19, series resistance, R_s in plotted against $1/r_t$ for these experiments. The linear plot thus obtained demonstrates the invariance of solution resistance with signal frequency and polarisation potential. A similar set of results is tabulated in table 24 for Runs 38, 39 and 40, and figure 20 again shows the overall linearity of the $R_s / 1/r_t$ graph. While the gradients of the best straight line through the points of any one run are almost equal to each other, the position of the intercept shows a slight variation. This was to be expected since while the intercept given by the theory, $\frac{\kappa}{4\pi r'}$, refers to a perfect sphere, the anode in the present work only approximated to one. Apart from the holes in the net, the shape was not geometrically exact, nor was the D.M.E. accurately centred.

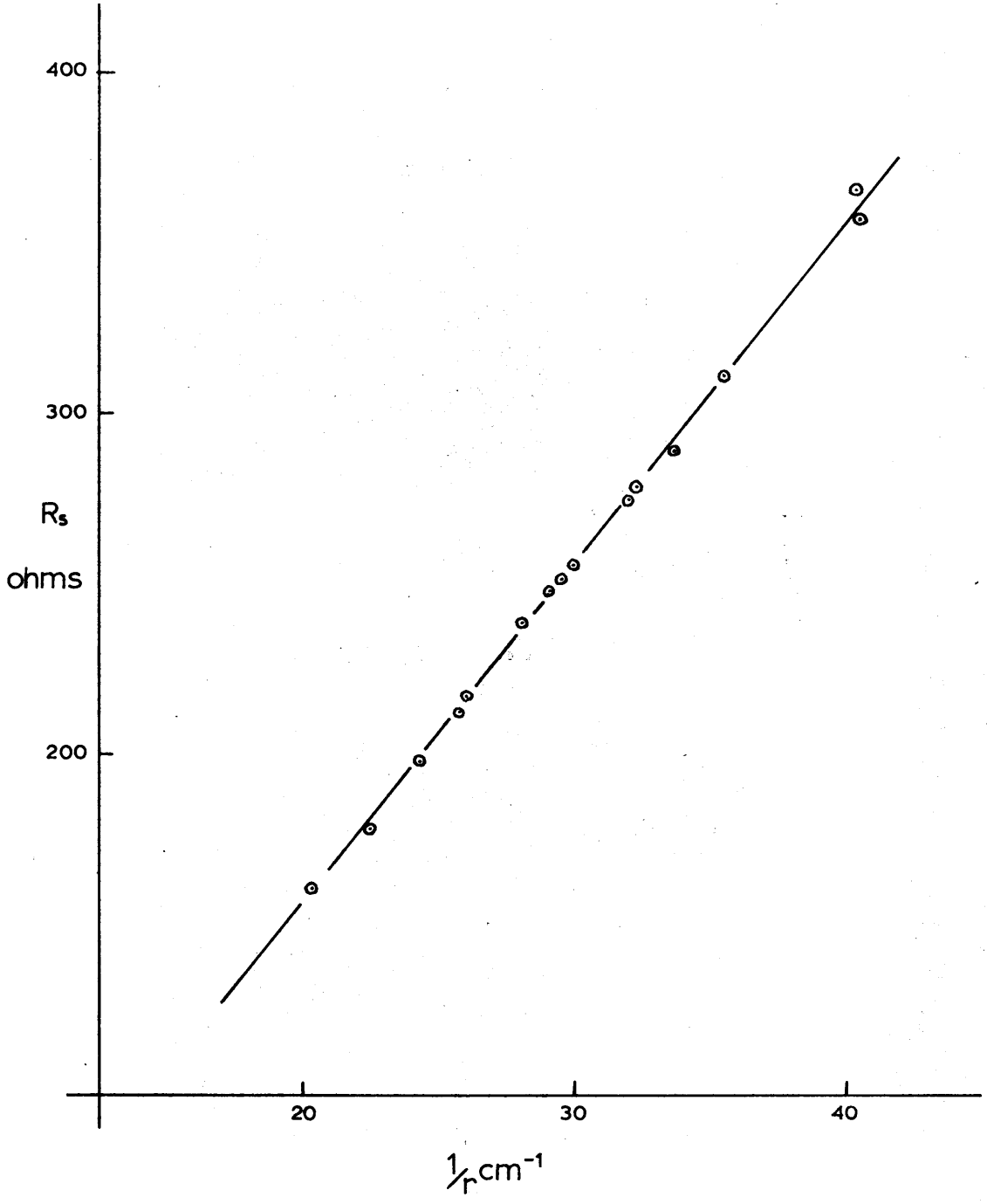

FIG. 19 RUNS 38;39;40.

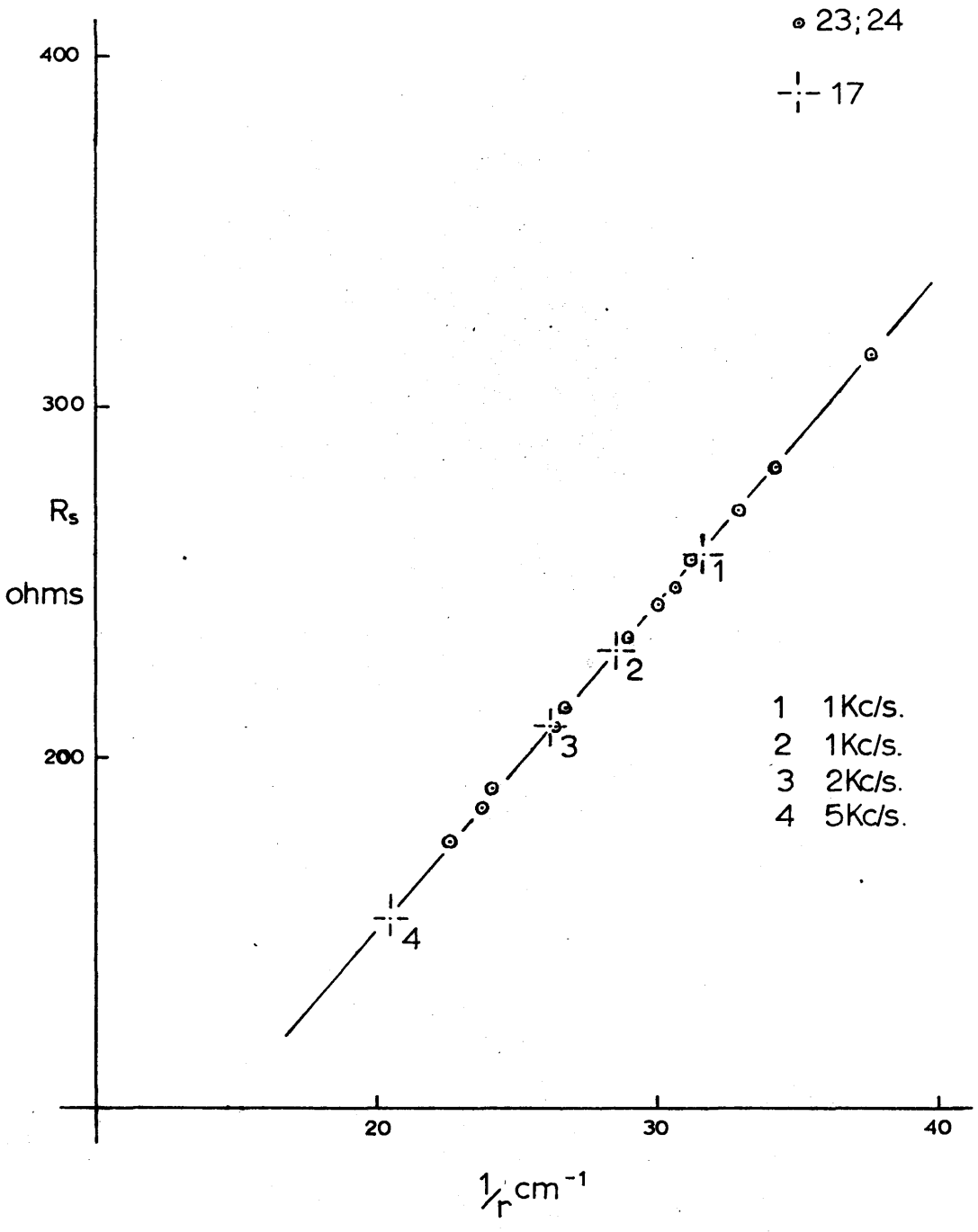

FIG. 20 RUNS 17;23;24.

A_s sq.cm.	$4\pi r_t^2$ sq.cm.	r_t cm.	$1/r_t$ $cm.^{-1}$
0.010735	0.010756	0.029256	34.18
0.013775	0.013796	0.033133	30.18
0.017941	0.017962	0.037807	26.45
0.022234	0.022255	0.042083	23.76
0.024496	0.024517	0.044170	22.63
0.008881	0.008902	0.026616	37.57
0.013380	0.013401	0.032656	30.62
0.014950	0.014971	0.034515	28.97
0.011645	0.011666	0.030468	32.82
0.013019	0.013040	0.032151	31.11
0.017719	0.017740	0.037573	26.61
0.021960	0.021981	0.041823	23.91
0.015425	0.015449	0.03506	28.52
0.012504	0.012528	0.03158	31.67
0.017676	0.017700	0.03754	26.38
0.029814	0.029838	0.04872	20.53

TABLE 23

E volts	C_p μF	G_p mMho	Q	f cps	R_s ohms
-1.250	0.1571	0.3020	3.26851	1000	283.4
-1.250	0.1980	0.4200	2.96207	1000	243.6
-1.250	0.2517	0.6000	2.63578	1000	209.7
-1.250	0.3036	0.7950	2.39945	1000	186.2
-1.250	0.3300	0.9000	2.30383	1000	176.2
-0.400	0.2351	1.0080	1.46546	1000	315.2
-0.400	0.3119	1.6000	1.22481	1000	250.0
-0.400	0.3356	1.8000	1.17146	1000	234.2
-1.200	0.1699	0.3400	3.13973	1000	270.9
-1.200	0.1878	0.4000	2.94995	1000	257.7
-1.200	0.2481	0.6000	2.59810	1000	215.0
-1.200	0.2984	0.8000	2.34362	1000	192.5
-1.200	0.2193	0.4960	2.77803	1000	231.3
-0.400	0.3000	1.4950	1.26084	1000	258.4
-1.200	0.1828	1.7200	1.33555	2000	208.9
-1.200	0.0779	5.5280	0.44271	5000	151.3

A_s sq.cm.	$4\pi r_t^2$ sq.cm.	r_t cm.	$1/r_t$ $cm.^{-1}$
0.010011	0.010032	0.028255	35.39
0.012428	0.012449	0.031475	31.77
0.014599	0.014620	0.034109	29.32
0.019173	0.019194	0.039082	25.59
0.021364	0.021385	0.041252	24.24
0.025378	0.025399	0.044958	22.24
0.031051	0.031075	0.049728	20.11
0.007502	0.007526	0.024472	40.86
0.015182	0.015206	0.034786	28.75
0.011022	0.011046	0.029648	33.73
0.009709	0.009733	0.027830	35.93
0.011953	0.011977	0.030872	32.39
0.014020	0.014044	0.033431	29.91
0.007298	0.007322	0.024139	41.43
0.012711	0.012735	0.031834	31.41
0.016049	0.016073	0.035763	27.96
0.019155	0.019179	0.039005	25.64
0.032100	0.032124	0.050659	19.74

TABLE 24

E volts	C_p μF	G_p mMho	Q	f cps	R_s ohms
-1.400	0.1485	0.3000	3.1102	1000	312.3
-1.400	0.1811	0.4000	2.8447	1000	275.0
-1.400	0.2092	0.5000	2.6289	1000	252.8
-1.400	0.2680	0.7000	2.4056	1000	210.5
-1.400	0.2948	0.8000	2.3154	1000	196.5
-1.400	0.3415	1.0000	2.1457	1000	178.4
-1.450	0.4845	0.4000	3.8053	500	161.5
-1.250	0.1021	0.4000	2.4057	1500	368.3
-1.250	0.1839	1.0000	1.7332	1500	249.8
-1.250	0.1248	1.0100	1.5667	2000	289.2
-1.050	0.1492	0.3000	3.1248	1000	309.7
-1.050	0.1787	0.4000	2.8201	1000	279.2
-1.050	0.2076	0.5000	2.6088	1000	256.2
-1.100	0.1180	0.0500	7.4142	500	357.3
-1.050	0.2080	0.1730	5.5708	500	266.1
-1.050	0.2600	0.1600	5.1051	500	230.9
-1.100	0.3010	0.1990	4.7519	500	213.1
-1.050	0.5250	0.1820	5.4374	300	179.9

The mean gradient for R_s-$1/r_t$ plots was found to be 10.07 ohm.cm. which gave a resistivity of 126 ohm/c.c. This was high compared with the value of 81.0 ohm/c.c. calculated using the formula of Shedlovsky (75) for the equivalent conductivity of aqueous potassium chloride solutions:-

$$\Lambda = 149.9 - 93.85c^{\frac{1}{2}} + 50\,c \qquad \text{.....70}$$

where c was the solution normality. Such a difference, however, was to be expected since the other electrode was not a completely closed spherical shell, and hence the effective "cell constant" used was too high.

A NEW METHOD FOR THE CALCULATION OF DIFFERENTIAL CAPACITANCE PER UNIT AREA AT A D.M.E.

The linearity of the R_s-$1/r_t$ plots suggested that a method might be found of determining the differential capacitance per unit area of a D.M.E. without having recourse to either the birth-balance time, or the rate of flow of the mercury.

Since $R_s = \frac{\kappa}{4\pi}(1/r_t) + x$, where x is a constant, r_t could be calculated from R_s, provided that κ and x were known. Taking the electrode area as $(4\pi r_t^2 - A_s)$, the capacitance per unit area could then be found. Run 21 was calculated using only impedance data together with values of κ and x from other runs; the capacitance data thus derived had a standard deviation of ± 1.8% as compared with values calculated using areas determined from measurements of t and M. This method of calculation had two disadvantages, however:

(i) the values of κ and x had to be known, and with the latter especially, it was inaccurate, as shown above, to use a value obtained in a different experiment.

(ii) the relative change in resistance during drop growth was small, and thus a calculation dependent on the measurement of impedance at only one instant during the life of a drop could not be accurate.

Accordingly, in an attmpt to overcome these problems, a new method was developed. This relied on the fact that independent functions

of resistance and capitance could be found which bore linear relationships either directly to, or to a simple function of drop radius.

For any one static polarisation potential:

$$C_s = (4\pi r^2 - A_s).C_o$$

$$\therefore (C_s + C_o A_s)^{\frac{1}{2}} = 2(\pi C_o)^{\frac{1}{2}}.r \quad \ldots\ldots\ldots\ldots\ldots\ldots\ldots\ldots 71$$

and $$R_s = \left(\frac{\chi}{4\pi}\right). 1/r + x \quad \ldots\ldots\ldots\ldots\ldots\ldots 72$$

If any value was chosen for C_o, then values of r, $r_{calc.}$, could be derived from equation 71 corresponding to experimental determination of C_s. The experimental R_s values could now be plotted against their equivalent $1/r_{calc.}$ values. This graph would result in a straight line, only if

$$1/r_{calc.} = 1/r \quad \ldots\ldots\ldots\ldots\ldots\ldots\ldots\ldots\ldots\ldots 73$$

i.e. only if the C_o value chosen for substitution into equation 71 had been the correct one. Therefore it is seen that the linearity of the R_s vs. $1/r_{calc.}$ plots indicated that a correct value of C_o had been selected.

A value of C_o having been selected, $1/r_{calc.}$ terms were derived for one set of experimental R_s values. By means of a Deuce programme using least square methods, the best straight line was drawn through the $1/r_{calc.}$-R_s points and extrapolated to meet the R_s-ordinates of a second set of experimental measurements. This gave rise to a term, designated by $1/r_{extrap.}$ for each of the R_s values of this second series.

The criterion for the best value of C_o, was a minimum in

$$p \sum_{i-1} \Delta \left(1/r_i \right)$$

where p was the gradient of the R_s vs. $1/r_{calc.}$ graph and $\Delta (1/r_i)$ was the difference between $1/r_{calc.}$ and $1/r_{extrap.}$ for any one of the second sets of points. While this minimum could be found with any required degree of precision, C_o values have not yet been accurately determined due to programming difficulties and the fact that a fairly large number of readings had to be taken if random errors were to be eliminated. Further development of the method would be useful, however, since it should enable C_o to be found without the use of t, t_g, $\mathcal{T}$ or $\bar{m}$. Since the calculation is independent of $\bar{m}$, the mercury flow rate, an irregular flow would not adversely affect an experiment.

PART 3

DIFFERENTIAL CAPACITANCE OF THE DOUBLE LAYER IN NON-AQUEOUS SOLVENTS

INTRODUCTION.

In recent years it has been proposed that the solvent has a very important influence on the structure of the electrical double layer (13,19,20,76,77). Molecules of solvent near the interface are subjected to the action of very high electrical fields and thus behave differently from those in the bulk of the solution. In typical capacitance measurements, for instance, the potential difference across the interface may be greater than 1 volt, and as it acts over a distance of only a few Å-units, the field produced is about 2×10^7 volt/cm. Now the average field necessary to orientate a molecule with dipole moment μ is approximately $F = kT/\mu$.

Solvent.	μ esu. of charge x cm.	F volt/cm.
Formamide.	3.25×10^{-18}	3.80×10^6
Water.	1.85×10^{-18}	6.67×10^6
Methanol.	1.70×10^{-18}	7.26×10^6

Thus polar solvent molecules in the immediate environment of the electrode are expected to show strong dielectric saturation, as is the case with those in the hydration sheath of an ion. Polar solvents often have large dielectric constants due to the dipoles of single molecules associating into groups with large electrical moments (17). Depending on molecular structure, however, such associations can also cause dielectric orientation saturation to extend past the region of influence of a field.

Another effect of the large electric field is compression of the solvent layer at the interface caused by strong attraction towards the electrode of ions in the O.H.P. (19,78). The compressibility of the solvent is thus a governing factor in the assessment of double layer capacitance, since under cathodic polarisation, this is largely determined by the thickness of the charge-free region. Grahame (20) has also considered that solvent molecules would be distorted in the field with consequent separation of charge centroids and a corresponding increase in effective dielectric constant. Macdonald (76), however, considered this "electrostriction" effect to be small.

Since ionic solvation energies vary from solvent to solvent, the potential energy barrier to be surmounted for the partial or complete desolvation of an ion must depend on the solvent. This consideration is important in the assessment of specific adsorption effects for both anions and cations.

The present section of the thesis describes the measurement of differential capacitance in a non-aqueous solvent, formamide and an attempt to obtain similar measurements in formic acid solutions. Formamide is an excellent polar solvent with a dielectric constant of 109 at room temperature (79) : alkali metal chlorides dissolve readily to give 0.1 m solutions and above. Unfortunately, the fluorides are not so soluble. Impedance measurements were made in 0.1 m lithium and caesium chloride solutions and in potassium chloride solutions at 0.05 m, 0.1 m and 0.5 m.

EXPERIMENTAL.

1. Preparation of Materials.

Formamide. Gaseous ammonia was added to B.D.H. "98%" formamide until the latter was slightly alkaline. Any ammonium formate present was filtered off and the formamide was twice distilled under vacuum. Since formamide tends to decompose at high temperature, the distillate was collected at about 110-120°C and about 15 m.m. pressure. It was necessary to incorporate an efficient spray trap in the distillation system.

Pure formamide had an M.P. of 2.5°C. (reported M.P. 2.55°C.)

Formic acid. Formic acid (Hopkins and Williams Ltd.) which ha a specific gravity of 1.22 and a purity of 98% was further purified by distillation and differential crystallisation techniques. The final product had a M.P. of 7.94°C. ("98%": 6.46°C; reported M.P.: 8.39°C).

Ammonium formate. AnalaR ammonium formate was used after drying over phosphorus pentoxide.

Alkali metal chlorides. AnalaR materials were recrystallised three times from conductivity water before use.

2. Preparation of Solutions.

Since traces of moisture were liable to affect measurements in non-aqueous solvents, solutions were generally prepared in a

"glove box" filled with pure dry nitrogen under a slightly positive pressure. The glove box contained a balance together with the necessary apparatus and chemicals. Solutions were made up by weight in 250 ml. flasks with Quickfit necks. A special head fitted the latter which enabled the solution to be blown over into the cell by dry nitrogen without coming in contact with the atmosphere. Concentrations in non-aqueous solvents were all expressed on the molal scale.

3. Reference Electrodes.

The quinhydrone electrode used with formic acid solutions is illustrated in figure 14. AnalaR quinhydrone was recrystallised in an atmosphere of nitrogen by the method of Harned and Wright (80), as also described by Dunsmore (81), and was dried over phosphorus pentoxide in a nitrogen-filled dessicator. C, in figure 14, was a heat-conditioned gold wire and D a fine sintered glass filter surmounted by a glass wool pad which guarded against diffusion of quinhydrone into the cell. Some "Araldite" resin was cast at the bottom of electrode tube H to act as a Pyrex-gold seal. When a small quantity of quinhydrone had been placed in limb B, the electrode was filled by immersing E in a flask of test solution, that had been vigorously blown out with nitrogen, and applying suction at A. Care was taken to ensure that no air was trapped at F or G.

The silver-silver chloride electrodes (figure 14) used with chloride solutions in formamide were similar to those described by Harned (82) and, in detail, by McAuley (83). A platinum wire was would in a helix and sealed into one end of a Pyrex tube, the other end of which was attached to a Quickfit B 29 cone. The helix was filled with a thick paste of spectroscopically pure silver oxide in conductivity water. The electrode after having been dried at 100°C was heated in a muffle furnace at 400°C until the metallic oxide had completely decomposed to grey lustrous silver. Another coating of the oxide was applied and the electrode heated as before. This process was continued until none of the platinum was visible through the silver. Some "Araldite" resin was then cast in the electrode tube to ensure a complete Pyrex-platinum seal. The electrode was then chloridised in the absence of light by electrolysis in normal hydrochloric acid (aqueous) at a current density of approximately 1 amp/sq.cm. for three hours, using a platinum cathode. It was finally thoroughly washed with formamide containing a small quantity of potassium chloride, and allowed to age in the dark for several weeks in a similar solution. Before a run the electrode was washed several times in cell solution.

4. General Run Procedure.

Capacitance measurements were made in a similar manner to that described for aqueous solutions in Part 2. Precautions were taken to prevent moisture from entering the cell at any time. Densities of solutions were found by using a pyknometer.

RESULTS AND DISCUSSION

I. 0.1 m AMMONIUM FORMATE IN FORMIC ACID

Figure 21 shows the results of several sets of differential capacitance measurements in the above solution. The potential scale is referred to a quinhydrone electrode in 0.1 m $HCOONH_4/HCOOH$.

While capacitance values on the anodic branch of the curve are fairly reproducible, cathodic capacitance values varied from run to run in a random manner. When a polarogram of the solution was investigated, it was found that at cathodic potentials, the electrode was no longer perfectly polarised and that the solvent was breaking down. As this process was irreversible, no pseudo-capacitance peaks were observed. Experiments using a pool anode as "reference" showed similar irreproducibility and thus proved that the decomposition was not being catalysed by the quinhydrone.

The anodic branch of the C_c/E curve showed no evidence of the "hump", familiar in aqueous solutions. The capacitance minimum of slightly less than 9 μF/sq.cm., occuring around - 1.1 volts with respect to the quinhydrone electrode was close to the value of 9.2 μF/sq.cm. found by Grahame (20) for methanol.

The potential of the E.C. maximum was estimated from drop life time measurements to be approximately -1.15 volts.

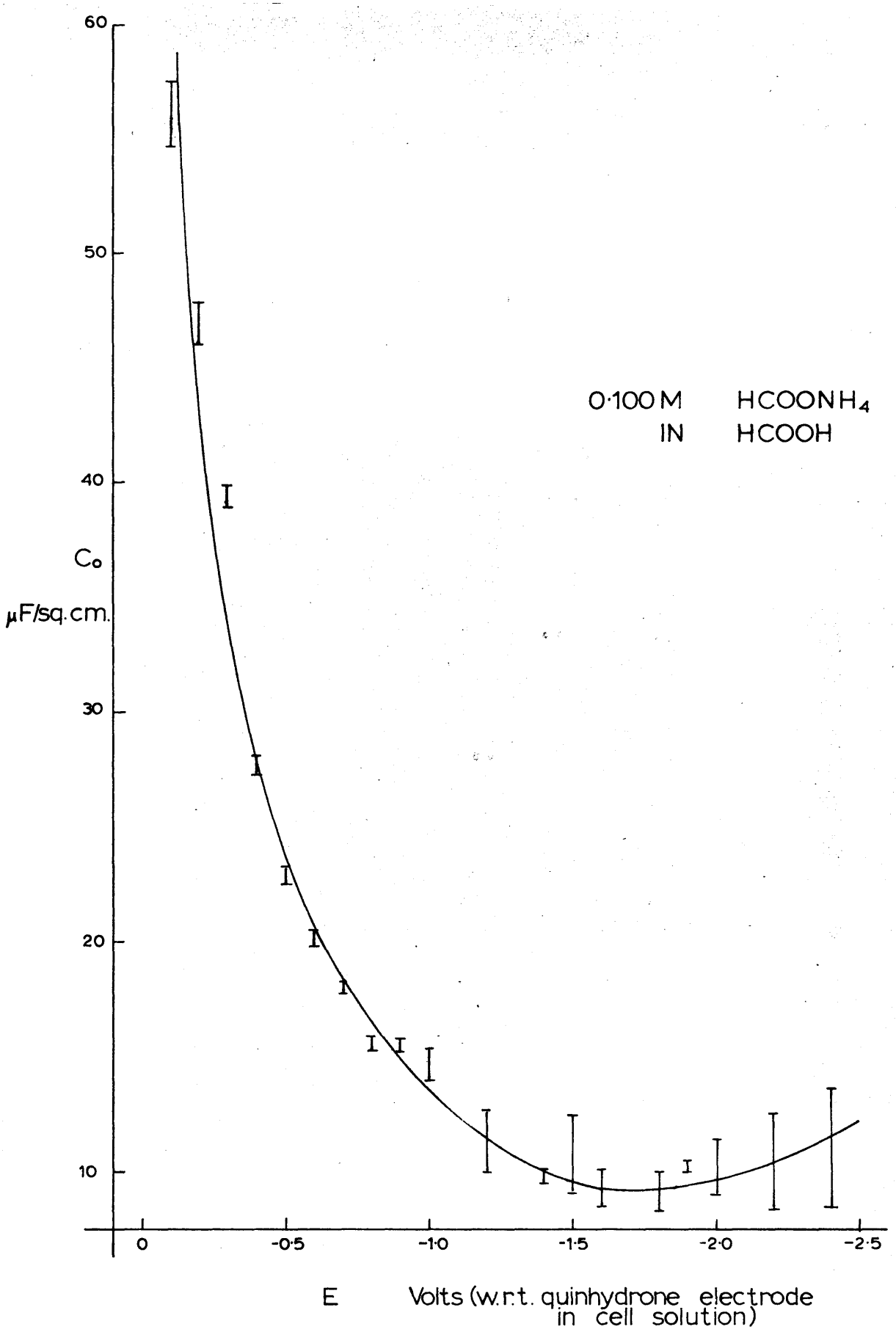

FIG. 21 DIFFERENTIAL CAPACITANCE vs APPLIED POTENTIAL

2. ALKALI METAL SOLUTIONS IN FORMAMIDE.

The results of capacitance measurements of alkali metal chlorides in formamide from Runs 44-50 are given in tables 25-31, in which potentials are referred to a Ag/AgCl electrode in cell solution. All measurements were made at a temperature of 25°C and a bridge frequency of 1 Kc./sec. Run 45(a) was used to compute a value of w_o (table 32). It is noted that the magnitude of w_o, 0.0884 mgm., corresponding to an A_o of 1.670×10^{-3} sq.cm., is appreciably larger than that found for aqueous solutions with a capillary of similar bore.

The potentials of the E.C. maximum were determined for each concentration of solution:-

TABLE 33

Solution	$E_{E.C.Max.}$ with respect to Ag/AgCl
0.500 m KCl in formamide	-0.473 volts
0.100 m KCl " "	-0.478 volts
0.050 m KCl " "	-0.484 volts
0.100 M KCl aqueous	-0.514 volts

TABLE 25 RUN 44

E volts	t_g sec.	t sec.	C_T μF	G_T mMho
-0.100	3.69439	1.43126	0.03605	1.2000
-0.200	3.80299	1.95564	0.06180	1.3000
-0.200	3.80299	2.01815	0.06060	1.3000
-0.300	3.89459	2.49041	0.08600	1.3000
-0.300	3.89459	2.49064	0.08570	1.3000
-0.400	3.93072	2.71367	0.10698	1.2000
-0.500	3.93703	1.27805	0.09100	0.7008
-0.600	3.92981	1.44224	0.09740	0.7000
-0.700	3.89947	1.36168	0.09300	0.7000
-0.800	3.86703	1.24895	0.08970	0.7000
-0.900	3.80336	1.15576	0.08629	0.7000
-1.000	3.71814	1.05202	0.08160	0.6800
-1.100	3.61520	1.04663	0.08140	0.6780

h 33.143 cm.

$\bar{m}$ 1.83555 mgm/sec.

M 1.93961 mgm/sec.

Equation for M :-

$$3.89459\,M - 0.25188\,M^{2/3} - 0.01086\,M^{1/3} - 7.14871 = 0$$

0.100 m CsCl IN FORMAMIDE

γ dyne/cm.	A sq.cm.	C_s μF	C_o μF/sqcm
369.3	0.016336	1.04785	64.14
379.6	0.020079	0.75449	37.58
379.6	0.020505	0.76701	37.41
388.3	0.023577	0.58377	24.76
388.3	0.023578	0.58521	24.82
391.7	0.024963	0.44794	17.94
392.3	0.015104	0.22771	15.08
391.6	0.016367	0.32483	13.74
388.7	0.015761	0.22646	14.37
385.7	0.014890	0.22807	15.32
379.5	0.014159	0.23013	16.25
371.5	0.013326	0.22514	16.90
361.8	0.013301	0.22445	16.87

w_2	7.1487 mgm.
ρ	2.7660×10^{-3} cm.
d	1.14243 gm./ml.

TABLE 26 RUN 45(b)

E volts	t_g sec.	t sec.	C_P μF	G_P mMho
-0.100	4.01283	1.65896	0.03545	1.2000
-0.500	4.22873	2.20865	0.10530	0.9230
-0.600	4.21560	1.53519	0.09445	0.7000
-0.700	4.19551	1.47607	0.09350	0.7000
-1.000	3.97144	1.20067	0.08420	0.7000
-1.100	3.85599	1.20384	0.08340	0.7020
-1.200	3.71734	1.25416	0.08643	0.6960
-1.300	3.56448	1.34072	0.09028	0.6959
-1.400	3.35301	1.38219	0.09277	0.6900

h 31.209 cm.

$\bar{m}$ 1.69309 mgm/sec.

M 1.79559 mgm/sec.

Equation for M :-

$$4.22873\,M - 0.28301\,M^{2/3} - 0.01263\,M^{1/3} - 7.15962 = 0$$

0.100 m CsCl IN FORMAMIDE

γ dyne/cm	A sq. cm.	C_s μF	C_o μF/sqcm
372.8	0.017062	1.06438	62.38
391.7	0.020598	0.31023	15.06
390.5	0.016160	0.22586	13.98
388.8	0.015748	0.22625	14.37
369.2	0.013779	0.23161	16.81
359.0	0.013826	0.23122	16.72
346.8	0.014233	0.22840	16.05
333.3	0.014905	0.22616	15.17
314.5	0.015253	0.22277	14.61

w_1	7.1596 mgm.
ρ	2.7660×10^{-3} cm.
d	1.14243 gm./ml.

TABLE 27 RUN 46

E volts	t_g sec.	t sec.	C_p μF	G_p mMho
0.100	3.94126	1.08112	0.03420	1.0200
0.200	4.09241	0.61983	0.04800	0.7000
0.300	4.16416	0.78817	0.06061	0.7198
0.400	4.18981	1.06225	0.07500	0.7500
0.500	4.21143	1.36176	0.08645	0.7400
0.700	4.10962	1.29400	0.08490	0.6800
0.800	4.03012	1.18538	0.08141	0.6749
1.300	3.53847	1.29557	0.08680	0.6700
1.400	3.36666	1.40991	0.09580	0.6700
1.600	3.18187	1.41211	0.09100	0.6500

h 31.138

$\hat{m}$ 1.71852

M 1.82368

Equation for M :-

$$4.21143\,M - 0.28610\,M^{2/3} - 0.01296\,M^{4/3} - 7.23743 = 0$$

0.100 m KCl IN FORMAMIDE

γ dyne/cm	A sq.cm.	C_s μF	C_o μF/sqcm
369.4	0.012983	0.80477	61.99
382.9	0.009017	0.30658	34.00
389.2	0.010518	0.27714	26.35
391.5	0.012784	0.26498	20.73
393.4	0.015062	0.24690	16.39
384.4	0.014582	0.22286	15.28
377.3	0.013777	0.22313	16.20
333.4	0.014714	0.21780	14.80
317.9	0.015596	0.21449	13.75
301.3	0.015652	0.20860	13.33

w_q	7.2374 mgm.
ρ	2.7660×10^{-3} cm.
d	1.13327 gm./ml.

TABLE 28 RUN 47

E volts	t_g sec.	t sec.	C_p μF	G_p mMho
-0.100	3.94742	3.32099	0.21398	4.0052
-0.200	4.07615	2.67794	0.30080	3.0000
-0.300	4.15816	2.18207	0.32082	2.0050
-0.400	4.19576	3.25042	0.36748	2.0000
-0.500	4.20179	3.51302	0.36490	1.7000
-0.600	4.19010	2.58969	0.30500	1.2000
-0.700	4.15286	2.72880	0.31510	1.2000
-0.800	4.09064	2.11039	0.27679	1.0000
-0.900	4.00248	2.10013	0.27698	1.0000
-1.000	3.89771	1.98440	0.26360	0.9000
-1.100	3.76765	2.22371	0.27039	0.9000
-1.200	3.61965	2.56483	0.27961	0.9000
-1.300	3.46133	2.89179	0.28532	0.9000
-1.400	3.28871	2.34058	0.24845	0.7000
-1.500	3.10486	2.49121	0.25098	0.7000
-1.600	2.89869	2.54441	0.25280	0.7000

h 31.236 cm.

$\bar{m}$ 1.69754 mgm/sec.

M 1.79987 mgm/sec.

Equation for M :-

$$4.20179\ M - 0.28032\ M^{2/3} - 0.01247\ M^{1/3} - 7.13271 = 0$$

0.500 m KCl IN FORMAMIDE

γ dyne/cm	A sq.cm.	C_s µF	C_o µF/sqcm.
367.7	0.027200	2.11293	77.68
379.0	0.023512	1.05868	45.03
386.2	0.020480	0.63822	31.16
389.5	0.026743	0.64320	24.05
390.0	0.028274	0.56552	20.07
389.0	0.022961	0.42459	18.49
385.7	0.023791	0.43086	18.11
380.3	0.020044	0.36830	18.37
372.6	0.019999	0.36843	18.42
363.4	0.019281	0.34144	17.71
351.9	0.020835	0.34627	16.62
338.8	0.022957	0.35299	15.38
324.8	0.024917	0.35723	14.34
309.4	0.021678	0.29841	13.77
293.0	0.022644	0.30043	13.27
274.6	0.023017	0.30190	13.11

w_q	7.1327 mgm.
ρ	2.7660×10^{-3} cm.
d	1.14846 gm./ml.

TABLE 29 RUN 48

E volts	t_g sec.	t sec.	C_p μF	G_p mMho
-0.100	4.05463	3.67845	0.01200	0.9000
-0.200	4.16443	2.05487	0.01828	0.7000
-0.300	4.23855	2.17864	0.02601	0.7000
-0.400	4.25837	3.27834	0.02781	0.7000
-0.500	4.26355	2.66516	0.04119	0.7000
-0.600	4.25488	2.75928	0.04413	0.7000
-0.700	4.22242	1.96459	0.04052	0.6000
-0.800	4.18256	1.87681	0.03830	0.6000
-0.900	4.11162	1.79586	0.03600	0.6000
-1.000	4.02439	1.76270	0.03479	0.6000
-1.100	3.91267	1.77142	0.03439	0.6000
-1.200	3.78546	1.82046	0.03645	0.6000
-1.300	3.63790	1.27825	0.03480	0.5060
-1.400	3.46455	1.33104	0.03678	0.5200
-1.500	3.28685	1.37225	0.03775	0.5200
-1.600	3.10428	1.39539	0.03898	0.5200

h 31.156 cm.

$\bar{m}$ 1.68176 mgm/sec.

M 1.78394 mgm/sec.

Equation for M :-

$$4.26355\ M - 0.28566\ M^{2/3} - 0.01276\ M^{1/3} - 7.17026 = 0$$

0.050 m KCl IN FORMAMIDE

γ dyne/cm	A Sq.cm.	C_s μF	C_o μF/sqcm
374.4	0.028934	1.72179	59.51
384.0	0.019560	0.69726	35.65
389.6	0.020325	0.50320	24.76
392.2	0.026725	0.47412	17.74
392.6	0.023255	0.34252	14.73
391.8	0.023805	0.32539	13.67
389.0	0.018969	0.26507	14.00
385.6	0.018407	0.27639	15.02
379.4	0.017890	0.28930	16.17
371.8	0.017689	0.29690	16.78
362.0	0.017702	0.29955	16.86
350.9	0.018127	0.28663	15.81
338.0	0.014370	0.22116	15.39
322.7	0.014794	0.22300	15.07
307.0	0.015131	0.21919	14.49
290.9	0.015337	0.21469	14.00

w_s	7.1703mgm.
ρ	2.7660×10^{-3} cm.
d	1.13126 gm./ml.

TABLE 30 RUN 49

E volts	t_q sec.	t sec.	C_p μF	G_p mMho
-0.100	3.00481	1.40009	0.02722	1.0050
-0.200	3.12513	1.18717	0.04068	0.9000
-0.300	3.23999	0.83729	0.05098	0.7000
-0.400	3.30083	1.01910	0.06149	0.7000
-0.500	3.33944	1.25451	0.07143	0.7000
-0.600	3.32084	1.39810	0.07727	0.7000
-0.700	3.31418	1.38266	0.07630	0.7000
-0.800	3.29674	1.31269	0.07375	0.7000
-0.900	3.25808	1.24869	0.07108	0.7000
-1.000	3.18993	1.22495	0.07050	0.7000
-1.100	3.12609	1.23632	0.07080	0.7000
-1.200	3.03525	1.29566	0.07359	0.7000
-1.300	2.88977	1.38577	0.07720	0.7000
-1.400	2.68633	1.47014	0.07980	0.7000
-1.500	2.47143	1.52020	0.08128	0.7000
-1.600	2.28009	1.55808	0.08201	0.7000

h 31.332 cm.

$\bar{m}$ 1.79380 mgm/sec.

M 1.90923 mgm/sec.

Equation for M :-

$$3.33944\,M - 0.24112\,M^{2/3} - 0.01161\,M^{1/3} - 5.99029 = 0$$

0.100 m LiCl IN FORMAMIDE

γ dyne/cm	A sq.cm.	C_s μF	C_o μF/sqcm
354.6	0.015932	0.96713	60.70
368.0	0.014255	0.54504	38.23
380.8	0.011310	0.29444	26.03
387.5	0.012849	0.26334	20.49
391.8	0.014729	0.24519	16.65
389.7	0.015832	0.23790	15.03
389.0	0.015717	0.23897	15.21
387.1	0.015189	0.24205	15.93
382.8	0.014705	0.24570	16.71
375.2	0.014537	0.24655	16.96
368.1	0.014642	0.24611	16.81
358.0	0.015127	0.24225	16.01
341.8	0.015855	0.23798	15.01
319.0	0.016543	0.23534	14.23
294.8	0.016973	0.23398	13.79
273.0	0.017304	0.23336	13.48

w_2 5.9903 mgm.

ρ 2.2999×10^{-3} cm.

d 1.13131 gm./ml.

TABLE 31 RUN 50

E volts	t_g sec.	t sec.	C_P μF	G_P mMho
-0.100	3.18367	1.00110	0.03383	1.0000
-0.200	3.33857	0.92740	0.05120	0.9000
-0.300	3.43517	0.70739	0.06148	0.7000
-0.400	3.49108	0.94263	0.07593	0.7000
-0.500	3.49858	1.18973	0.08648	0.7000
-0.600	3.48134	1.32810	0.09119	0.7000
-0.600	3.48134	2.49026	0.10881	1.0000
-0.700	3.44611	1.29378	0.09021	0.7000
-0.800	3.39521	1.19997	0.08658	0.7000
-0.900	3.35610	1.12226	0.08359	0.7000
-1.000	3.30793	1.09624	0.08243	0.7000
-1.100	3.21130	1.11974	0.08389	0.7000
-1.200	3.09758	1.20877	0.08741	0.7000
-1.300	2.95980	1.33219	0.09261	0.7000
-1.400	2.80828	1.44352	0.09618	0.7000
-1.500	2.64462	1.49741	0.09700	0.7000
-1.600	2.48561	1.53635	0.09740	0.7000

h 30.945 cm.

$\bar{m}$ 1.76808 mgm/sec.

M 1.88196 mgm/sec.

Equation for M :-

$$3.49858\,M - 0.25158\,M^{2/3} - 0.01206\,M^{1/3} - 6.18577 = 0$$

0.100 m KCl IN FORMAMIDE

γ dyne/cm	A sq.cm.	C_s μF	C_o μF/sqcm
358.1	0.012634	0.78258	61.94
374.5	0.011981	0.45193	37.72
384.7	0.010024	0.26336	26.27
390.6	0.012075	0.23939	19.83
391.4	0.014075	0.23000	16.34
389.6	0.015144	0.22730	15.01
389.6	0.023040	0.34160	14.83
385.9	0.014892	0.22780	15.30
380.5	0.014181	0.22994	16.21
376.4	0.013577	0.23207	17.09
371.3	0.013580	0.23300	17.41
361.0	0.013592	0.23184	17.06
349.0	0.014324	0.22940	16.10
334.3	0.015309	0.22663	14.80
318.1	0.016183	0.22523	13.92
300.4	0.016623	0.22496	13.53
283.3	0.016949	0.22483	13.36

w_g	6.1858 mgm.
ρ	2.3797×10^{-3} cm.
d	1.13327 gm./ml.

TABLE 32 — 0.100 m CsCl IN FORMAMIDE — RUN 45(a)

C_T μF	G_P mMho	t sec.	C_s μF	$(C_s + C_o A_s)^{3/2}$	A* sq.cm.	f(t)
0.05241	0.3000	0.35549	0.09591	0.02988	0.005721	0.54943
0.07260	0.4850	0.78334	0.15467	0.06105	0.009938	1.25792
0.08944	0.7000	1.38542	0.22821	0.10929	0.014737	2.27151
0.10530	0.9230	2.20865	0.31023	0.17311	0.020298	3.67185

* Back-pressure corrected, but with no allowance for w_o or A_s.

$\bar{m}$	1.69309 mgm./sec.	E	-0.500 volts
t_g	4.22873 sec.	M	1.79559 mgm./sec.
γ	391.7 dynes/cm.	w_g	7.1596 mgm.
h	31.209 cm.	ρ	2.7660×10^{-3} cm.

Equation for M :-

$$4.22873\,M - 0.28301\,M^{2/3} - 0.01263\,M^{1/3} - 7.15962 = 0$$

$(C_s + C_o A_s)^{3/2}$ vs. f(t) plot.

Gradient	0.046066
Intercept	0.004073
w_o	0.08841 mgm.
A_o	16.68×10^{-4} sq.cm.
C_o	15.07 μF/sq.cm.

TABLE 34 SURFACE TENSION DATA FOR FORMAMIDE SOLUTIONS

E volts	KCl 0.5m	KCl 0.1m	KCl 0.1m	KCl 0.05m	LiCl 0.1m	CsCl 0.1m	CsCl 0.1m
-0.100	367.7*	369.4	358.1	374.4	354.6	369.3	372.8
-0.200	379.0	382.9	374.5	384.0	368.0	379.6	-
-0.300	386.2	389.2	384.7	389.6	380.8	388.3	-
-0.400	389.5	391.5	390.6	392.1	387.5	391.7	-
-0.500	390.0	393.4	391.4	392.6	391.8	392.3	391.7
-0.600	389.0	-	389.6	391.8	389.7	391.6	390.5
-0.700	385.8	384.4	385.9	389.0	389.0	388.7	388.8
-0.800	380.3	377.3	380.5	385.5	387.1	385.7	-
-0.900	372.6	-	376.4	379.4	382.8	379.5	-
-1.000	363.4	-	371.3	371.8	375.2	371.5	369.2
-1.100	351.9	-	361.0	362.0	368.1	361.8	359.0
-1.200	338.8	-	349.0	350.9	358.0	-	346.8
-1.300	324.8	333.4	334.3	338.0	341.8	-	333.3
-1.400	309.4	317.9	318.1	322.7	319.0	-	314.5
-1.500	293.0	-	300.4	307.0	294.8	-	-
-1.600	274.5	301.3	283.3	290.9	273.1	-	-

* All surface tension values are given in dynes/cm.

TABLE 35 KCl IN FORMAMIDE

	0.500m		0.100m		0.050m	
E volts	q μC/sqcm	C_o μF/sqcm	q μC/sqcm	C_o μF/sqcm	q μC/sqcm	C_o μF/sqcm
+0.400	+16.32	88.0	+13.15	67.5	+12.04	63.4
+0.300	+ 9.39	50.8	+ 7.78	41.8	+ 7.02	38.6
+0.200	+ 5.24	34.31	+ 4.35	28.25	+ 3.87	26.07
+0.100	+ 2.30	25.46	+ 1.90	21.42	+ 1.65	18.70
0	0	20.98	0	16.80	0	15.00
-0.100	- 1.97	18.79	- 1.58	15.10	- 1.42	13.74
-0.200	- 3.81	18.14	- 3.08	15.18	- 2.74	13.89
-0.300	- 5.62	18.30	- 4.64	16.00	- 4.17	14.72
-0.400	- 7.47	18.50	- 6.29	17.01	- 5.71	15.98
-0.500	- 9.30	18.04	- 8.02	17.46	- 7.35	16.69
-0.600	-11.05	17.00	- 9.76	17.22	- 9.03	16.90
-0.700	-12.68	15.71	-11.44	16.32	-10.70	16.34
-0.800	-14.20	14.62	-13.02	15.19	-12.30	15.67
-0.900	-15.62	13.85	-14.48	14.20	-13.84	15.10
-1.000	-16.98	13.34	-15.87	13.64	-15.32	14.55
-1.100	-18.30	13.05	-17.22	13.31	-16.75	14.02
-1.200	-	-	-	-	-18.13	13.59

TABLE 36 0.100 m SOLUTIONS IN FORMAMIDE

E volts	LiCl q μC/sqcm	LiCl C_o μF/sqcm	KCl q μC/sqcm	KCl C_o μF/sqcm	CsCl q μC/sqcm	CsCl C_o μF/sqcm
+0.400	+13.05	65.0	+13.15	67.5	+12.76	68.8
+0.300	+ 7.77	42.0	+ 7.78	41.8	+ 7.41	40.8
+0.200	+ 4.36	27.70	+ 4.35	28.25	+ 3.97	26.95
+0.100	+ 1.92	21.40	+ 1.90	21.42	+ 1.70	19.39
0	0	17.38	0	16.80	0	15.48
-0.100	- 1.61	15.28	- 1.58	15.10	- 1.46	14.00
-0.200	- 3.12	15.13	- 3.08	15.18	- 2.86	14.16
-0.300	- 4.66	15.80	- 4.64	16.00	- 4.32	15.10
-0.400	- 5.28	16.59	- 6.29	17.01	- 5.88	16.14
-0.500	- 7.97	16.94	- 8.02	17.46	- 7.53	16.72
-0.600	- 9.66	16.91	- 9.76	17.22	- 9.21	16.83
-0.700	-11.32	16.25	-11.44	16.32	-10.87	16.27
-0.800	-12.90	15.25	-13.02	15.19	-12.46	15.49
-0.900	-14.38	14.40	-14.48	14.20	-13.97	14.71
-1.000	-15.79	13.85	-15.87	13.64	-15.40	13.82
-1.100	-17.15	13.50	-17.22	13.31	-	-

TABLE 37

CALCULATED CAPACITANCE OF THE DIFFUSE DOUBLE LAYER

IN FORMAMIDE SOLUTIONS

±q μC/sqcm	0.1mKCl μF/sqcm	0.1mCsCl μF/sqcm	0.1mLiCl μF/sqcm	0.5mKCl μF/sqcm	0.05mKCl μF/sqcm
0	89.8	89.7	89.8	199.1	63.5
2	97.8	97.7	87.8	202.8	74.4
4	118.5	118.5	118.6	213.6	100.1
6	146.7	146.7	146.8	230.5	132.4
8	179.0	178.9	179.0	252.1	167.3
10	213.2	213.2	213.4	277.7	203.8
12	249.0	249.0	249.1	305.9	240.7
14	285.4	285.4	285.4	336.3	278.3
16	322.4	322.4	322.4	368.0	316.0
18	359.5	359.5	359.6	401.1	354.1
20	397.3	397.3	397.3	435.2	392.2

TABLE 38

CAPACITANCE OF INNER REGION

OF SOLUTIONS IN FORMAMIDE

q μC/sqcm	0.1mKCl μF/sqcm	0.1mCsCl μF/sqcm	0.1mLiCl μF/sqcm	0.5mKCl μF/sqcm	0.05mKCl μF/sqcm	Mean μF/sqcm
+12	(87.11)	(88.03)	(81.12)	(84.18)	(85.98)	(85.28)
+10	(70.37)	(69.83)	(68.97)	(69.35)	(71.94)	(70.69)
+ 8	(56.27)	(56.27)	(56.71)	(55.68)	(56.27)	(56.24)
+ 6	(45.45)	(45.11)	(44.58)	(44.50)	(44.84)	(44.90)
+ 4	(35.47)	(34.97)	(34.54)	(34.60)	(35.55)	(35.02)
+ 2	(27.56)	(26.44)	(27.50)	(28.02)	(26.57)	(27.22)
0	(20.67)	(18.71)	(21.55)	(23.45)	(19.63)	(20.80)
- 2	(17.73)	(16.43)	(18.04)	(20.67)	(16.87)	(17.95)
- 4	17.88	16.76	17.59	19.85	16.95	17.81
- 6	19.04	18.19	18.58	20.05	18.25	18.82
- 8	19.35	18.55	18.71	19.92	18.63	19.03
-10	18.28	18.12	18.27	18.68	18.21	18.31
-12	16.87	16.91	16.87	17.10	16.85	16.92
-14	15.36	15.50	15.42	15.35	15.84	15.49
-16	14.20	14.10	14.36	14.09	14.72	14.29
-18	13.54	-	13.56	13.54	14.14	13.66

Since Grahame (84) has shown that the cation has only a very small effect on the potential of the E.C. maximum, it was assumed to be the same for 0.100m lithium and caesium chloride solutions as for the 0.100m potassium chloride solution.

Interfacial tension data, calculated using Tate's Law are given in table 34 for all the solutions. Despite the high boiling point and viscosity of formamide, the maximum surface tension recorded in 0.100m KCl solution was 393.4 dynes/cm., as compared with 426.2 dynes/cm. at the electrocapillary maximum in aqueous 0.100 M KCl solutions.

The charge on the electrode was found by integrating the capacitance/potential plots using Simpson's Rule, and taking as the limit, q = 0 at the potential of the E.C. maximum. Tables 35 and 36 give values of charge and capacitance at potentials referred to the E.C. maximum. In figure 22, the charge is plotted against potential for three concentrations of KCl in formamide; a similar graph for 0.100 M aqueous KCl is included for comparison.

If it is assumed that specific adsorption of anions is absent, the differential capacitance of the diffuse double layer may be calculated using equations 15 and 18, derived on page 11. Such an assumptionwas valid when the electrode was polarised cathodically, but the procedure was inaccurate near the E.C. maximum potential and on the anodic side, where there was probably some specific adsorption of chloride ions. In table 36 calculated values are given for diffuse layer differential capacitance.

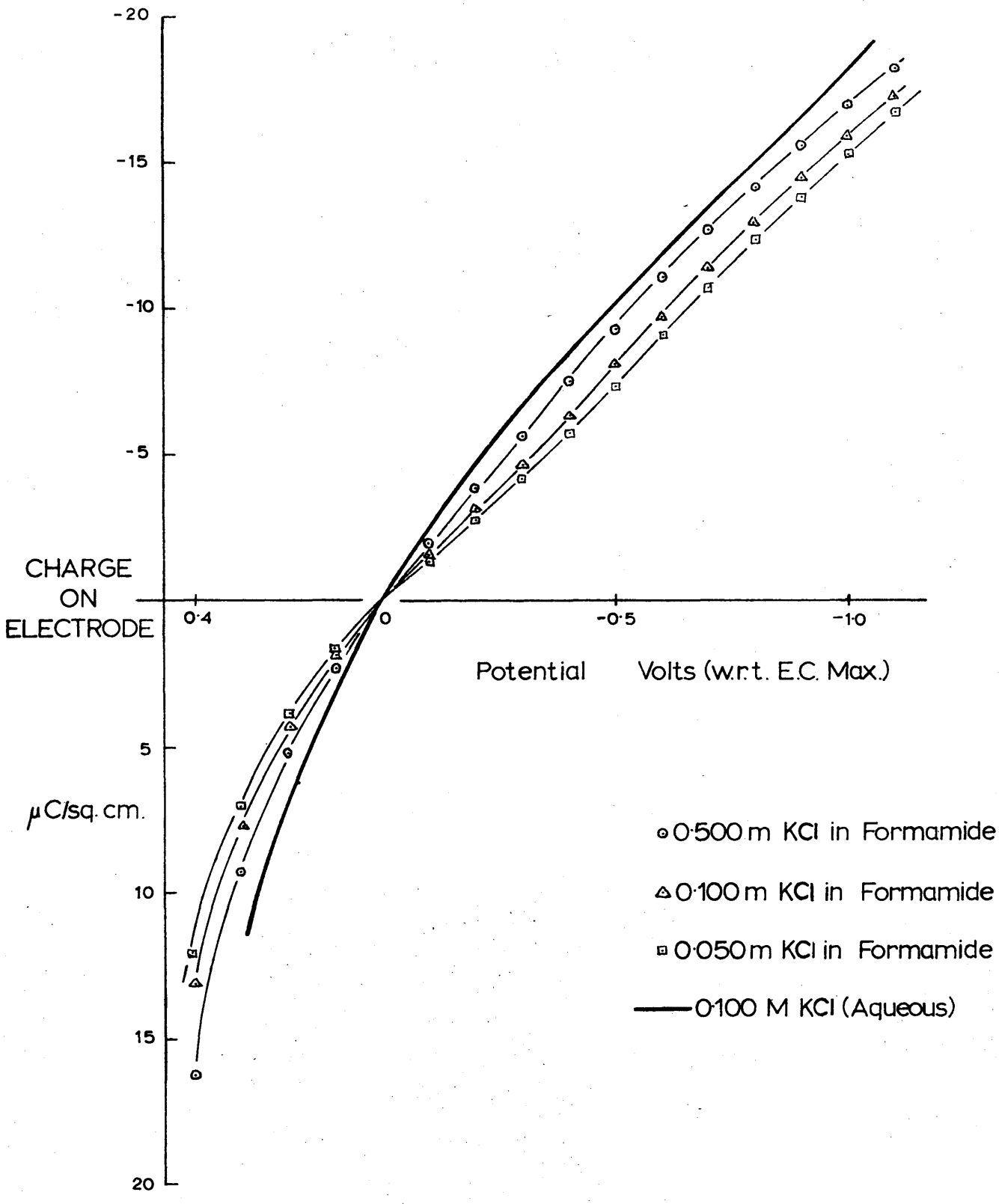
-20
-15
-10
-5
CHARGE ON ELECTRODE
0·4
0
-0·5
-1·0
Potential Volts (w.r.t. E.C. Max.)
5
μC/sq. cm.
10
15
20
⊙ 0·500 m KCl in Formamide
△ 0·100 m KCl in Formamide
⊡ 0·050 m KCl in Formamide
—— 0·100 M KCl (Aqueous)

FIG. 22

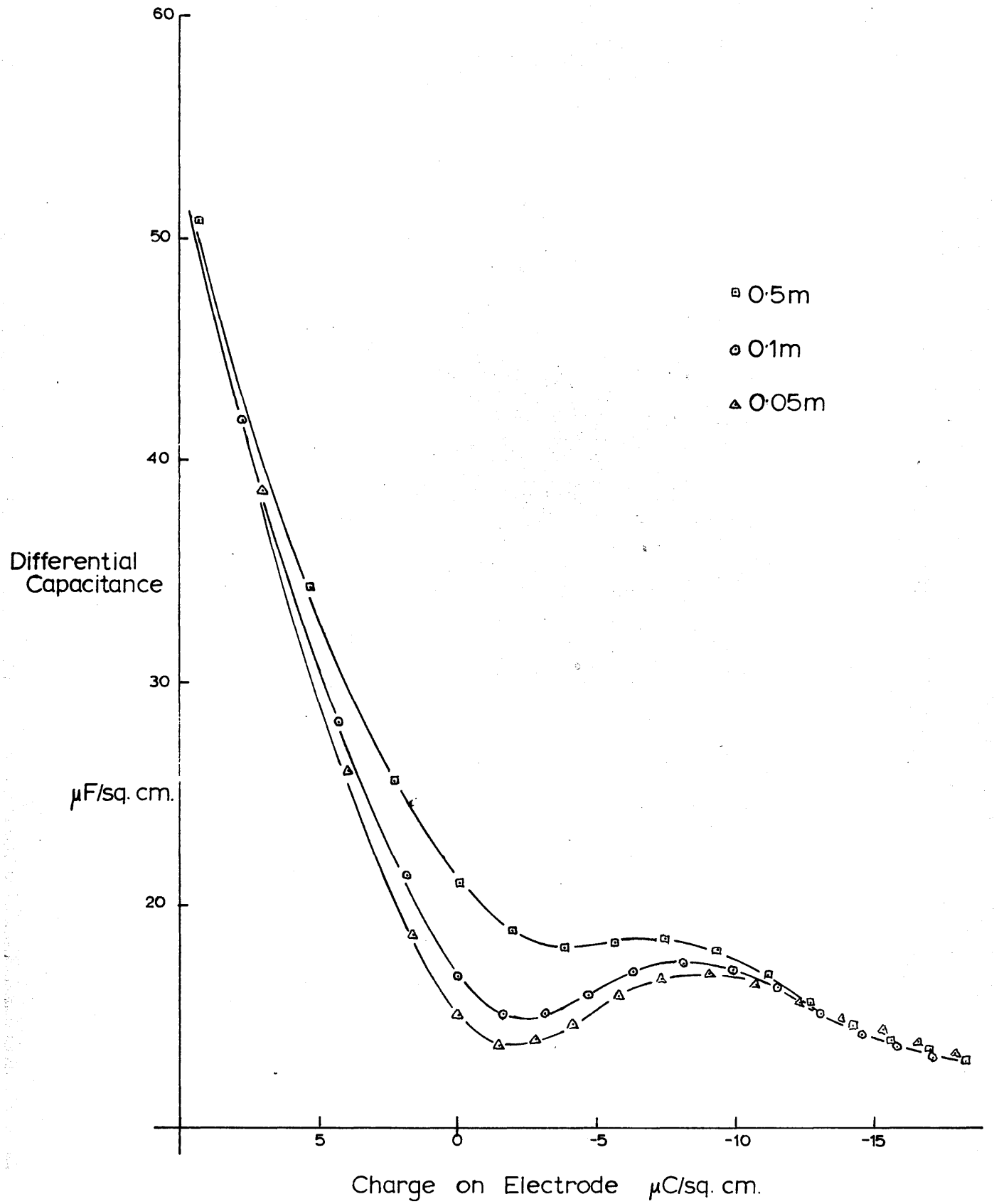

FIG. 23 K Cl SOLUTIONS IN FORMAMIDE

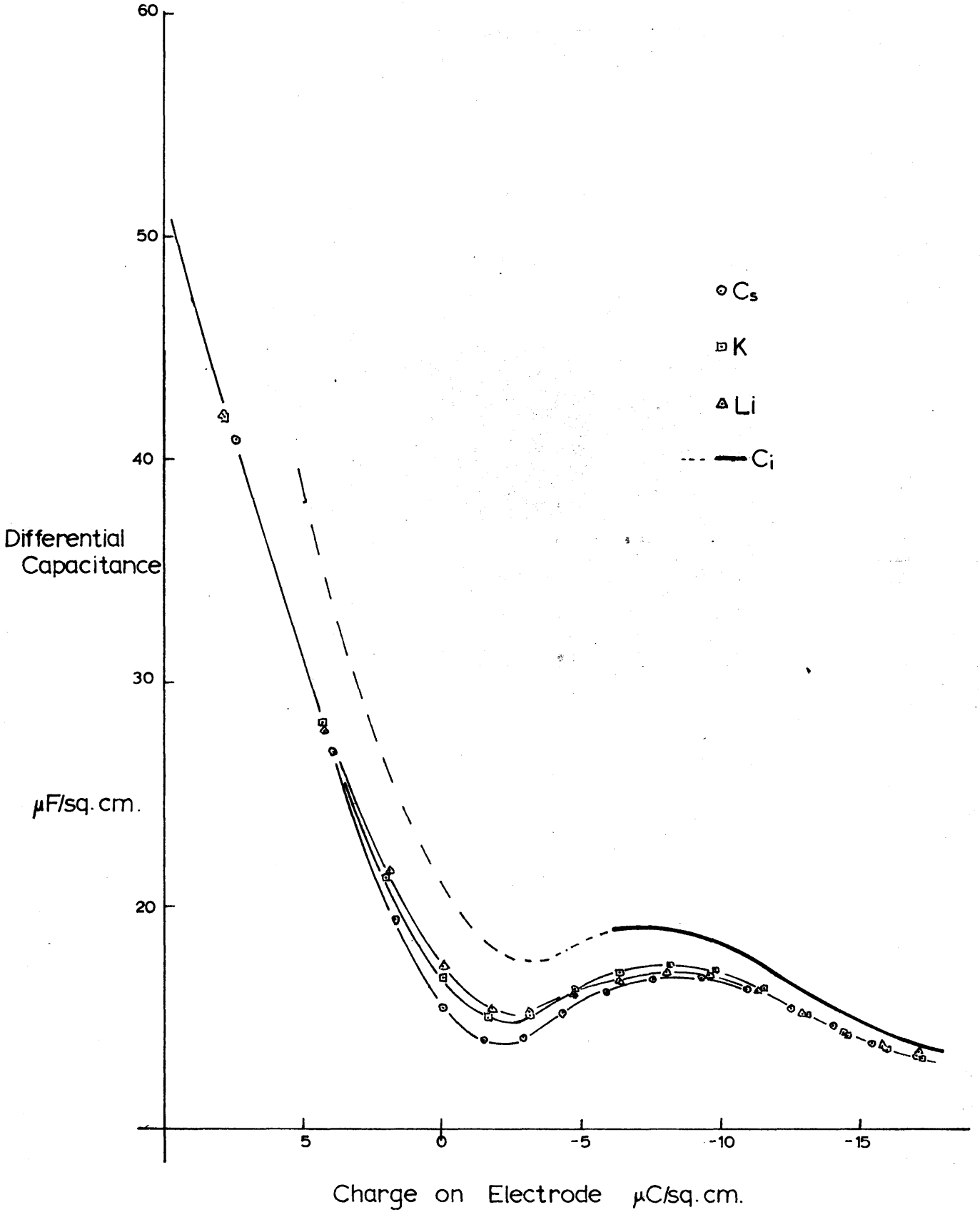

FIG. 24 0·1m ALKALI METALS IN FORMAMIDE

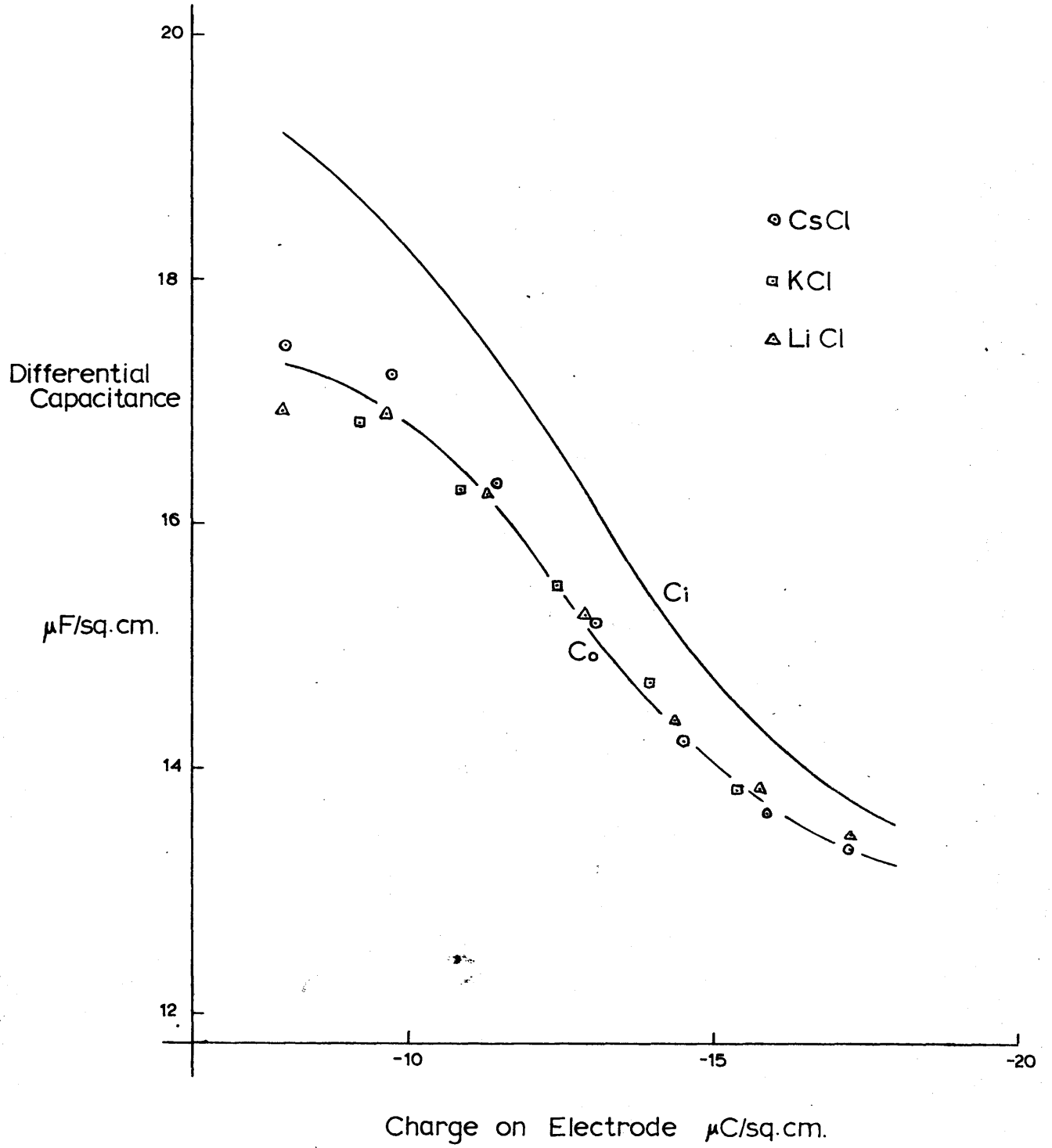
20
18
16
14
12
Differential Capacitance
μF/sq.cm.
CsCl
KCl
Li Cl
Ci
Co
-10
-15
-20
Charge on Electrode μC/sq.cm.

FIG. 25

Finally, the capacitance of the inner region of the double layer was calculated using the equation

$$1/C_i = 1/C_o - 1/C_d$$

Values of C_i for a given charge on the electrode are given in table 37 for all the solutions investigated. As predicted by theory, the value of C_i for a given q is little affected by the concentration of the solution. Near the potential of the E.C. maximum and on the anodic branch, agreement is less good, due to concentration dependent specific adsorption of chloride ions. In figure 23, C_o is plotted against q for three concentrations of potassium chloride. In figures 24 and 25, a similar graph is drawn for 0.100 m lithium, potassium and caesium chloride solutions. Also included is a plot of the mean value of the differential capacitance of the inner region.

There are several significant differences in the charge/capacitance curves of formamide solutions from those of aqueous solutions:

(i) First, although there is no capacitance maximum on the anodic branch of the curve, such an effect does occur on the cathodic side.

(ii) Second, as the charge is increased cathodically, the differential capacitance decreases.

(iii) Finally, at high cathodic polarisation, the size of the cation has almost no effect on the differential capacitance, as is illustrated in figure 25.

In terms of the theory outlined in the introductory section, these three observations may be interpreted as described in the following :

(i) The capacitance maximum.

It has been shown on page 18 that the contribution of solvent dipoles to the total capacitance is a maximum when the probabilities of their being parallel or anti-parallel to a normal of the electrode surface are equal. It was pointed out that this would occur at the potential of the E.C. maximum, where the "applied" field is zero, only if the "bonding energies" for parallel or anti-parallel directions were equal, i.e. if V = 0 in equation 32. In water where the capacitance "hump" occurs at an anodic potential even in the absence of specific adsorption, it is evident that there is a preferential direction of bonding with the positive end of the water molecule dipole towards the metal. When the applied field cancels this effect, the solvent contribution to the capacitance is at a maximum. This may be expressed in another way, by stating that when the field in the inner region, composed of the applied field and the solvent dipole field, is at a minimum, then so also is the dielectric saturation in that region. In the case of formamide it is apparent that the preferential bonding direction has the negative end of the dipole towards the metal and the capacitance peak therefore occurs on the cathodic side of the E.C. maximum. Unfortunately the wave mechanics of formamide are not so fully developed as those of water. It does appear, however, that the formamide dipole has its

positive region centred mainly on the carbon atom, with the negative region residing mainly on the oxygen and, to a smaller extent on the nitrogen. A closer approach to the metal can therefore be made by the negative end of the dipole, which results in a preferential bonding direction. In figure 26 the capacitance maxima for 0.100 M aqueous KCl and for 0.100 m KCl in formamide are drawn with displaced axes to show their similarity in shape. It is to be noted that this similarity is not apparent in capacitance/potential plots, since in the aqueous case the maximum occurs in a region where C_o (i.e. dq/dE) is high compared with that for the formamide solutions, and hence is laterally compressed.

It is noteworthy that near the maximum and towards the zero charge potential, the size of the cation is important in determining the magnitude of the double layer capacitance. Since solvent from the inner region is under the influence of minimum field strength in this range, the capacitance depends primarily on the position of the O.H.P. as fixed by the radius of the cation. In general, over this polarisation range, the capacitance follows the sequence $Li^+ > K^+ > Cs^+$ as would be predicted. (The opposite trend has been noted for water (84) and methanol (85) under strong cathodic polarisation where a limited amount of specific cation adsorption may occur.)

While different sizes of cation do not affect the capacitance maximum in aqueous solutions, a similar effect would be expected for

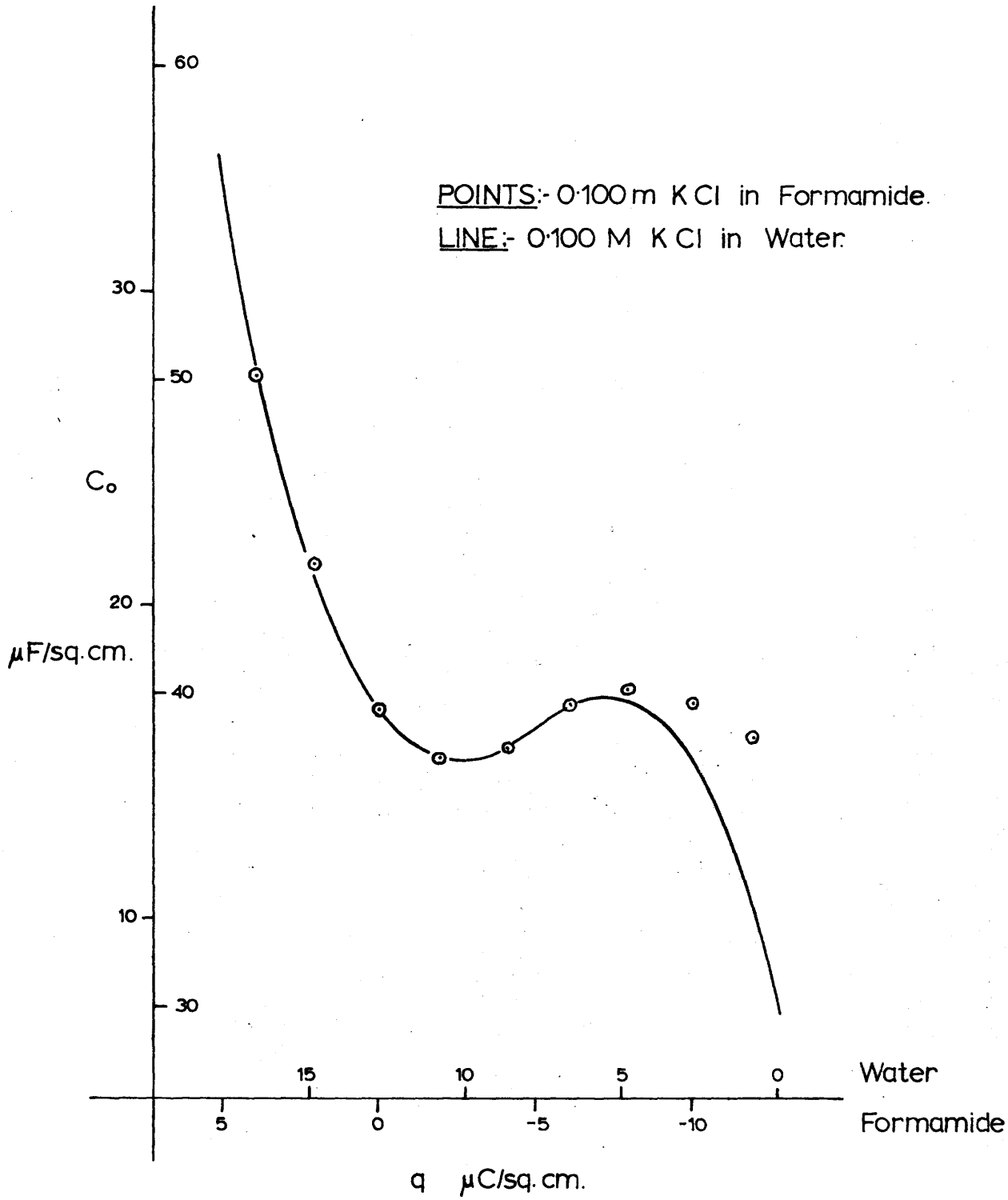

FIG. 26 CHARGE/CAPACITANCE CURVES

different sizes of non-adsorbed anions. Unfortunately this theory is difficult to test since only the fluoride anion fulfills the condition of not being specifically adsorbed. Also adion adsorption is likely to mask the effect.

Watts-Tobin (13) has suggested that the reason for the absence of capacitance maxima in methanolic and ethanolic solutions may be that alcohol molecules have a very strong preferential orientation on mercury, so that they do not turn over in the useable range of polarisation. Also their freezing points are lower and measurements in them should perhaps be compared with those in water at high temperatures where the maximum disappears. It will be of interest to study the effect of temperature on the double layer capacitance of solutions in formamide.

(ii) Decrease in capacitance with increasing negative polarisation

In the absence of specific adsorption, two effects determine the shape of the capacitance/potential or capacitance/charge curves under cathodic polarisation :

(a) the rate at which orientation polarisation of the solvent is being achieved, and

(b) the rate of increase of compression of the inner region by the electric field.

In the case of water when the electrode has a charge of approximately -12 μC/sq.cm., solvent dipoles in the inner region are almost completely orientation polarised, and hence increasing the applied

field does not tend to lower the capacitance much further. Compressional forces are now significant, however, and contraction of the inner region leads to an increase in capacitance. In contrast, for formamide the solvent dielectric saturation is still increasing at a similar value of electrode charge, and hence the dipole contribution to the capacitance is still decreasing. While no capacitance minimum can be observed due to electroreduction of solvent, if greater cathodic potentials were attainable without depolarisation of the electrode, an eventual increase in double layer capacitance would be expected. In the case of formamide, compressional forces would act over the whole range between the capacitance maximum and minimum turning points, whereas for water they act over only part of the range. Assuming the same compression coefficient for both solvents, it is therefore to be inferred that the potential difference between the turning points would be slightly greater for water than for formamide.

(iii) Effect of cation size on capacitance of the cathodic region

Grahame (84) has shown that in aqueous solutions of alkali metal chlorides, there is a regular increase in cathodic differential capacitance in going from lithium to caesium; $C_{o(Cs^+)} - C_{o(Li^+)}$ rises from 1.12 μF/sq.cm. to 4.39 μF/sq.cm. as the potential with respect to a 0.100 M calomel electrode rises from -0.700 volts to -1.940 volts. Minc and Jastrzebska (85) have

pointed out that the corresponding capacitance differences for lithium and sodium chloride solutions in methanol and ethanol are even larger than in water. In constrast, the differences observed in formamide solutions are very small and show no trends (figure 25).

The higher capacitance displayed by the large ions in aqueous solutions was considered by Grahame (84) to be largely due to the fact that for a given potential, since the inner region would be slightly broader, the field strength across it would be smaller and hence the effects of dielectric saturation would be reduced. He also favoured the idea, however, that some desolvation would take place on the side of the cation facing the metal and that this might occur more readily for large cations whose solvent sheaths were less tightly bound. Minc, Jastrzebska and Brzostowska (77) observed that cation desolvation must depend to a great extent on the solvent, since solvation energy varies greatly from one to another. If it is assumed, therefore, that the solvation energy of formamide is high, since it has a high dipole moment (3.25×10^{-18} e.s.u..cm. as compared with 1.85×10^{-18} e.s.u..cm. for water), the effect of cation size should be small.

Mott, Parsons and Watts-Tobin (18) however, consider that in general cations bind their primary hydration sheaths so strongly that these remain intact. Cathodic capacitance values are almost independent of temperature, whereas specific adsorption of cations

would be temperature dependent. These authors note that for water, the dielectric constant may rise to a high value between the metal and the O.H.P., so that the field never reaches the centre of a cation and thus its extra size does not lower the capacitance. Therefore, provided that solvent molecules in the second layer next to the electrode do not have their orientations determined to any great extent by the (polarised) molecules next to the electrode surface, the centres of ions lie in a plane located mainly in a region of high dielectric constant. Thus the potential drop occurs almost entirely before the O.H.P. This theory would not hold in concentrated solutions where the second solvent layer, even if not saturated by dipole forces from the first layer, would be polarised by a heavily populated O.H.P.

The structure of solid formamide has been determined by X-ray diffraction analysis (86) and a schematic diagram of the structure based on this is given in figure 27. It is seen that the high dielectric constant of formamide, 109.5 ± 0.2 at 25°C (79) is probably due to the formation of chains of molecules caused by the preferential breaking of the weaker (longer) of the two types of hydrogen bonds. The structure of the compound is such that a formamide molecule will only be orientated by another if the latter is in certain particular positions relative to it. Therefore it is very likely that if a formamide molecule was firmly orientated by the mercury surface, it would not be in a favourable position to restrict the movement of molecules

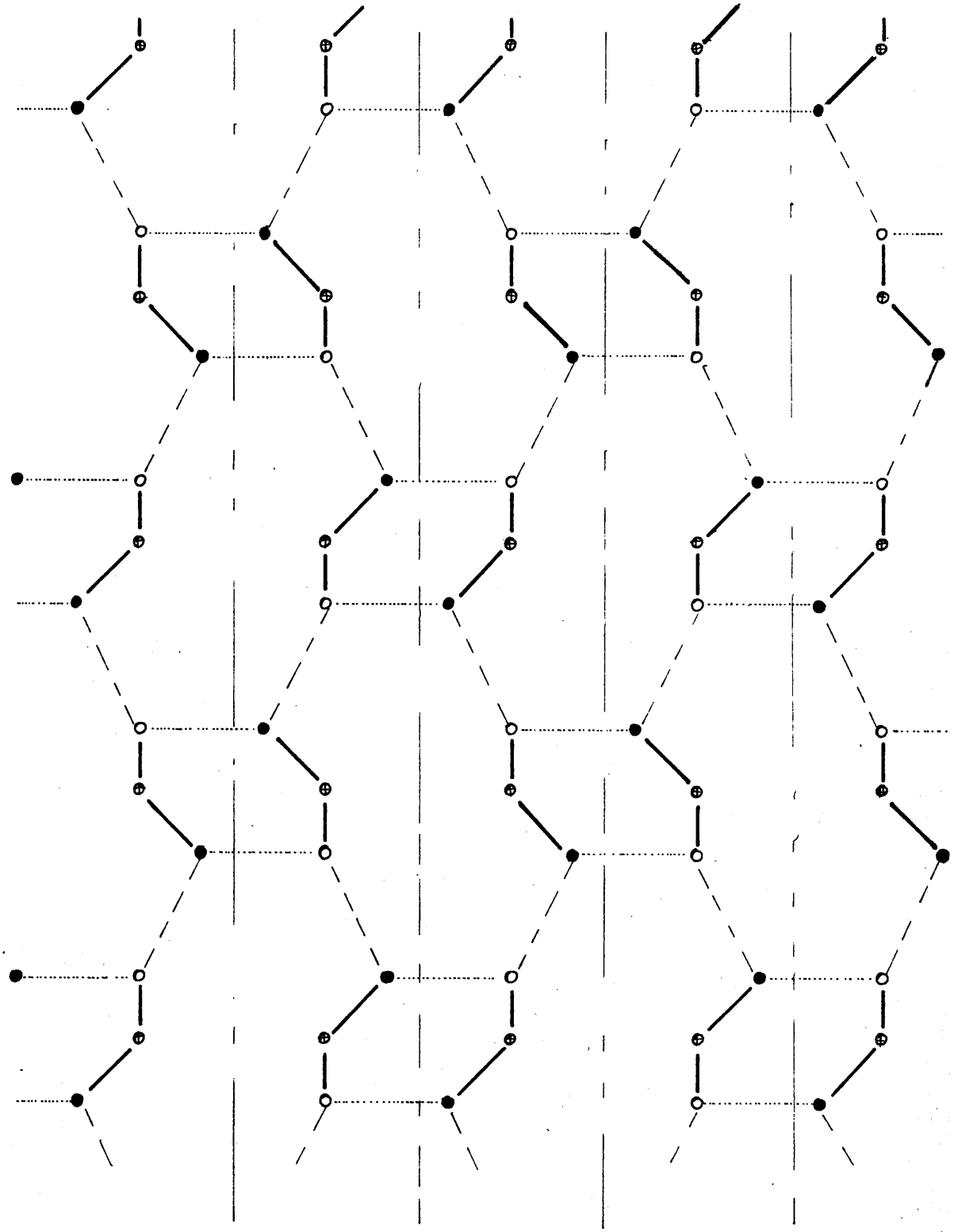

FIG. 27 SOLID FORMAMIDE STRUCTURE (SCHEMATIC)

in the second layer. It may be noted that as the formamide molecules next to the electrode become further polarised with increasing applied potential, the effect of cations size decreases.

THE VALUE OF THE CAPACITANCE MINIMUM

Minc et al. (77) have claimed that a linear relationship exists between the lowest value of the double layer differential capacitance and the bulk solvent dielectric constant: such a claim can be invalidated on both experimental and theoretical grounds. Firstly their authority (89) for taking the bulk dielectric constant of formamide as 84 does not appear very reliable (79,87,88), and in any case, the minimum for 0.1 m LiCl in formamide is below 13.5 μF/sq.cm., whereas for 0.1 M LiCl in water, it is 15.46 μF/sq.cm.

Secondly theoretical considerations make it very unlikely that such a relationship holds. In the absence of specific adsorption of cations, the value of the minimum depends on the extent to which solvent in the inner region is orientation polarised before the onset of appreciable compression. The degree of orientation polarisation depends on the position of the capacitance maximum which in turn is determined by the relative energies of adsorption of solvent dipoles towards, or away from, the metal. No correlation between capacitance minimum and the bulk dielectric constant is therefore expected.

BIBLIOGRAPHY

1.	Parsons.	Modern Aspects of Electrochemistry.	1954, Butterworths, London.
2.	Helmholtz.	Wied. Ann.	1879, 7, 337.
3.	Gouy.	Ann. de Phys.	1917, 7, 129.
4.	Chapman.	Phil. Mag.	1913, 25, 475.
5.	Stern.	Z. Elektrochem.	1924, 30, 508.
6.	Grahame and Whitney.	J. Chem. Phys.	1941, 9, 827.
7.	Grahame.	Chem. Rev.	1947, 41, 441.
8.	Devanathan.	Trans. Farad. Soc.	1954, 50, 373.
9.	Mott and Watts-Tobin.	Electrochim. Acta.	1961, 4, 79.
10.	Grahame.	J. Chem. Phys.	1950, 18, 903.
11.	Conway, Bockris and Ammar.	Trans. Farad Soc.	1951, 47, 756.
12.	Macdonald.	J. Chem. Phys.	1954, 22, 1857.
13.	Watts-Tobin.	Phil. Mag.	1961, 6, 133.
14.	Grahame and Parsons.	J.A.C.S.	1961, 83, 1291.
15.	Austin and Parsons.	Proc. Chem. Soc.	1961, 239.
16.	Grahame.	J.A.C.S.	1957, 79, 2093.
17.	Kirkwood.	J. Chem. Phys.	1939, 7, 911.
18.	Mott, Parsons and Watts-Tobin.	Phil. Mag.	1962, 7, 483.
19.	Macdonald.	J. Chem. Phys.	1954, 22, 1857.
20.	Grahame.	Z. Elektrochem.	1955, 59, 743.
21.	Rice.	Phys. Rev.	1928, 31, 1051.
22.	Pauling.	Proc. Roy. Soc. A.	1927, 114, 181.

23.	Lipmann.	Ann. Chim. Phys.	1875,	(3)5,	496.
24	Gouy.	Ann. Chim. Phys.	1903,	29,	145.
25.	Gouy.	Ann. Chim. Phys.	1906,	8,	291.
26.	Devanathan and Parsons.	Trans. Farad. Soc.	1953,	49,	673.
27.	Devanathan and Peries.	Trans. Farad. Soc.	1954,	50,	1236.
28.	Craxford and MacKay.	J. Phys. Chem.	1935,	39,	545.
29.	Corbusier and Gierst.	Anal. Chim. Acta.	1956,	15,	254.
30.	Smith.	Trans. Farad. Soc.	1951,	47,	63.
31.	Smolders and Duyvis.	Rec. Trav. Chim.	1961,	80,	635.
32.	Frumkin.	Acta. Scient. (Paris).	1936,	373.	
33.	Hickling.	Disc. Farad. Soc.	1947,	1,	277.
34.	Bowden and Grew.	Disc. Farad. Soc.	1947,	1,	91.
35.	Brodd and Hackerman.	J. Electrochem. Soc.	1957,	104,	704.
36.	McMillan and Hackerman.	J. Electrochem. Soc.	1959,	106,	341.
37.	Philpot.	Phil. Mag.	1935,	13,	775.
38.	Frumkin.	Z. Phys. Chem.	1923,	103,	55.
39.	Loveland and Elving.	J. Phys. Chem.	1952,	56,	250.
40.	Proskurnin and Frumkin.	Trans. Farad. Soc.	1935,	31,	110.
41.	Randles.	Disc. Farad. Soc.	1947,	1,	11.
42.	Wien.	Ann. Phys. (Leipzig).	1896,	58,	37.
43.	Jones and Christian.	J.A.C.S.	1935,	57,	272.

44.	Grahame.	J.A.C.S.	1949, 71, 2975.
45.	Robertson.	J. Electrochem Soc.	1953, 100, 194.
46.	Randles.	Trans.Farad. Soc.	1954, 50, 1246.
47.	Nancollas and Vincent.	Chem. and Ind.	1961, 506.
48.	Calvert et al.	J. Phys. Chem.	1958, 62, 47.
49.	Grahame.	J.A.C.S.	1946, 68, 301.
50.	Hickling and Bruce.	J. Sci. Inst.	1938, 15, 22.
51.	Barker and Gardner.	A.E.R.E. (Harwell).	1958, Cir 2297.
52.	Newcombe.	Electrochim. Acta.	1962, 7, 685.
53.	Newcombe.	Advances in Polarography 11 p.482.	1960, Pergammon.
54.	Belton.	Electronic Eng.	1958, 30, 454.
55.	Grahame.	J.A.C.S.	1941, 63, 1207.
56.	Peacock.	Ph.D. Thesis.	1954, Glasgow.
57.	Hans, Henne and Meurer.	Z Elektrochem.	1954, 58, 836.
58.	Barker.	Advances in Polarography 1 p.330.	1960, Pergammon.
59.	Los and Murray.	" 11 p.425.	1960, Pergammon.
60.	Lingane.	J.A.C.S.	1953, 75, 788.
61.	Newcombe.	Chem. and Ind.	1955, 1473.

62.	Newcombe.	Chem. and Ind.	1957, 1120.
63.	Newcombe.	Trans. Farad. Soc.	1961, 57, 130.
64.	Davies and Nancollas.	Chem. and Ind.	1950, 129.
65.	Bourdillon.	J.C.S.	1913, 791.
66.	Campbell, J.R.	Private communication	
67.	Barker.	Symposium on Electrode Processes (Philadelphia).	1959, Wiley. p.366.
68.	Harkins and Brown.	Int. Crit.Tables (New York).	1928, 4, 435.
69.	MacNevin and Balis.	J.A.C.S.	1943, 65, 660.
70.	Parsons, R.	Private communication.	
71.	Matsuda.	Bull. Chem. Soc. Japan.	1953, 26, 342.
72.	Bockris, J. O'M.	Private Communication.	
73.	Bockris and Conway.	J. Chem. Phys.	1958, 28, 707.
74.	Vincent, C.A.	Unpublished work.	
75.	Shedlovsky.	J.A.C.S.	1932, 54, 1405.
76.	Macdonald.	J. Chem. Phys.	1956, 25, 364.
77.	Minc Jastrzebska and Brzostowska.	J. Electrochem Soc.	1961, 108, 1160.
78.	Macdonald and Barlow.	J. Chem. Phys.	1962, 36, 3062.
79.	Leader.	J.A.C.S.	1951, 73, 806.
80.	Harned and Wright.	J.A.C.S.	1933, 55, 4849.
81.	Dunsmore.	Ph.D. Thesis.	1953, Glasgow.
82.	Harned.	J.A.C.S.	1929, 51, 416.

83.	McAuley.	Ph.D. Thesis.	1961, Glasgow.
84.	Grahame.	J. Electrochem. Soc.	1951, 98, 343.
85.	Minc and Jastrzebska.	J. Electrochem Soc.	1960, 107, 136.
86.	Ladell and Post.	Acta. Cryst.	1954, 7, 559.
87.	-	National Bureau of Standards.	Circular 514, 109.
88.	-	Handbook of Chemistry and Physics.	1959-60. 41st Edn. Chem. Rubber Pub. Co.
89.	Calton and Brooker.	J. Phys. Chem.	1958, 62, 1595.